gJR.

[redacted]

CENTRAL RESEARCH LIBRARY
DOCUMENT COLLECTION

ORNL-2061, Part IV
C-85 – Reactors-Aircraft Nuclear Propulsion Systems

cy. 123-A

AEC RESEARCH AND DEVELOPMENT REPORT

CENTRAL RESEARCH LIBRARY
DOCUMENT COLLECTION
LIBRARY LOAN COPY
DO NOT TRANSFER TO ANOTHER PERSON
If you wish someone else to see this document, send in name with document and the library will arrange a loan.

MARTIN MARIETTA ENERGY SYSTEMS LIBRARIES
3 4456 0251028 1

AIRCRAFT NUCLEAR PROPULSION PROJECT

QUARTERLY PROGRESS REPORT

FOR PERIOD ENDING MARCH 10, 1956

DECLASSIFIED
CLASSIFICATION CHANGED TO:
BY AUTHORITY OF: AEC 1-25-66
BY: C. Rackenmeister 2-14-67

[redacted]

OAK RIDGE NATIONAL LABORATORY
OPERATED BY
UNION CARBIDE NUCLEAR COMPANY
A Division of Union Carbide and Carbon Corporation
UCC
POST OFFICE BOX P · OAK RIDGE, TENNESSEE

[redacted]
This document contains Restricted Data as defined in the Atomic Energy Act of 1954. Its transmittal or the disclosure of its contents in any manner to an unauthorized person is prohibited.

[redacted]

LEGAL NOTICE

This report was prepared as an account of Government sponsored work. Neither the United States, nor the Commission, nor any person acting on behalf of the Commission:

A. Makes any warranty or representation, express or implied, with respect to the accuracy, completeness, or usefulness of the information contained in this report, or that the use of any information, apparatus, method, or process disclosed in this report may not infringe privately owned rights; or

B. Assumes any liabilities with respect to the use of, or for damages resulting from the use of any information, apparatus, method, or process disclosed in this report.

As used in the above, "person acting on behalf of the Commission" includes any employee or contractor of the Commission to the extent that such employee or contractor prepares, handles or distributes, or provides access to, any information pursuant to his employment or contract with the Commission.

[redacted]

ORNL-2061, Part IV
C-85 – Reactors-Aircraft Nuclear Propulsion Systems

This document consists of 72 pages.
Copy 23 of 199 copies. Series A.

Contract No. W-7405-eng-26

AIRCRAFT NUCLEAR PROPULSION PROJECT

QUARTERLY PROGRESS REPORT

For Period Ending March 10, 1956

W. H. Jordan, Director
S. J. Cromer, Co-Director
A. J. Miller, Assistant Director

DATE ISSUED

JUN 12 1956

OAK RIDGE NATIONAL LABORATORY
Operated by
UNION CARBIDE NUCLEAR COMPANY
A Division of Union Carbide and Carbon Corporation
Post Office Box P
Oak Ridge, Tennessee

[redacted]

MARTIN MARIETTA ENERGY SYSTEMS LIBRARIES
3 4456 0251028 1

[redacted]

INTERNAL DISTRIBUTION

1. R. G. Affel
2. C. R. Baldock
3. C. J. Barton
4. M. Bender
5. D. S. Billington
6. F. F. Blankenship
7. E. P. Blizard
8. C. J. Borkowski
9. W. F. Boudreau
10. G. E. Boyd
11. M. A. Bredig
12. W. E. Browning
13. F. R. Bruce
14. A. D. Callihan
15. D. W. Cardwell
16. C. E. Center (K-25)
17. R. A. Charpie
18. G. H. Clewett
19. C. E. Clifford
20. J. H. Coobs
21. W. B. Cottrell
22. D. D. Cowen
23. S. Cromer
24. R. S. Crouse
25. F. L. Culler
26. J. H. DeVan
27. L. M. Doney
28. D. A. Douglas
29. E. R. Dytko
30. L. B. Emlet (K-25)
31. D. E. Ferguson
32. A. P. Fraas
33. J. H. Frye
34. W. T. Furgerson
35. H. C. Gray
36. W. R. Grimes
37. E. E. Hoffman
38. A. Hollaender
39. A. S. Householder
40. J. T. Howe
41. H. K. Jackson
42. W. H. Jordan
43. G. W. Keilholtz
44. C. P. Keim
45. M. T. [illegible]
46. F. Kertesz
47. E. M. King
48-49. J. A. Lane
50. R. S. Livingston
51. R. N. Lyon
52. F. C. Maienschein
53. W. D. Manly
54. E. R. Mann
55. L. A. Mann
56. W. B. McDonald
57. F. R. McQuilkin
58. R. V. Meghreblian
59. R. P. Milford
60. A. J. Miller
61. R. E. Moore
62. J. G. Morgan
63. K. Z. Morgan
64. E. J. Murphy
65. J. P. Murray (Y-12)
66. G. J. Nessle
67. R. B. Oliver
68. L. G. Overholser
69. P. Patriarca
70. R. W. Peelle
71. A. M. Perry
72. J. C. Pigg
73. H. F. Poppendiek
74. P. M. Reyling
75. A. E. Richt
76. M. T. Robinson
77. H. W. Savage
78. A. W. Savolainen
79. R. D. Schultheiss
80. E. D. Shipley
81. A. Simon
82. O. Sisman
83. M. J. Skinner
84. G. P. Smith
85. A. H. Snell
86. C. D. Susano
87. J. A. Swartout
88. E. H. Taylor
89. R. E. Thoma
90. D. B. Trauger
91. E. R. Van Artsdalen
92. F. C. VanderLage
93. G. M. Watson

[redacted]

[redacted]

94. A. M. Weinberg
95. J. C. White
96. G. D. Whitman
97. E. P. Wigner (Consultant)
98. G. C. Williams
99. J. C. Wilson
100. C. E. Winters
101-110. ORNL – Y-12 Technical Library, Document Reference Section
111-120. Laboratory Records Department
121. Laboratory Records, ORNL R. C.
122-124. Central Research Library

EXTERNAL DISTRIBUTION

125. AF Plant Representative, Baltimore
126. AF Plant Representative, Burbank
127. AF Plant Representative, Marietta
128. AF Plant Representative, Santa Monica
129. AF Plant Representative, Seattle
130. AF Plant Representative, Wood-Ridge
131. Air Research and Development Command (RDGN)
132. Air Research and Development Command (RDZPA)
133. Air Technical Intelligence Center
134. Air University Library
135. Aircraft Laboratory, Design Branch (WADC)
136-138. ANP Project Office, Fort Worth
139. Argonne National Laboratory
140. Armed Forces Special Weapons Project, Sandia
141. Assistant Secretary of the Air Force, R&D
142-147. Atomic Energy Commission, Washington
148. Bureau of Aeronautics
149. Bureau of Aeronautics General Representative
150. Chicago Operations Office
151. Chicago Patent Group
152-153. Chief of Naval Research
154. Convair-General Dynamics Corporation
155. Director of Laboratories (WCL)
156. Director of Requirements (AFDRQ)
157. Director of Research and Development (AFDRD-ANP)
158-160. Directorate of Systems Management (RDZ-1SN)
161-163. Directorate of Systems Management (RDZ-1SS)
164. Equipment Laboratory (WADC)
165-168. General Electric Company (ANPD)
169. Hanford Area Office
170. Headquarters, Air Force Special Weapons Center
171. Lockland Area Office
172. Los Alamos Scientific Laboratory
173. Materials Laboratory Plans Office (WADC)
174. National Advisory Committee for Aeronautics, Cleveland
175. National Advisory Committee for Aeronautics, Washington
176. North American Aviation, Inc. (Aerophysics Division)
177. Nuclear Development Corporation
178. Patent Branch, Washington

[redacted]

[redacted]

179-181. Powerplant Laboratory (WADC)
182-185. Pratt & Whitney Aircraft Division (Fox Project)
186. Sandia Corporation
187. School of Aviation Medicine
188. USAF Project RAND
189. University of California Radiation Laboratory, Livermore
190-192. Wright Air Development Center (WCOSI-3)
193-198. Technical Information Extension, Oak Ridge
199. Division of Research and Development, AEC, ORO

[redacted]

[redacted]

FOREWORD

This portion, Part IV. Shielding Systems, of the Aircraft Nuclear Propulsion Project Quarterly Progress Report falls in AEC category C-85, Reactors – Aircraft Nuclear Propulsion Systems, and is therefore being issued separately in order not to further limit distribution of the material that falls in AEC category C-84, Reactors – Special Features of Aircraft Reactors, which has been issued as ORNL-2061, Parts I, II, III.

[redacted]

[redacted]

CONTENTS

FOREWORD v

SUMMARY 1

PART IV. SHIELDING SYSTEMS

15. TOWER SHIELDING FACILITY 5
- Gamma-Ray and Fast-Neutron Dose Rates in Air as a Function of Distance from the TSF Reactor 5
- Preliminary Differential Gamma-Ray Shielding Tests 6
- Measurements with the Reactor Off the Major Axis of the Crew Compartment 26
- Angular Distribution of Radiation in the GE R1 Crew-Compartment Mockup 26
  - Method of Determining Factor for Radiation from the Rear 27
  - Method of Determining Factor for Radiation from the Side 29
  - Calculation of Angular Distribution for GE Crew Compartment 31

16. AIRCRAFT SHIELD DESIGN 36
- Procedure for the Optimization of a Divided Gamma-Ray Shield for Circulating-Fuel Reactors 36
  - Expression for Total Crew-Compartment Gamma-Ray Dose Rate 36
  - Expression for Total Gamma-Ray Shield Weight 37
  - Determination of Shadow-Shield Volume 37
  - Method of Tapering the Shadow Shield 38
  - Determination of the Scattering Probability 38
  - Application of Lagrange Multipliers to Obtain Lead Thicknesses 39
  - Determination of Gamma-Ray Linear Attenuation Coefficients 40
  - Sample Calculation 41
- Shield Design Study for a Circulating-Fuel Reactor with a Fuel-to-Air Radiator 44
  - Reactor, Radiator, and Crew Compartment 44
  - Dose-Rate Criteria 46
  - Shield Design for a Circulating-Fuel Reactor with a Wrap-Around Radiator 46
  - Shield Design for a Circulating-Fuel Reactor with a Tandem Radiator 50
  - Total Weights 54
- Modification of the Procedure for Using TSF Data for the Optimization of a Divided Neutron Shield 54
  - Neglected Derivative Term 55
  - Changed Iteration Procedure 59
  - Results of a Sample Calculation 61

[redacted]

[redacted]

ANP PROJECT QUARTERLY PROGRESS REPORT

SUMMARY

PART IV. SHIELDING SYSTEMS

15. Tower Shielding Facility

Measurements of the gamma-ray and fast-neutron dose rates in air as a function of distance from the reactor have been made for distances as large as 4000 ft. The results indicate relaxation lengths (λ) in air of 785 ft for gamma rays and 630 ft for fast neutrons.

Preliminary gamma-ray shielding tests have been initiated. Measurements to determine the variation of the dose rate at the GE R1 crew compartment as a function of the reactor shield thickness and angle of radiation emission from the reactor are being made. Thermal-neutron flux measurements are also being made as part of the investigation to determine the cases for which neutron captures in air contribute significantly to the dose rate inside the crew compartment.

As a first step in a preliminary investigation of the effects of placing a reactor in the wing of an airplane, two configurations with the reactor off the major reactor–crew-compartment axis were investigated.

A calculation was performed to determine the effect of the angular distribution of the radiation leaving the inside surface of the GE crew compartment on the dose rate within the crew compartment. Factors which account for the angular distribution were calculated for the direct dose rate entering the crew compartment rear, the scattered dose rate entering the rear, and the scattered dose rate entering the side. The results indicate that the scattered radiation leaving the side has a $\cos^5 \theta$ distribution, while the direct radiation entering the rear has a $\cos^2 \theta$ distribution. The scattered radiation entering the rear is negligible compared with the contributions by other sources.

16. Aircraft Shield Design

The gamma-ray optimization procedure used previously in the calculation of total weights for various circulating-fuel reactors has been described in detail. The procedure was designed primarily for choosing the proper distribution of gamma-ray shielding material between the reactor and the crew compartment, but it also gives a distribution of material at these locations which probably is not far from that for minimum weight. In the procedure it is assumed that the neutron shield for a specified neutron dose rate in the crew compartment has already been optimized and that it will not be greatly affected by the optimization of the gamma-ray shield, and vice versa. The method of Lagrangian multipliers is then used to derive expressions for the optimum thickness of the lead at both the reactor and the crew compartment.

The preliminary shielding study for a 300-Mw circulating-fuel aircraft reactor system employing a direct fuel-to-air heat exchanger was completed. Both a wrap-around and a tandem heat exchanger arrangement were considered, but no attempt was made to design a heat exchanger or air ducts or to evaluate the increased efficiency for a fuel-to-air heat exchanger system. Divided shield weights were

[redacted]

determined for the condition of 1 rem/hr in the crew compartment and 1000 rep/hr at 50 ft from the reactor. For the wrap-around heat exchanger the total weight was 115,400 lb; for the tandem arrangement the weight was 121,200 lb. When the dose rate for radiation damage and activation was permitted to increase to 100,000 rep/hr at 50 ft from the shielded reactor, the total weights were reduced to 94,700 and 85,700 lb, respectively.

The procedure for the optimization of a divided neutron shield through the use of TSF data was modified in two respects: a derivative term was included which was neglected before, and the iteration procedure was changed in such a way that one of the Lagrangian multipliers converges more rapidly. The effect that these modifications have on the shield thicknesses and weights was determined by a sample shield calculation for the same reactor and crew compartment system as that used previously. The new procedure gave shield weights that were substantially the same though slightly lower than those given by the old procedure for the particular configuration considered.

Part IV

SHIELDING SYSTEMS

15. TOWER SHIELDING FACILITY

C. E. Clifford

J. L. Hull F. N. Watson
F. J. Muckenthaler
Applied Nuclear Physics Division

G. J. Rausa, Glenn L. Martin Co.

GAMMA-RAY AND FAST-NEUTRON DOSE RATES IN AIR AS A FUNCTION OF DISTANCE FROM THE TSF REACTOR

F. N. Watson

Measurements of the gamma-ray and fast-neutron dose rates in air as a function of distance from the Tower Shielding Facility (TSF) reactor have been made for distances as large as 4000 ft. The reactor was contained in the TSF reactor tank with 6 in. of water between the tank wall and the side of the reactor nearest the detector. The reactor altitude was 190 ft.

A curve (Fig. 15.1) drawn through the points for which the reactor was visible to the gamma-ray detector (i.e., the terrain did not interfere with the direct beam from the reactor) indicates a constant relaxation length (λ_γ) of 785 ft. The following formula was fitted to the curve:

$$D_\gamma = C_1 \frac{e^{-r/\lambda_\gamma}}{r^2} ,$$

where

D_γ = gamma-ray dose rate (mr/hr·w),

C_1 = 1.72×10^4 (a constant),

r = distance from the reactor (ft).

Fast-neutron dose-rate measurements (Fig. 15.2) for the same distances were made with a less reliable instrument that is directional in its response. Although there are several inconsistencies, a general trend in the data indicates an air relaxation length (λ_n) of approximately 630 ft. The following formula serves as a reasonable approximation to the response to be expected from this type of a directional detector:

$$D_n = C_2 \frac{e^{-r/\lambda_n}}{r^2} ,$$

where

D_n = fast-neutron dose rate (mrep/hr·w),

C_2 = 2.3×10^3 (a constant).

The gamma-ray dose-rate curve shows that the air-scattered gamma rays are still well collimated far from the reactor. This is indicated by the rather large decrease in the dose rate at points where the reactor was not visible to the detector and is in contrast to the fast-neutron measurements, where interposition of the terrain had little effect. Since the fast-neutron dose-rate measurements were detected

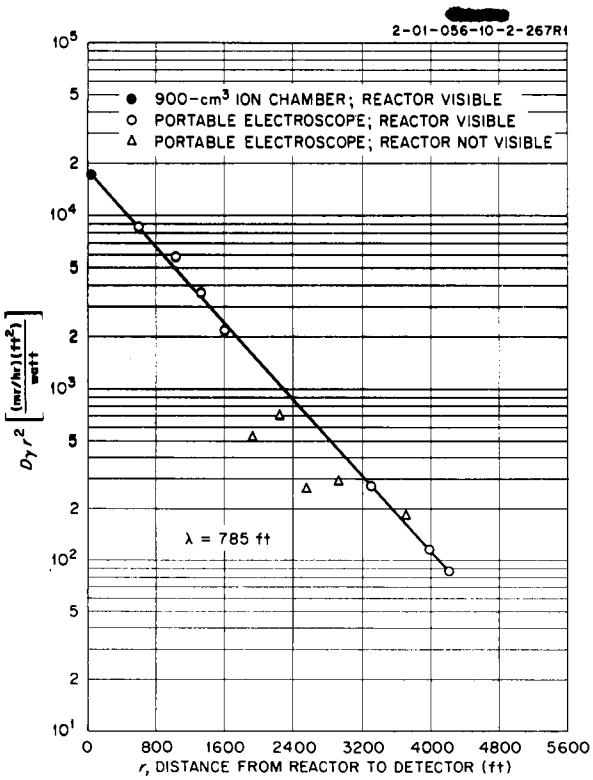

Fig. 15.1. Gamma-Ray Dose Rates in Air at the TSF.

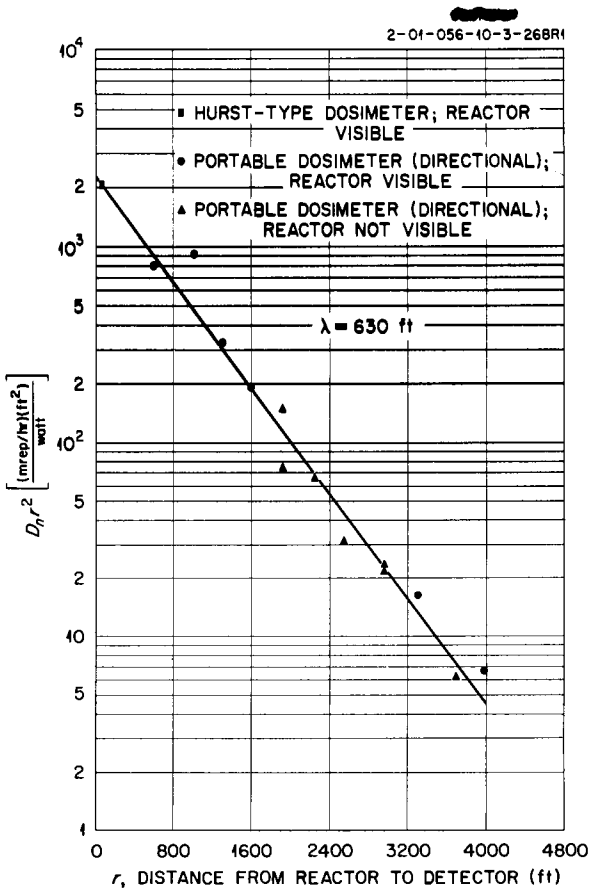

Fig. 15.2. Fast-Neutron Dose Rates in Air at the TSF.

with a directional detector and the neutrons were obviously not well collimated, the neutron dose rate shown in Fig. 15.2 could possibly be low by a factor of 2, except for the first point.

It should be noted that the first point in Fig. 15.2 was measured with a Hurst-type fast-neutron dosimeter which was submerged in the water of the TSF detector tank. Such a measurement results in the elimination of 2π radians of the solid angle from which radiation may be received by the detector from the air. The detector does, however, receive reflected neutrons from water behind it, which probably at least compensates for those not received from the air. The net error is expected to be small in this case.

PRELIMINARY DIFFERENTIAL GAMMA-RAY SHIELDING TESTS

F. N. Watson

A preliminary investigation of the variation of gamma-ray dose rates at the crew compartment as a function of the reactor water-shield thicknesses (ρ) and angles of radiation emission (θ) from the reactor shield was started. One of the early objectives of these tests will be to determine the cases in which neutron captures in air contribute significantly to the gamma-ray dose rate inside the crew compartment.

Gamma-ray dose rates at the outside rear of the GE R1 crew compartment[1] were measured for various reactor shield configurations. For these measurements the reactor was placed inside the TSF reactor tank,[2] and a separation distance of 64 ft was maintained between the center of the tank and the outside rear face of the GE crew compartment. The reactor-detector altitude was 195 ft for all the measurements. The dose rates were measured as a function of ρ for two values of θ, 0 and 180 deg. The dose rate showed a minimum at ρ = 60 cm and θ = 180 deg (Fig. 15.3). The relaxation length of the direct beam of gamma rays in the reactor shield water was approximately 28 cm. As the reactor approached the outside of the reactor tank the apparent relaxation length of the air-scattered gamma rays plus the air-capture gamma rays changed rapidly and approached 17 cm. The thermal-neutron flux measured at the rear of the GE crew compartment as a function of ρ and θ showed a minimum at ρ = 140 cm and θ = 180 deg (Fig. 15.3).

The gamma-ray dose rate was also measured inside and near the center of the GE crew compartment as a function of ρ (Fig. 15.3). In this case the direct-beam radiation exhibited a relaxation length of approximately 34 cm, except when the reactor was near the outside of the reactor tank. The apparent relaxation length of the air-scattered plus air-capture gamma-ray dose rate was 6.5 cm, and thus there is an indication that most of these gamma rays probably were produced by neutron and air interactions and did not originate in the reactor.

Other measurements made in order to further investigate the phenomena of air scattering of gamma rays and the production of gamma rays by neutrons captured in air are presented in Figs. 15.4 through 15.20; the analysis of these data will be presented in a future report. Figures 15.4 through 15.6 show the thermal-neutron flux at the outside rear of the GE crew compartment as a function of θ for reactor shield thicknesses (ρ) of 90, 16, and 45 cm, respectively. Corresponding gamma-ray dose-rate measurements are shown in Fig. 15.7 for ρ = 16 cm and in Fig. 15.8 for ρ = 30, 45, 60, 90, 120, and 156 cm.

Gamma-ray dose-rate measurements at the outside rear of the crew compartment were also made as a function of the altitude of the reactor tank (Figs. 15.9, 15.10, and 15.11). For these measurements the crew-compartment–detector altitude was held stationary at 100 ft, and the reactor shield thicknesses were 16, 45, 90, and 156 cm. Thermal-neutron-flux measurements as a function of reactor altitude for the same reactor shield thicknesses are shown in Figs. 15.12 through 15.15.

For another measurement a detector was placed on a tower leg[3] at an altitude of 140 ft, and the thermal-neutron flux was measured as a function of the distance between the detector and the center of the reactor tank at the same altitude. This essentially indicated the flux at a point in space. The fiducial line for the reactor orientation angle, θ, was left unchanged for this measurement; that is, an angle of 90 deg indicates that the reactor was on the side of the reactor tank nearest the detector. These data are shown in Figs. 15.16, 15.17, and 15.18 for θ = 0, 270, and 92 deg, respectively. (A measurement could not be obtained for θ = 90 deg owing to limitations of the reactor-positioning device.)

---

[1] F. N. Watson, *ANP Quar. Prog. Rep. Sept. 10, 1955*, ORNL-1947, p 217.

[2] C. E. Clifford *et al.*, *Preliminary Study of Fast Neutron Ground and Air Scattering at the Tower Shielding Facility*, ORNL CF-54-8-95 (Aug. 23, 1954).

[3] *Ibid.*, p 7; see TSF layout for leg No. 1.

[redacted]
2-01-056-11-1 to 10-285 A

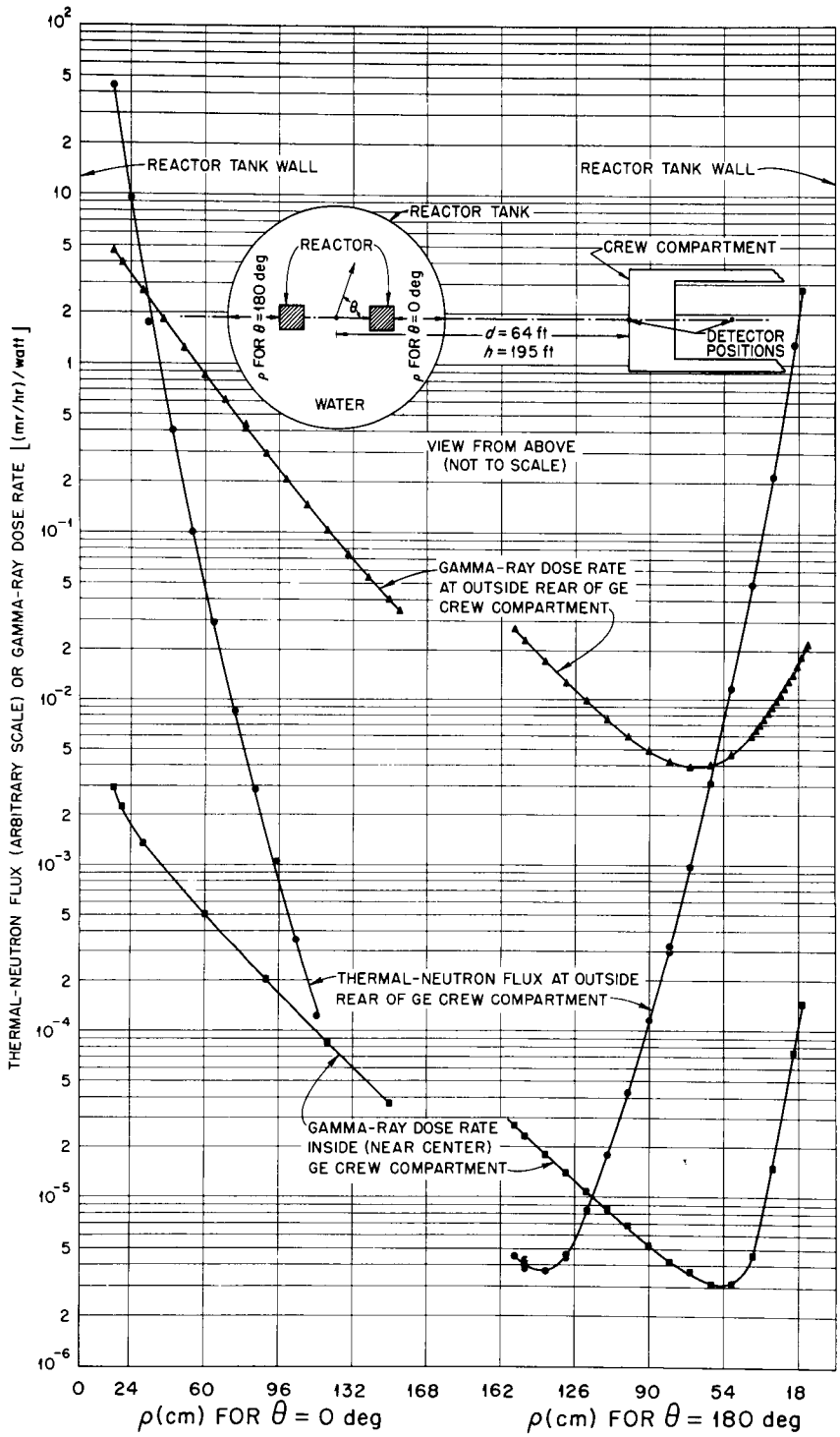

Fig. 15.3. Thermal-Neutron Flux and Gamma-Ray Dose Rate Inside and Outside GE Crew Compartment as a Function of Reactor Position Within the Tank.

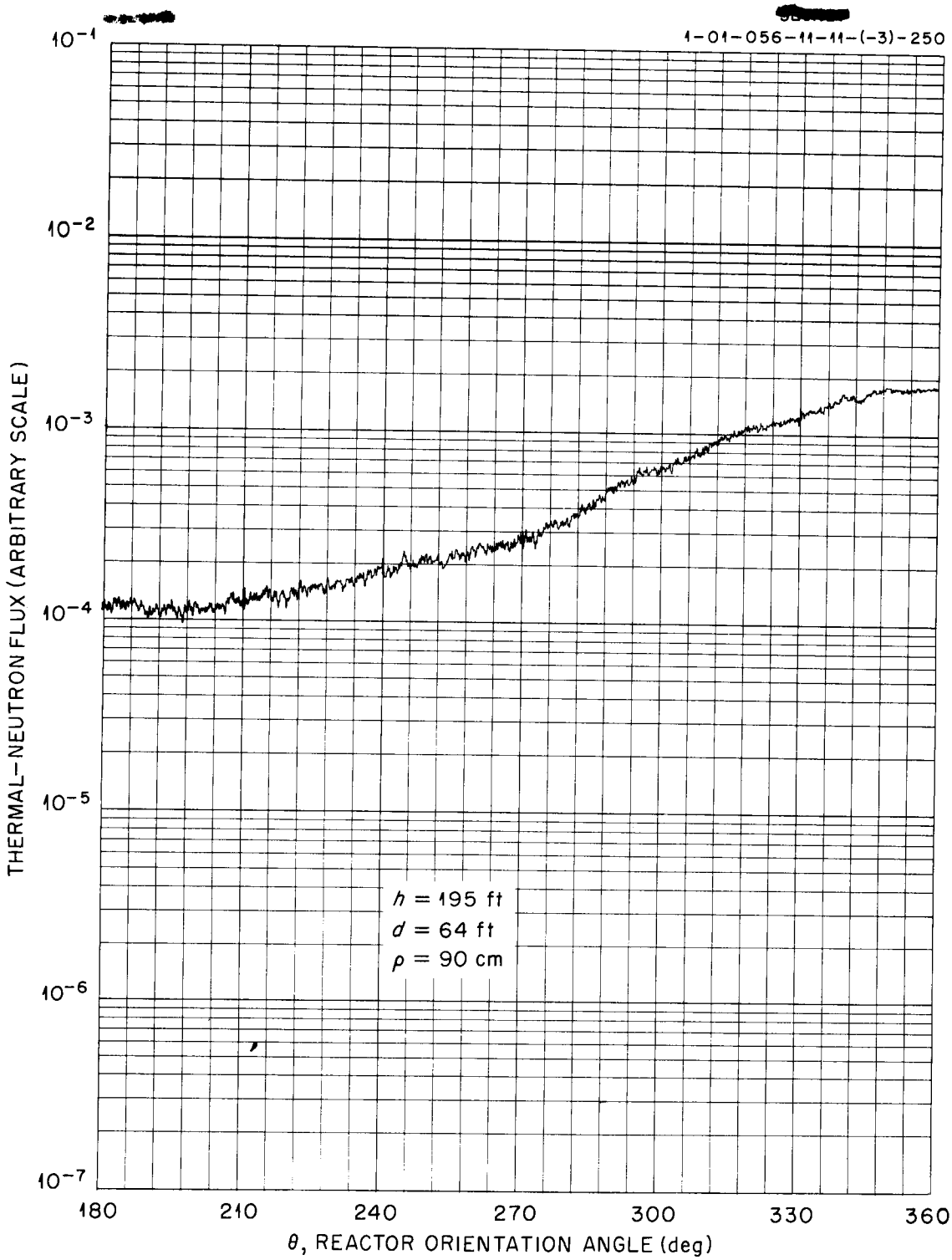

Fig. 15.4. Thermal-Neutron Flux at Outside Rear of GE Crew Compartment as a Function of θ for ρ = 90 cm.

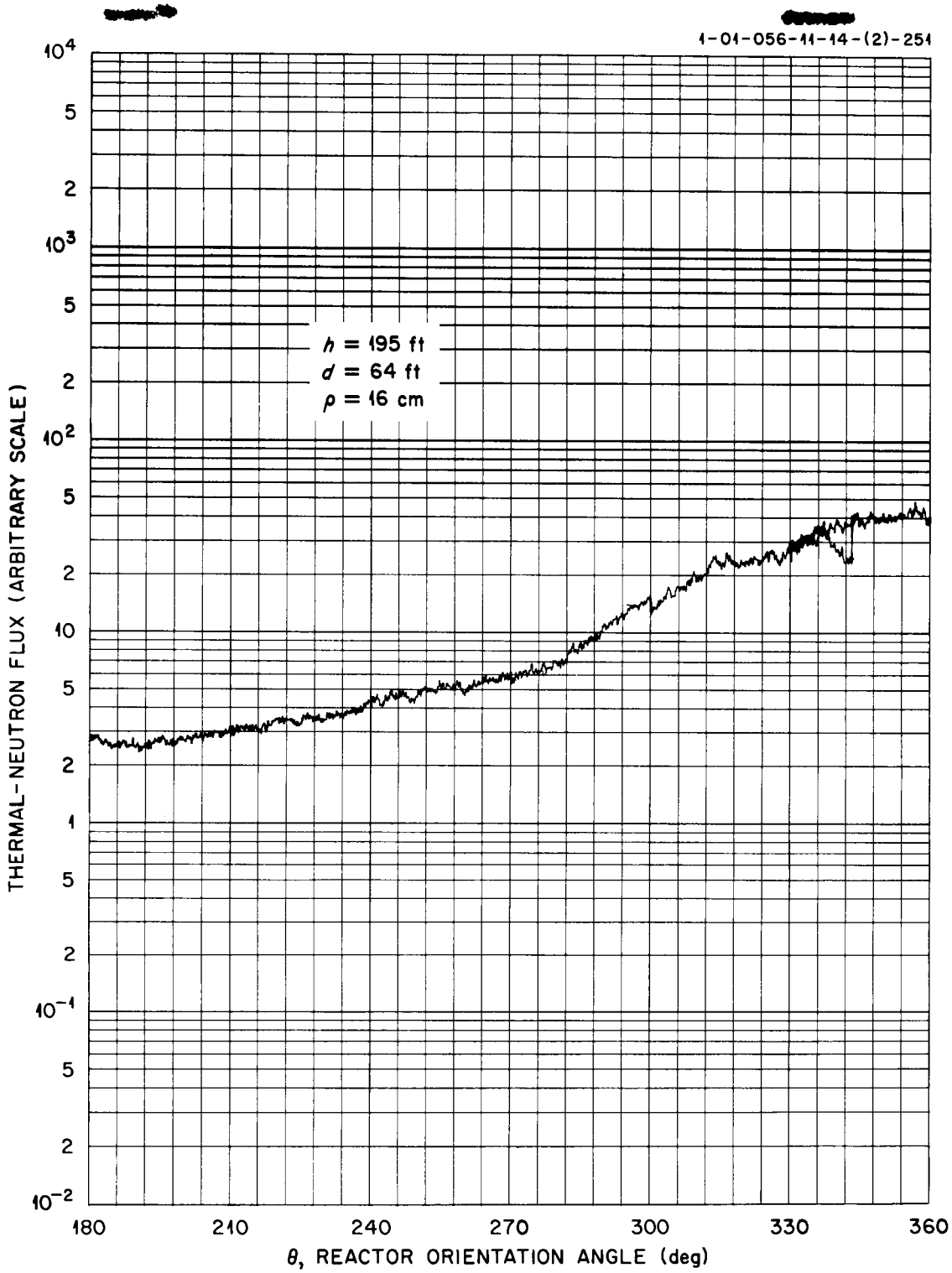

Fig. 15.5. Thermal-Neutron Flux at Outside Rear of GE Crew Compartment as a Function of θ for ρ = 16 cm.

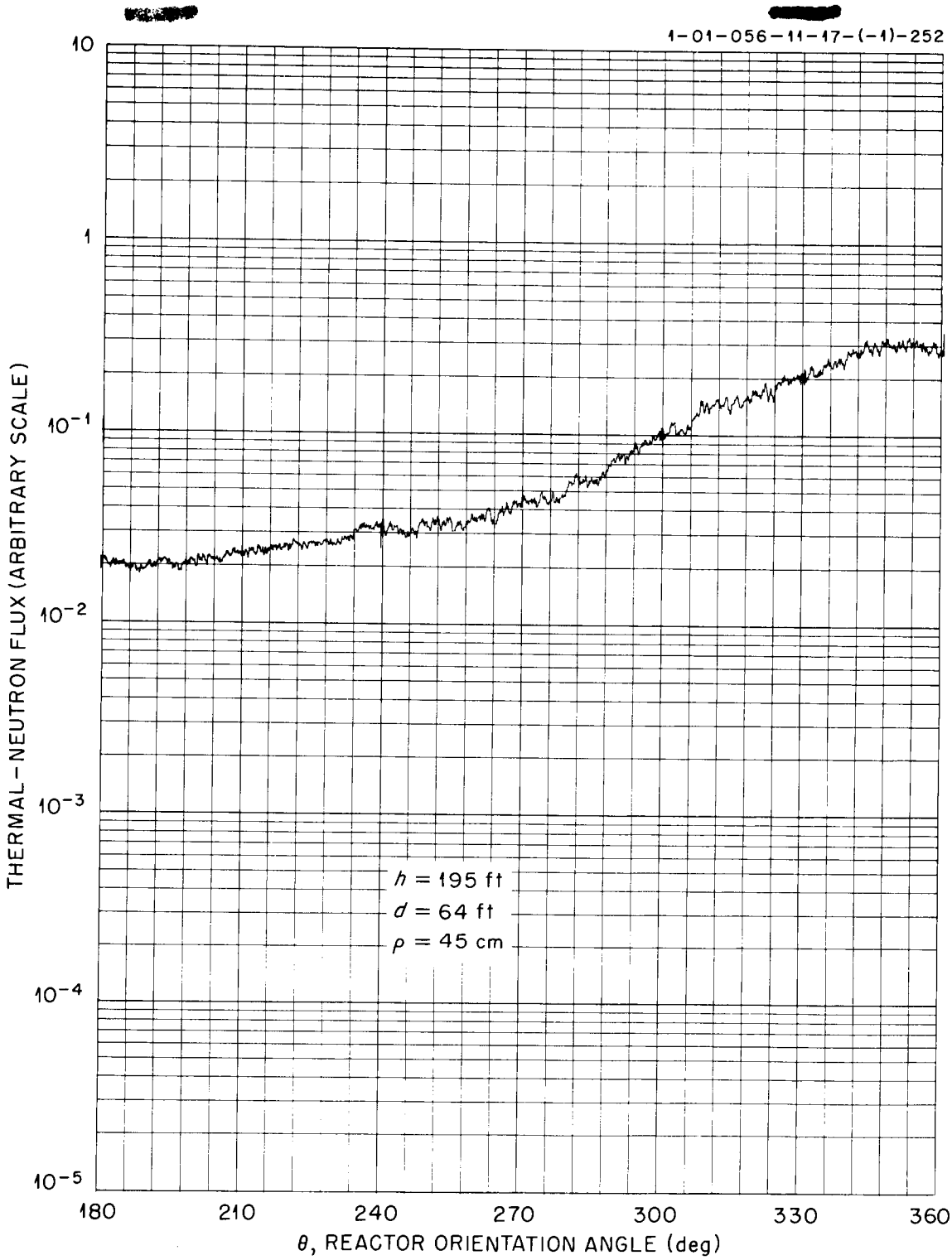

Fig. 15.6. Thermal-Neutron Flux at Outside Rear of GE Crew Compartment as a Function of θ for ρ = 45 cm.

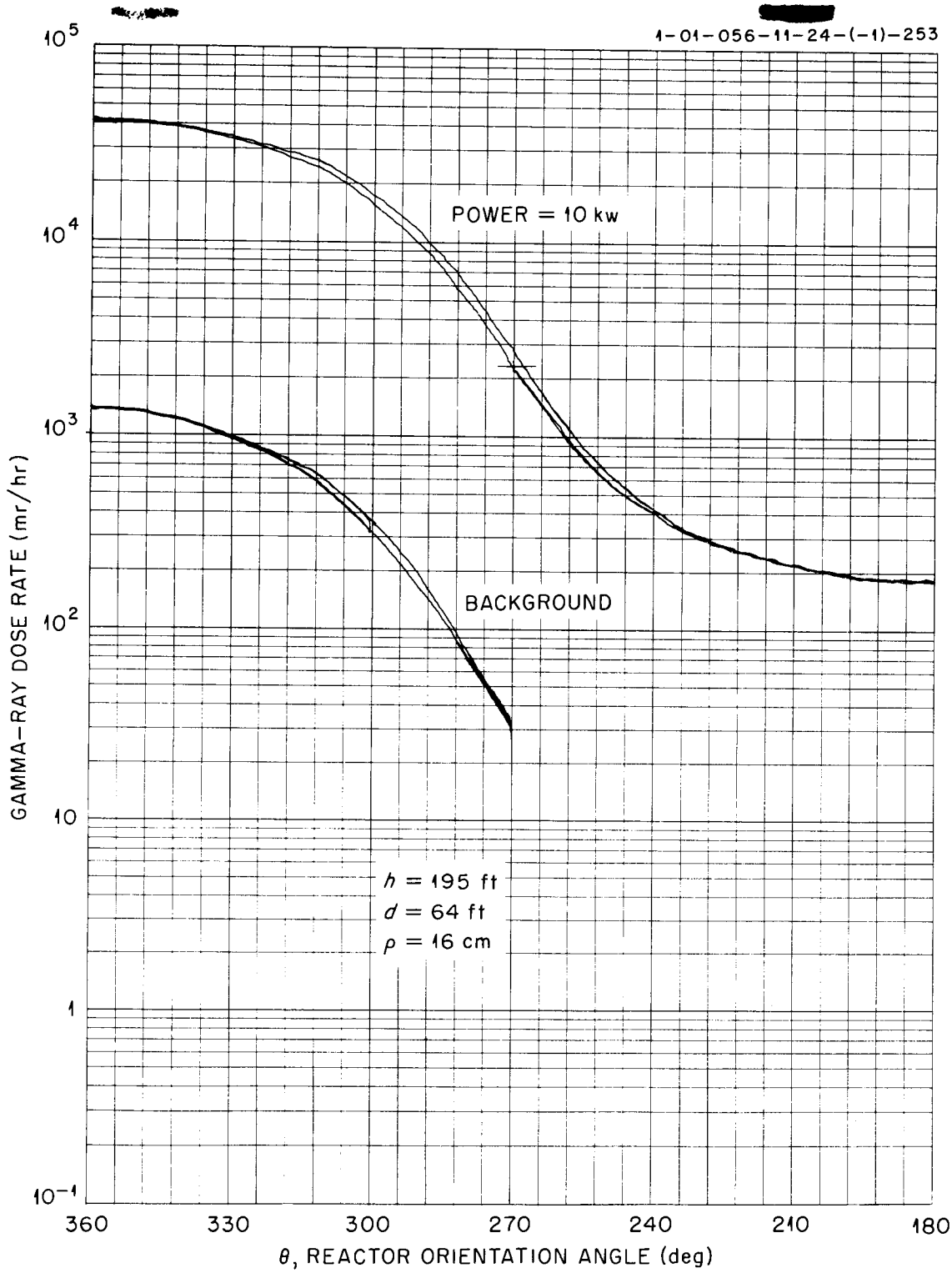

Fig. 15.7. Gamma-Ray Dose Rate at Outside Rear of GE Crew Compartment as a Function of θ for ρ = 16 cm.

[redacted] [redacted]

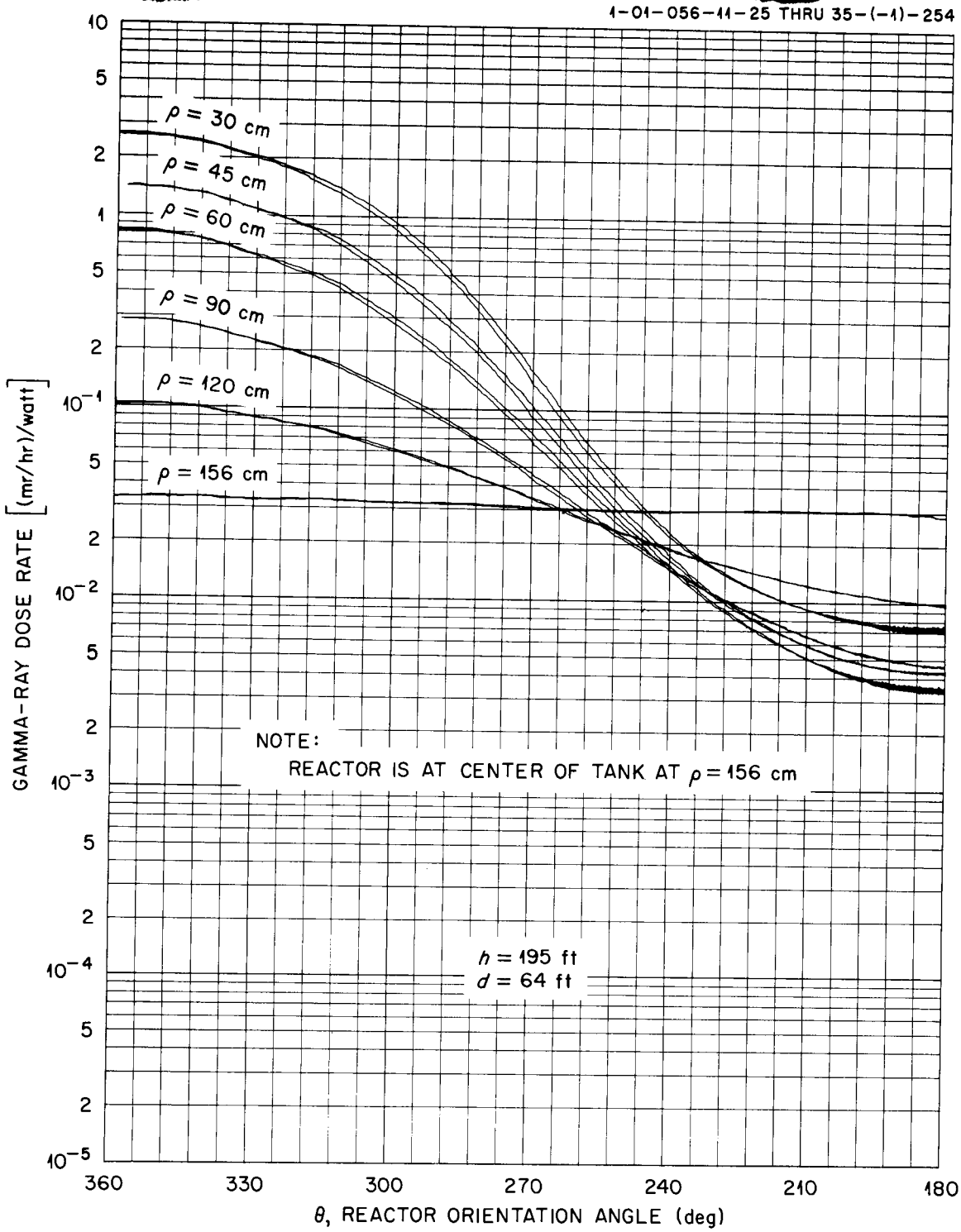

Fig. 15.8. Gamma-Ray Dose Rate at Outside Rear of GE Crew Compartment as a Function of θ for Various Values of ρ.

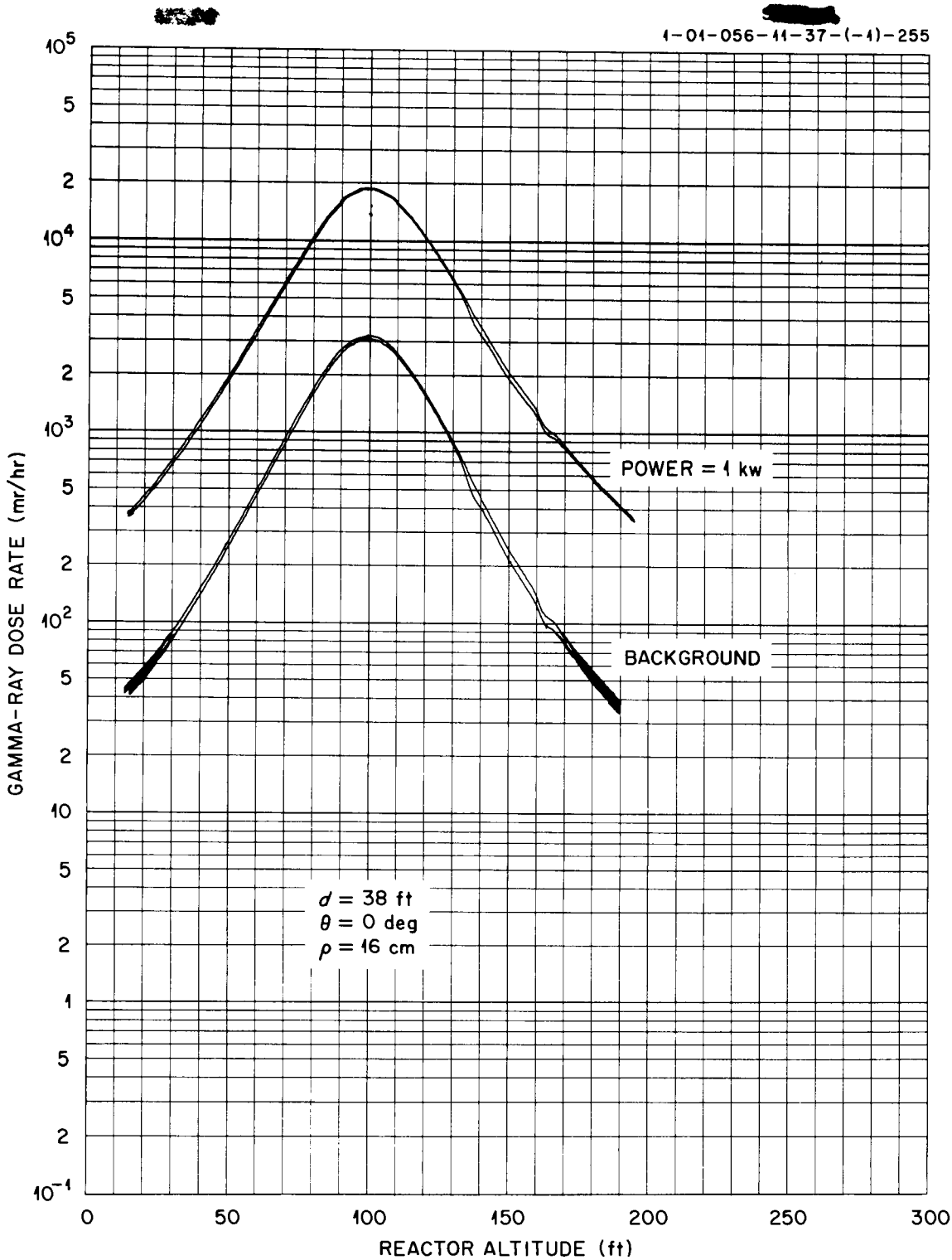

Fig. 15.9. Gamma-Ray Dose Rate at Outside Rear of GE Crew Compartment as a Function of Reactor Altitude for $\rho = 16$ cm.

[redacted] [redacted]

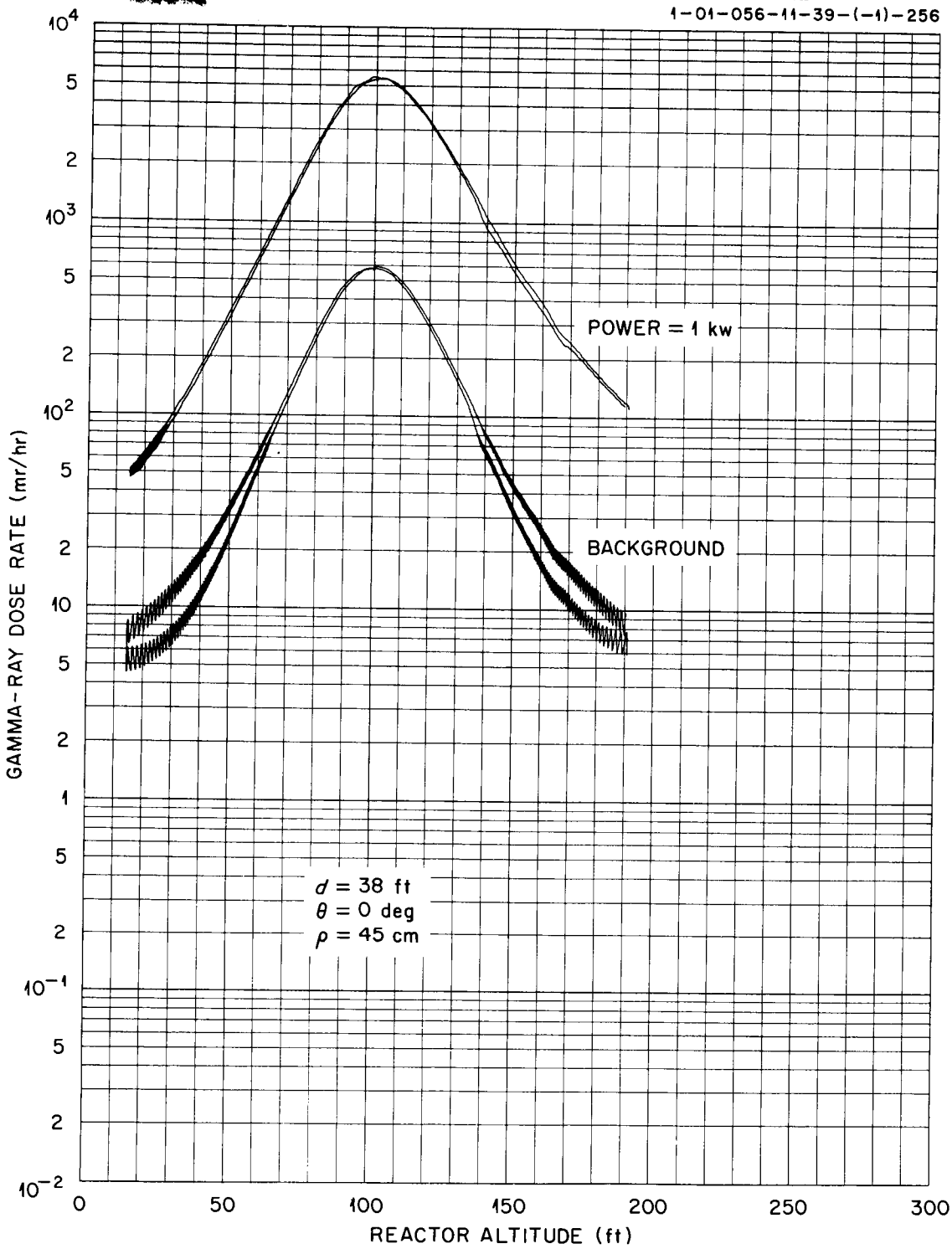

Fig. 15.10. Gamma-Ray Dose Rate at Outside Rear of GE Crew Compartment as a Function of Reactor Altitude for $\rho = 45$ cm.

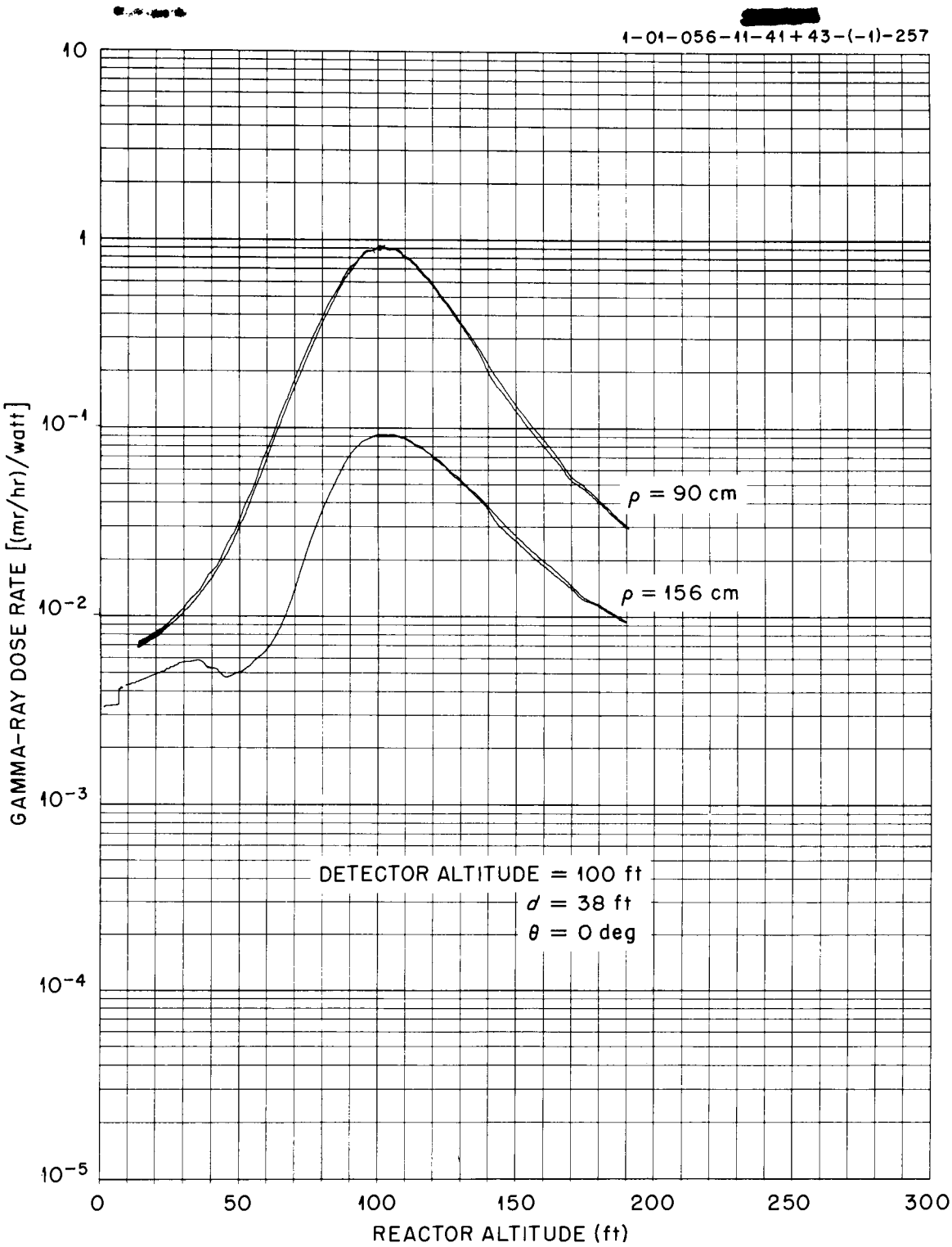

Fig. 15.11. Gamma-Ray Dose Rate at Outside Rear of GE Crew Compartment as a Function of Reactor Altitude for ρ = 90 and 156 cm.

[redacted] [redacted]

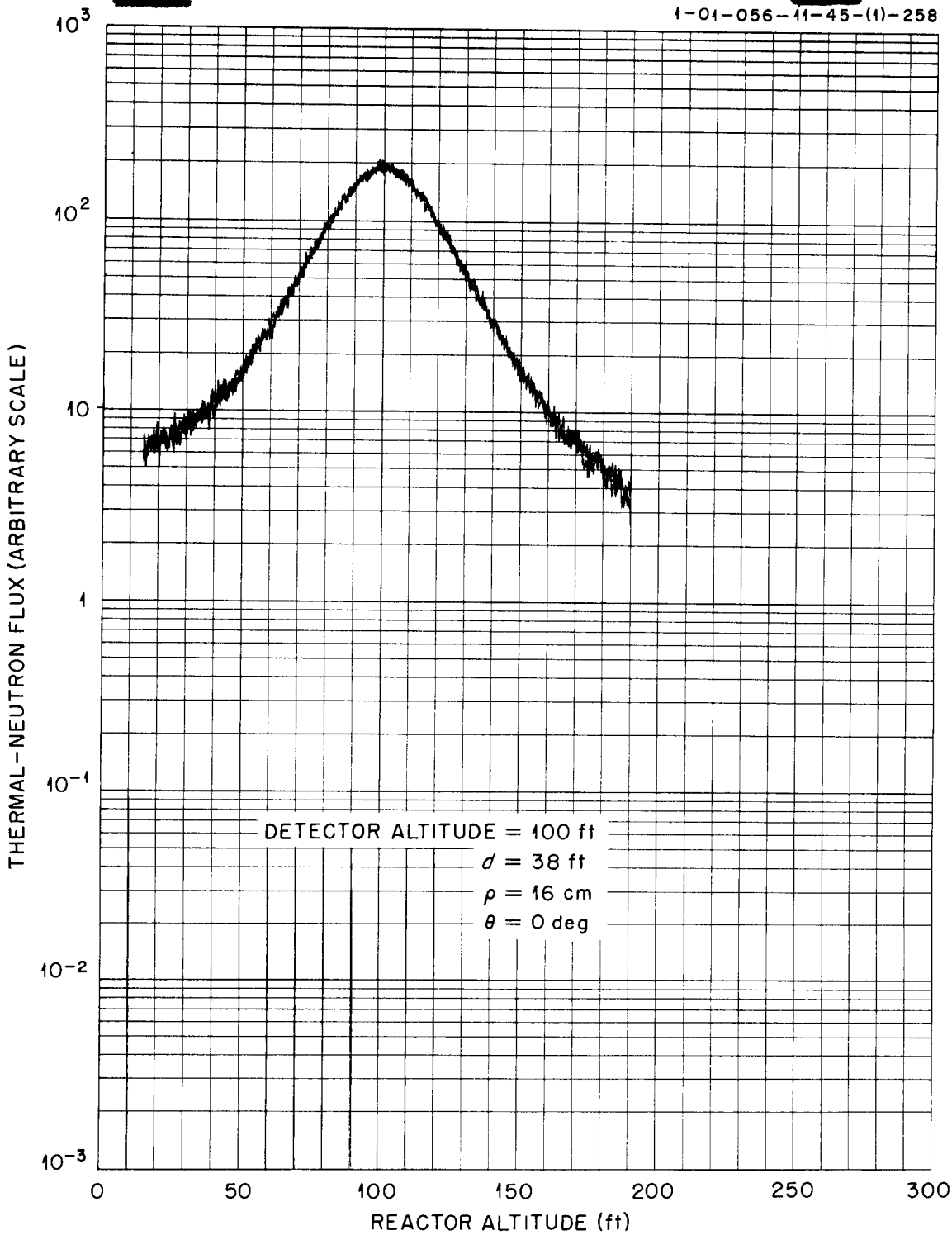

Fig. 15.12. Thermal-Neutron Flux at Outside Rear of GE Crew Compartment as a Function of Reactor Altitude for ρ = 16 cm.

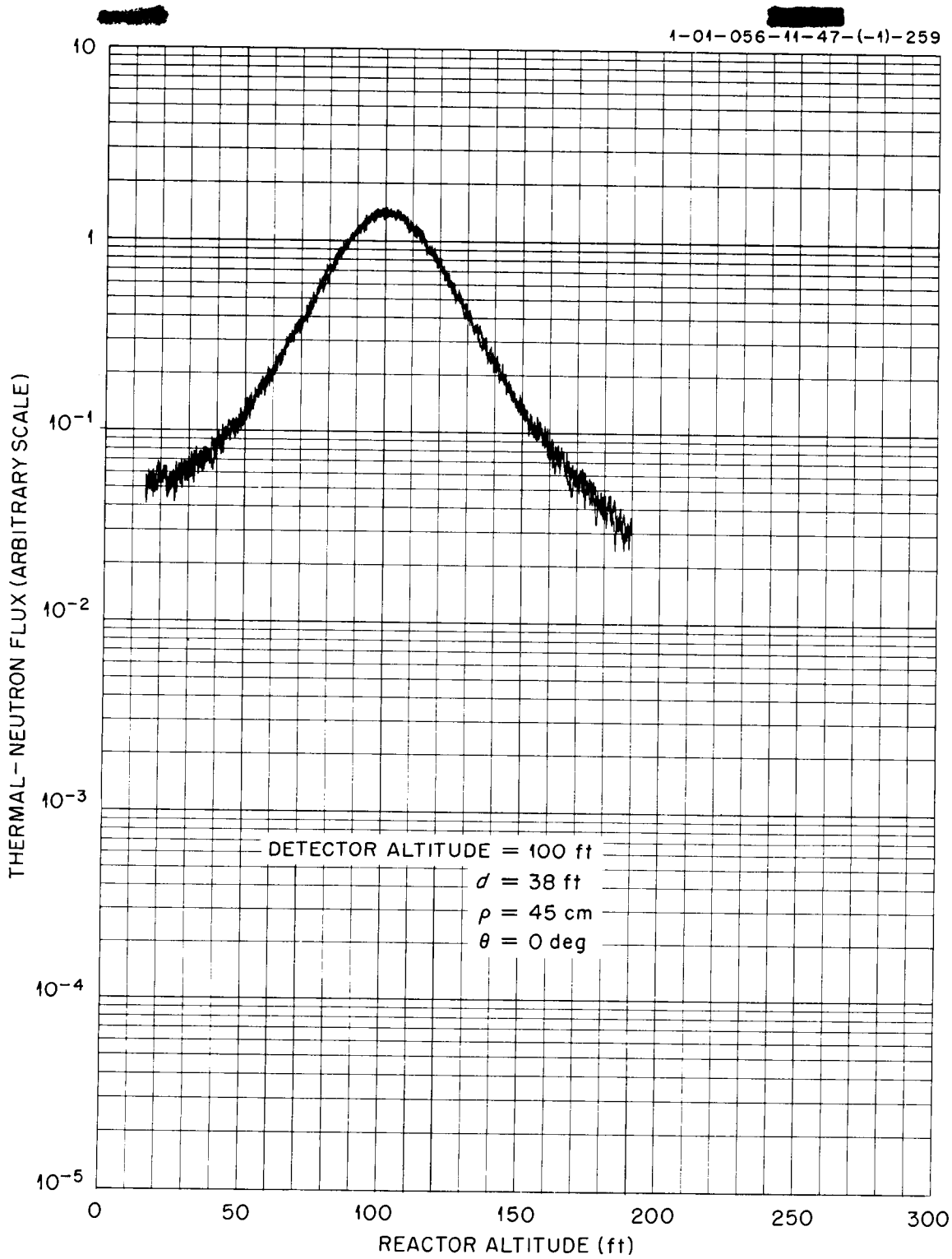

Fig. 15.13. Thermal-Neutron Flux at Outside Rear of GE Crew Compartment as a Function of Reactor Altitude for ρ = 45 cm.

[redacted] [redacted]

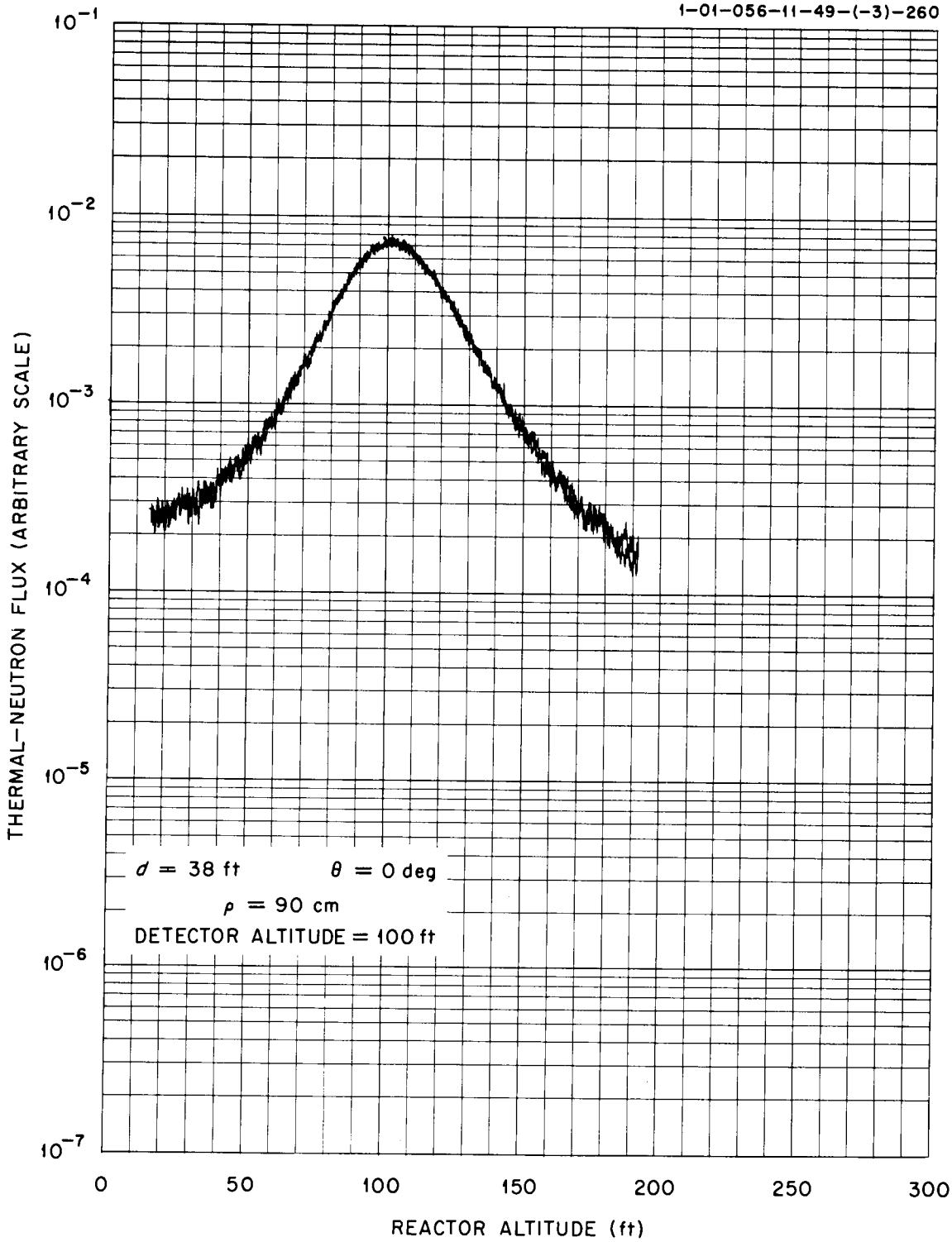

Fig. 15.14. Thermal-Neutron Flux at Outside Rear of GE Crew Compartment as a Function of Reactor Altitude for ρ = 90 cm.

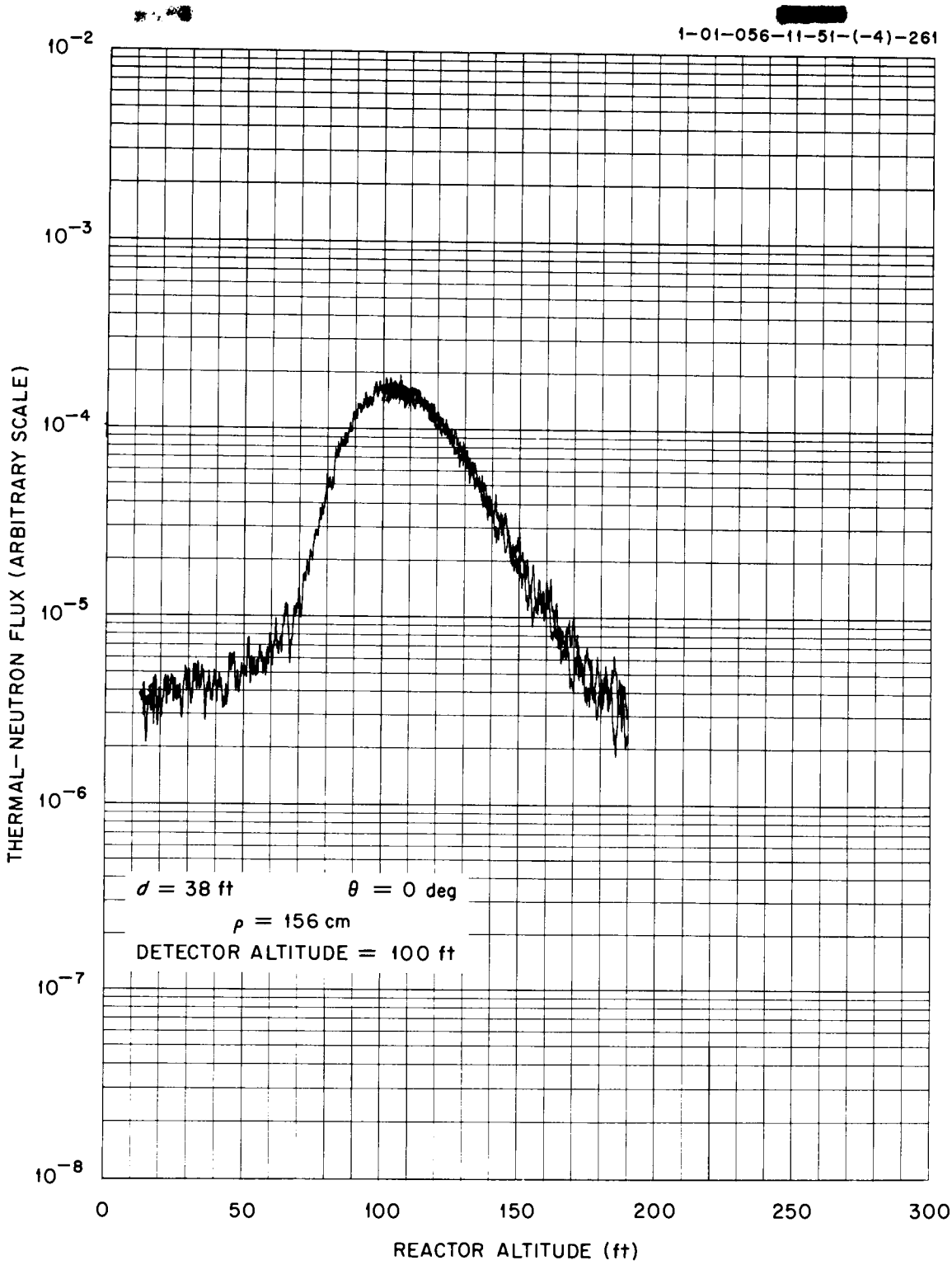

Fig. 15.15. Thermal-Neutron Flux at Outside Rear of GE Crew Compartment as a Function of Reactor Altitude for ρ = 156 cm.

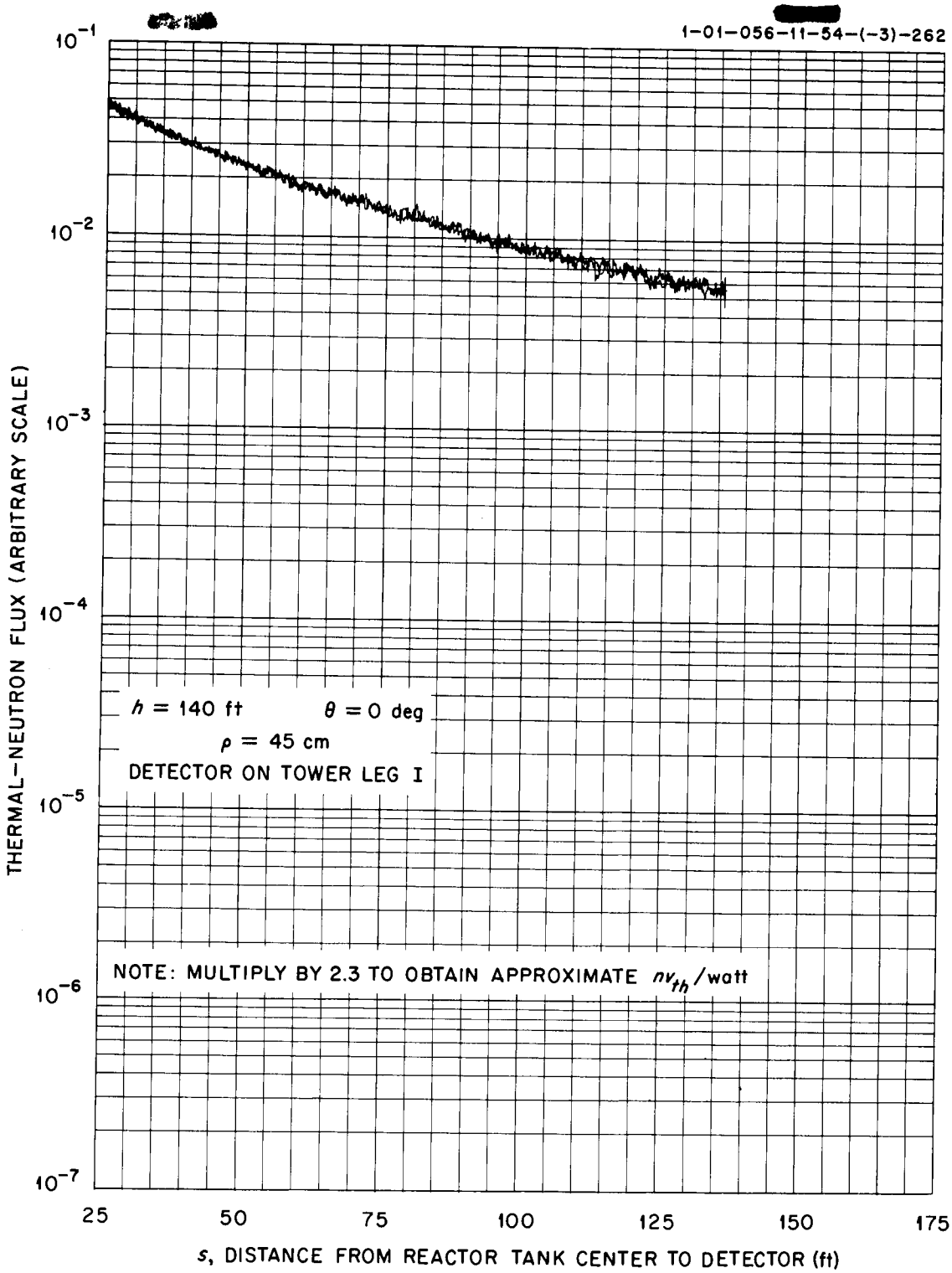

Fig. 15.16. Thermal-Neutron Flux in Air as a Function of Reactor-Detector Separation Distance for θ = 0 deg.

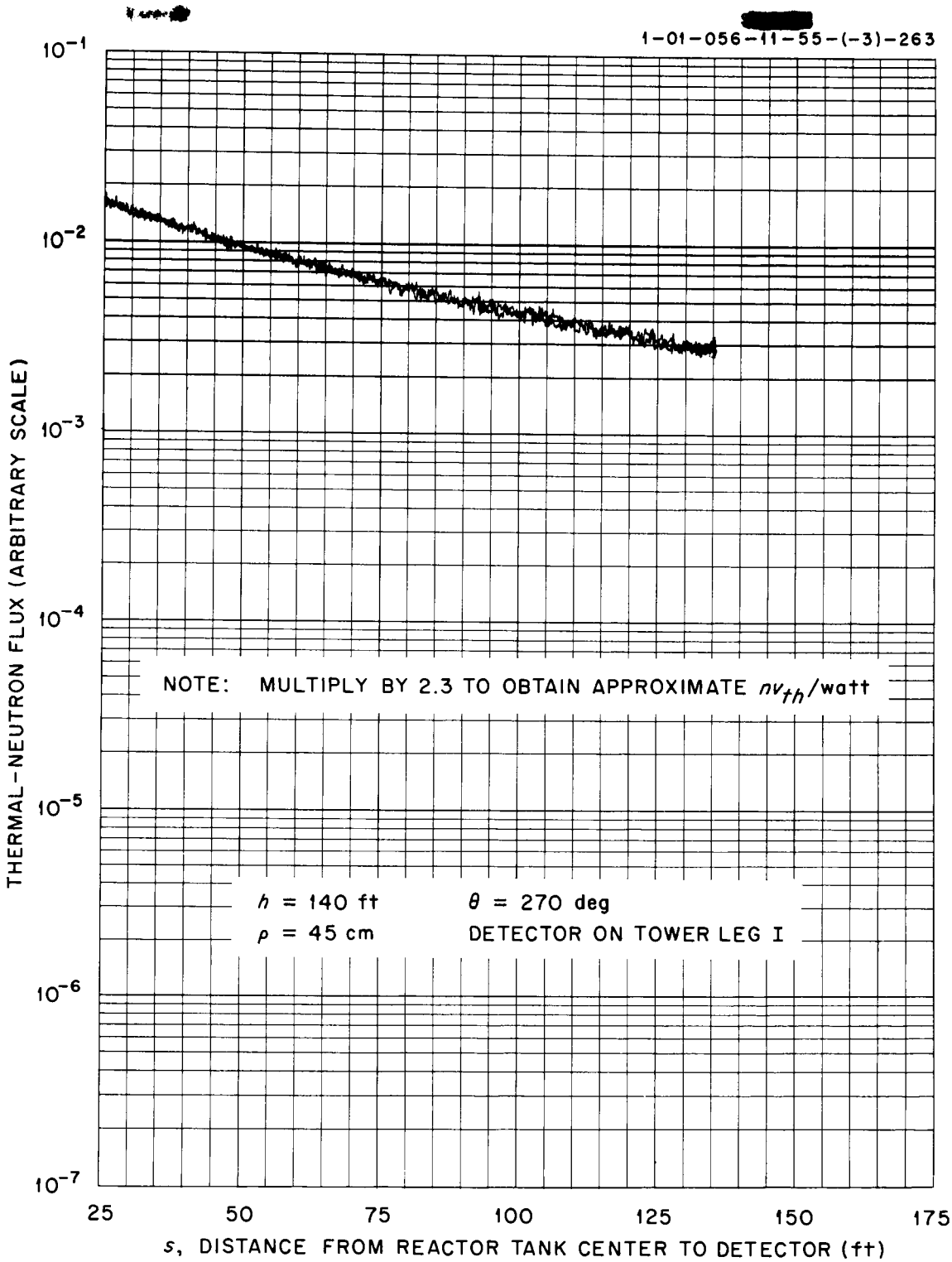

Fig. 15.17. Thermal-Neutron Flux in Air as a Function of Reactor-Detector Separation Distance for θ = 270 deg.

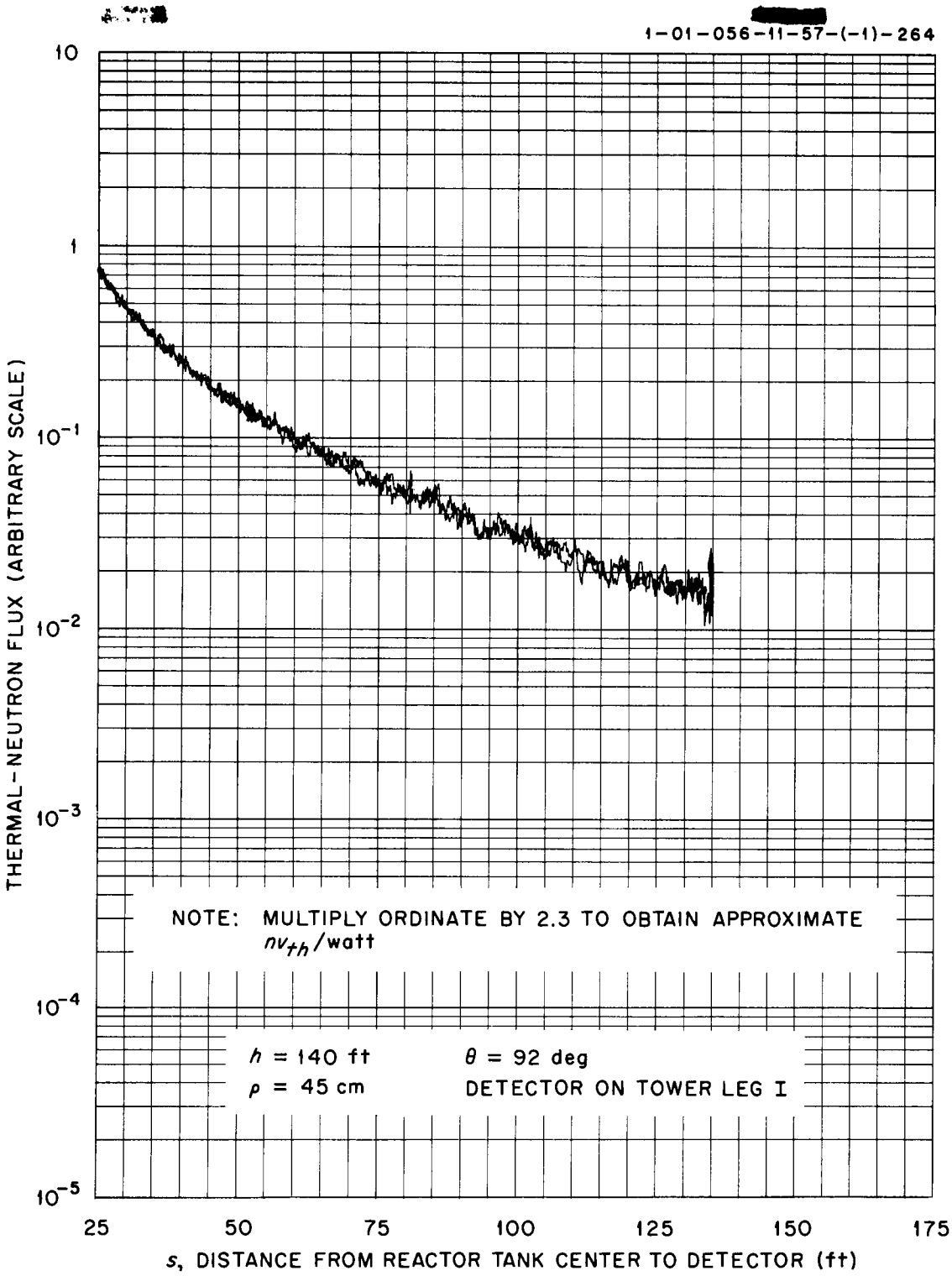

Fig. 15.18. Thermal-Neutron Flux in Air as a Function of Reactor-Detector Separation Distance for θ = 92 deg.

[redacted] [redacted]

1-01-056-11-59-(-1)-265

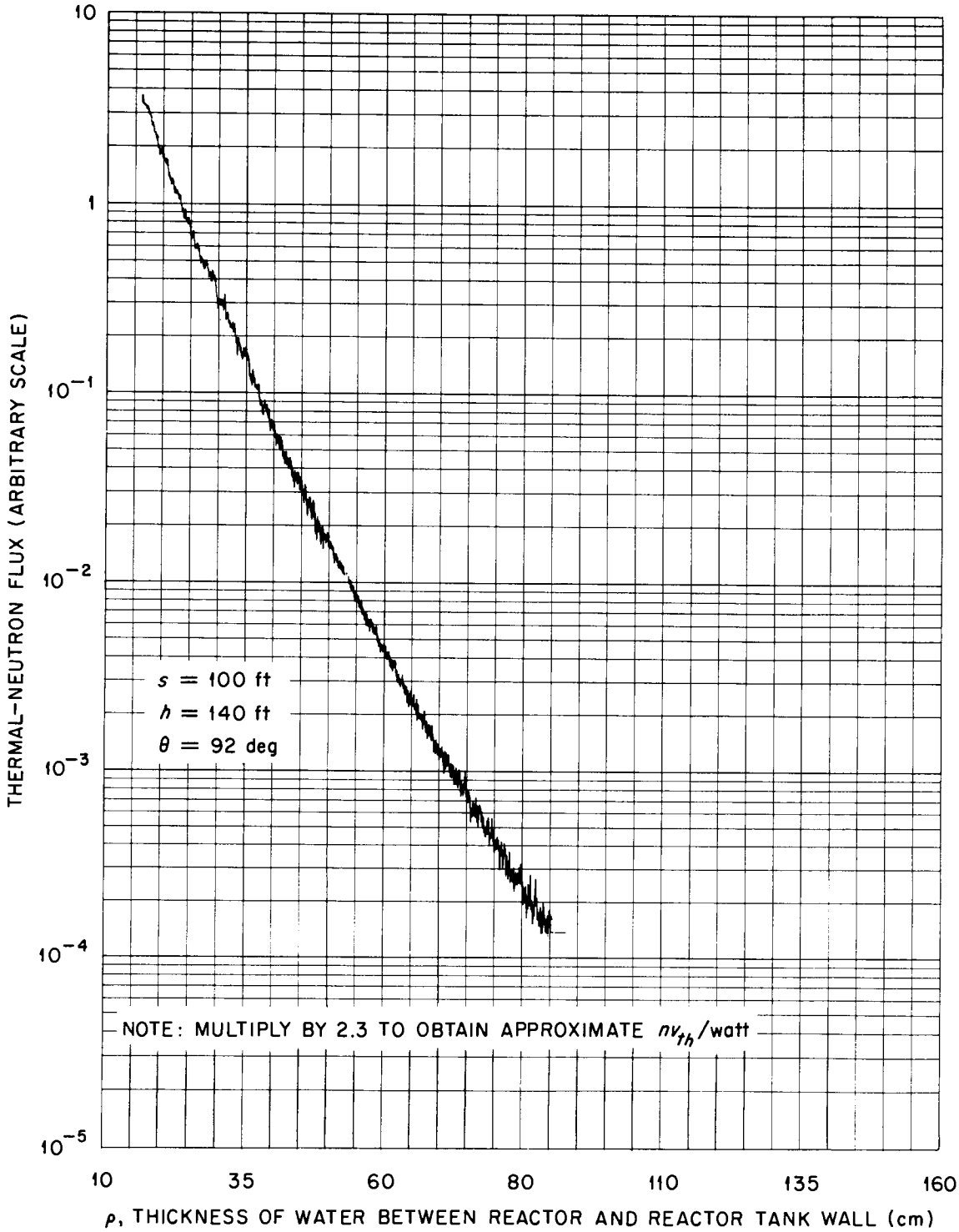

Fig. 15.19. Thermal-Neutron Flux in Air as a Function of Reactor Shield Thickness (ρ) for θ = 92 deg.

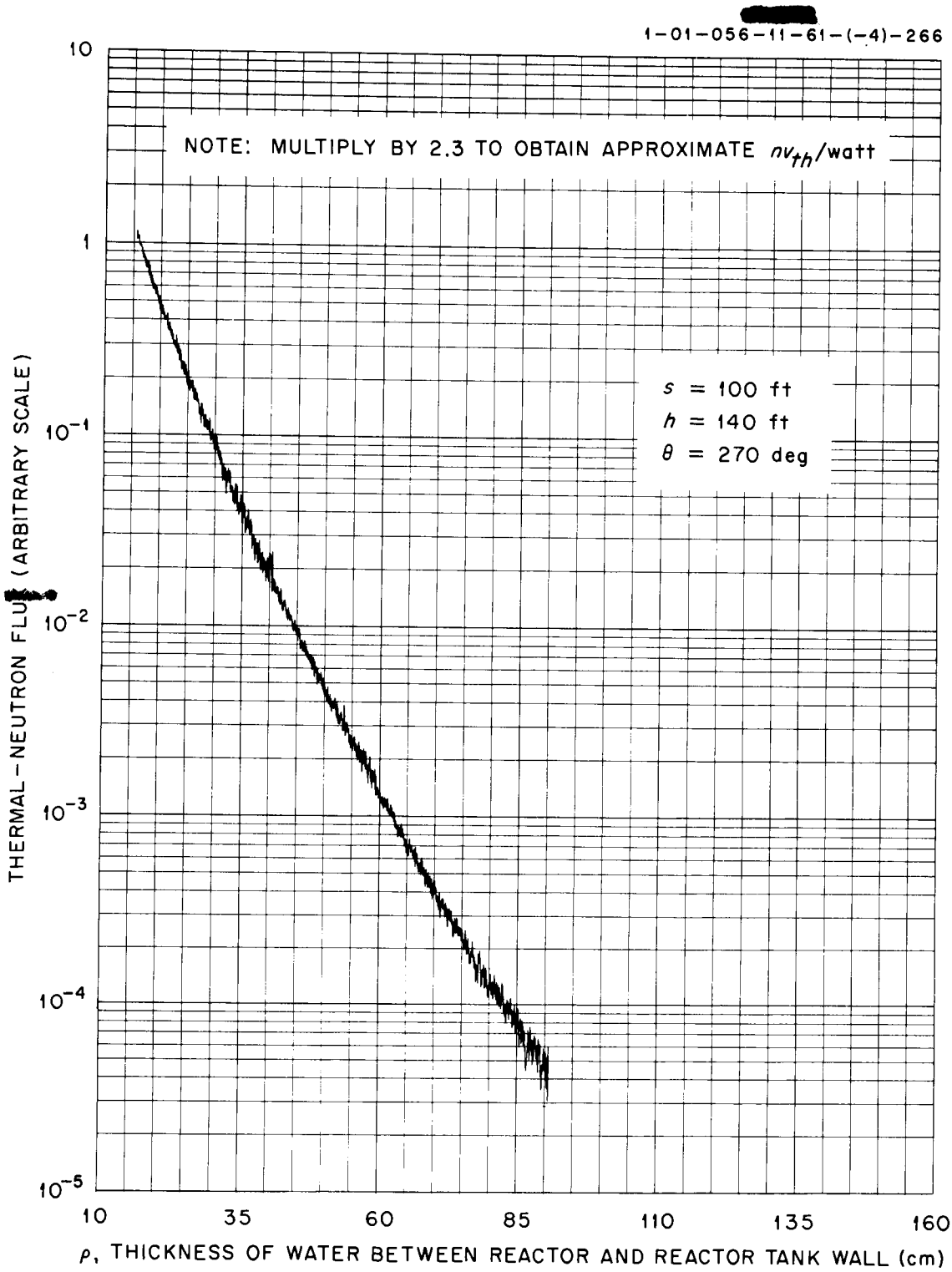

Fig. 15.20. Thermal-Neutron Flux in Air as a Function of Reactor Shield Thickness (ρ) for θ = 270 deg.

The thermal-neutron flux at the tower leg was also measured as a function of the reactor shield thickness for two values of θ, 92 and 270 deg, and a constant reactor-detector separation distance of 100 ft (Figs. 15.19 and 15.20).

The scale used in reporting these neutron data is the approximate thermal-neutron flux per watt. Cadmium difference measurements would result in a small correction.

MEASUREMENTS WITH THE REACTOR OFF THE MAJOR AXIS OF THE CREW COMPARTMENT

F. N. Watson

As a first step in a preliminary investigation of the effects of placing a reactor in the wing of an airplane, two configurations, as shown in Fig. 15.21, were investigated at the TSF. A BF_3 thermal-neutron detector and a scintillation-crystal gamma-ray detector were placed near the center of the GE crew compartment. The responses of these detectors were then recorded as a function of reactor position (ρ variable) for both configurations (Figs. 15.22 and 15.23).

ANGULAR DISTRIBUTION OF RADIATION IN THE GE R1 CREW-COMPARTMENT MOCKUP

G. J. Rausa

The angular distribution of the radiation leaving the inside surface of the crew compartment must be known for accurate shield design. At present there is no instrument at the TSF which will measure this

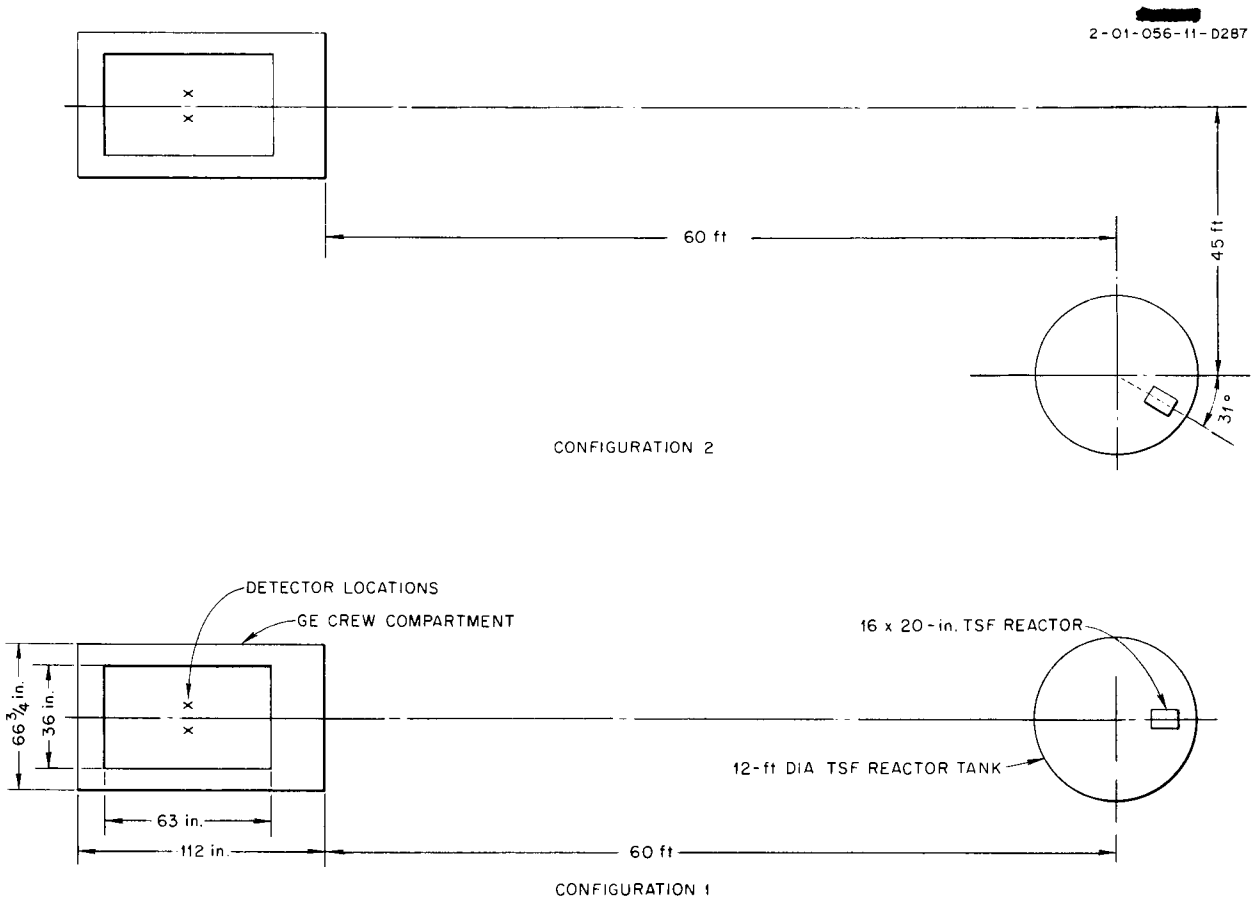

Fig. 15.21. TSF Configurations Used in Preliminary Investigation of Wing Pod Reactor Application.

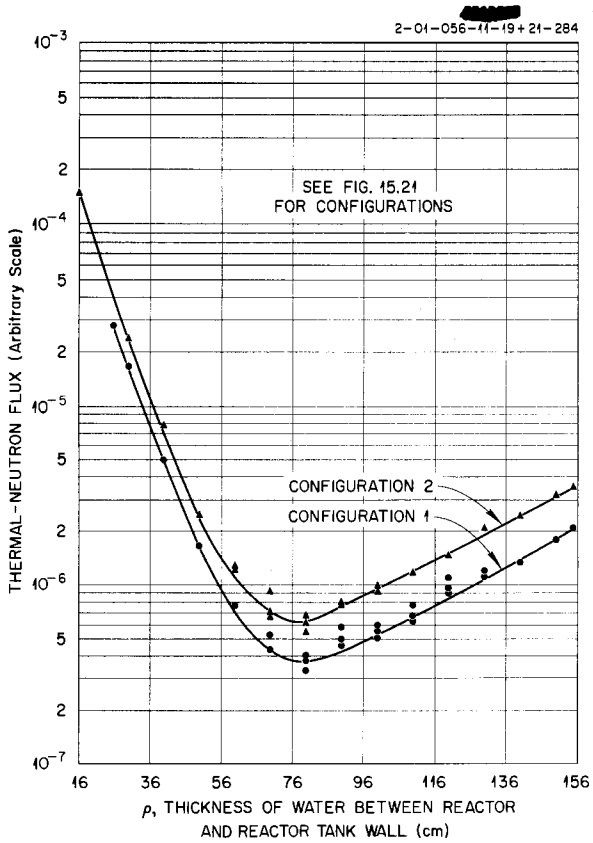

Fig. 15.22. Thermal-Neutron Flux Values for Two Reactor–Crew-Compartment Configurations.

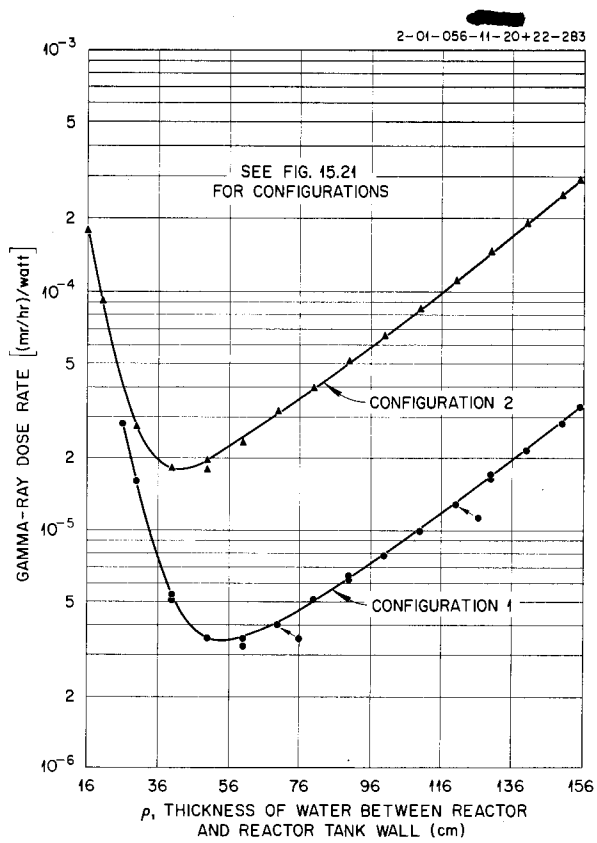

Fig. 15.23. Gamma-Ray Dose Rates for Two Reactor–Crew-Compartment Configurations.

quantity, but the effect of the angular distribution of radiation in a specific shield mockup can be calculated, and the results can then be applied to the design of other shields with the same geometry. The effect of the angular distribution of radiation within the cylindrical GE R1 crew compartment has been determined.

The dose rate at the point of interest within the crew compartment was considered, as previously,[4] to consist of three components: (1) the direct dose rate arriving through the rear of the shield, D_d^r; (2) the air-scattered dose rate arriving through the rear of the shield, D_s^r; and (3) the air-scattered dose rate arriving through the sides of the shield, D_s^s. These components can be assumed to be the result of sources on the inside surface of the crew compartment from which the radiation emerges with some angular distribution.

Method of Determining Factor for Radiation from the Rear

The dose rate at any point in the crew compartment from radiation leaving the rear (or front) inside surface of the shield (i.e., the dose rate from D_d^r and D_s^r) decreases as the distance between the surface and the point increases because of the geometry of the source and the angular distribution of the radi-

[4] M. F. Valerino and F. L. Keller, *ANP Quar. Prog. Rep. Sept. 10, 1955*, ORNL-1947, p 205.

ation. This can be seen from Fig. 15.24 and the following equations:

(1) $$D_p = \frac{m+1}{2\pi} \int_A D_0 \cos^m \theta \, d\Omega \, dA \ ,$$

where

p = distance from inside rear of the crew compartment to the point of interest,

D_p = dose rate at the point of interest within the shield from radiation entering the rear of the shield,

D_0 = dose rate at the inside rear surface ($p = 0$) from radiation entering the rear of the shield,

$(m + 1)/2\pi$ = normalizing factor to convert to dose rate per solid angle,

$\cos^m \theta$ = angular distribution of radiation about the normal to the surface,

θ = angle between the conical-shell beam of radiation and the reactor–crew-compartment axis,

$d\Omega = 1/r^2$,

r = distance from element of area to p

$= \sqrt{p^2 + \rho^2}$,

$dA = 2\pi\rho \, d\rho = 2\pi r \, dr$,

ρ = radius to element of area in the plane of the source;

or

(2) $$D_p = \frac{(m+1)}{2\pi} D_0 \int_p^{(p^2+\rho_{max}^2)^{1/2}} \frac{p^m}{r^{m+1}} \, dr = \int_p^{p(1+K_0^2)^{1/2}} \frac{p^m}{r^{m+1}} \, dr \ ,$$

where

ρ_{max} = radius of the crew compartment,

$K_0 = \dfrac{\rho_{max}}{p}$.

[redacted]

2-01-056-0-A315

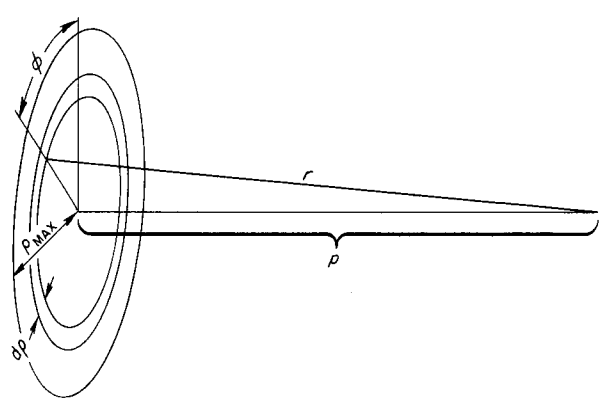

Fig. 15.24. Geometry for Angular Distribution Calculation.

The factor f^r for the radiation leaving the rear inside surface of the shield is then

$$f^r = \frac{D_p}{D_0} = 1 - \frac{1}{(1 + K_0^2)^{m/2}} \quad . \tag{3}$$

When this factor is determined for the direct radiation only, it is designated as f_d^r. When it applies only to scattered radiation, it is designated as f_s^r. It can be seen that this ratio is always less than 1 for $m > 0$, or, in effect, for defocusing.

In the case of the GE crew compartment, $\rho_{max} = 45.76$ cm. With the point of interest at the center of the crew compartment (i.e., at $p = 81$ cm), the value of K_0 is 0.565. Theoretical values of the factor f^r at this point in the shield for various assumed values of the angular distribution m are listed below:

m	f^r
0	0.07
1	0.13
2	0.24
3	0.34
4	0.42
5	0.50
6	0.56

Method of Determining Factor for Radiation from the Side

The dose rate at the point of interest in the crew compartment from radiation leaving the side of the crew compartment is the result of radiation scattered in air (D_s^s). Faulkner[5] has shown the "focusing" effect of this radiation from an infinite cylinder. His method was used in this calculation to determine values of the factor f_s^s for the center of the finite GE R1 crew compartment (length-to-diameter ratio of 1.78) for various assumed values of the angular distribution. As for Faulkner's infinite cylinder, it was assumed that the source strength per unit area and the angular distribution at the side were constant over the length of the cylinder. The results are compared with corresponding values for an infinite cylinder in Table 15.1.

It can be seen from Table 15.1 that, for practical purposes, any crew-compartment shield with a length-to-diameter ratio of 1.78 can be regarded as an infinite cylinder for $m \geqq 3$ when considering the dose rate at the center of the crew compartment. The distribution of dose rate along the axis of the crew compartment would be different, however. In the infinite crew shield, the dose rate along the axis would be constant, whereas in the finite crew compartment it would drop off at the ends of the crew compartment according to the distribution assumed.

The theoretical factor f_s^s (normalized to a maximum of 1) for the GE crew compartment is plotted as a function of distance from the rear for assumed angular distributions of $m = 1$, 3, and 5 in Fig. 15.25. (The abcissa in the figure is labeled y, a coordinate in the TSF geometrical system which coincides with p in this paper; $y = 0$ at the outside rear of the crew compartment.) As was expected, the factor

[5] J. E. Faulkner, *Focusing of Radiation in a Cylindrical Crew Compartment*, ORNL CF-54-8-100 (Aug. 18, 1954).

TABLE 15.1. THEORETICAL VALUES OF f_s^s IN CENTER OF GE R1 CREW COMPARTMENT FOR VARIOUS ASSUMED VALUES OF m COMPARED WITH THE VALUES FOR AN INFINITE CYLINDER

m	f_s^s	
	GE R1 Crew Compartment	Infinite Cylinder
0	2.1	3.14
1	3.5	4.0
2	4.4	
3	5.2	5.3
4	5.8	
5	6.4	6.5
6	6.8	

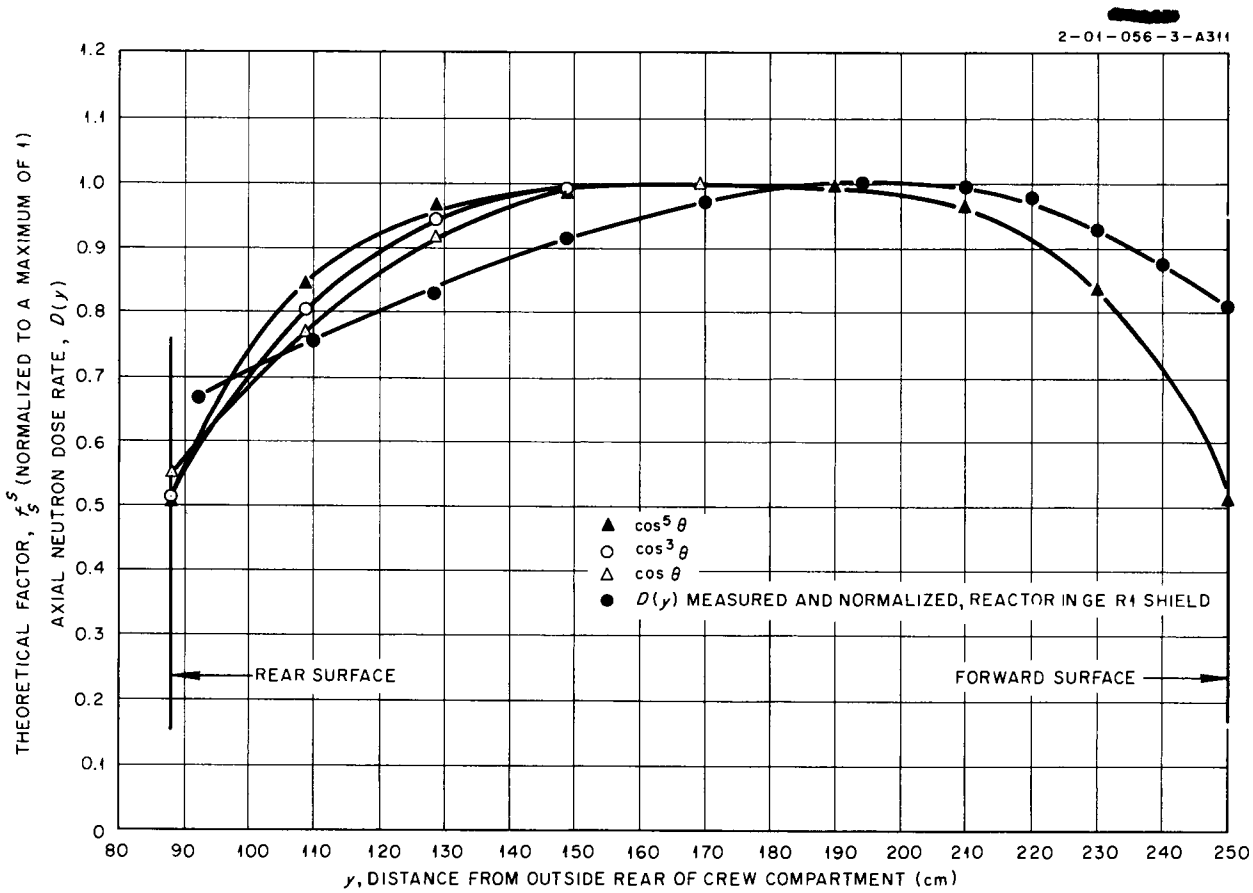

Fig. 15.25. Axial Neutron Dose Rate and Theoretical f_s^s Factors for GE R1 Crew Compartment (Normalized to a Maximum of 1).

for the $\cos^5 \theta$ distribution rises most rapidly as the distance from the end of the crew compartment is increased. In the calculations it was assumed that the radiation was distributed symmetrically about the normal to any inside surface of the shield. As mentioned above, it was also assumed that the source strength per unit area and the angular distribution at the side surface did not vary as functions of y. This assumption may be somewhat in error, since the curve of the measured dose rate in Fig. 15.25 peaks forward of the center of the crew compartment. This may be the result of the angular distribution being symmetrical about an axis which is not normal to the surface but, rather, is skewed in the forward direction.

Calculation of Angular Distribution for GE Crew Compartment

Since the neutron dose rate measured at the center of the GE crew compartment consists of three components, D^r_d, D^r_s, and D^s_s, it is necessary to know the magnitude of each component in order to determine the angular distribution of radiation from the inside surface. The dose contributions from a conical shell (Fig. 15.26) for direct, rear-scattered, and side-scattered radiations are calculated by using the following formulas developed from the results of the differential shielding experiments:[4,6]

[6] M. F. Valerino, *ANP Quar. Prog. Rep. June 10, 1955*, ORNL-1896, p 206.

[redacted]
2-01-056-3-A312

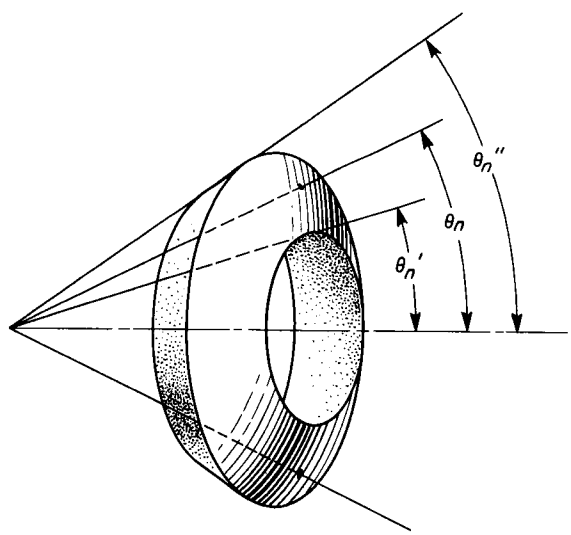

Fig. 15.26. Conical Shell Geometry.

$$D^r_{d,n} = \Delta \cos^{m+1} \theta_n f^r_d D_d(a,\ell) e^{-\int_0^{T_n} dt/\lambda_d} e^{-\int_0^{T_r} dy/\lambda^r_d}, \qquad \text{for } \theta = 0 \text{ to } \pi/2$$

(4)

$$D^r_{d,n} \cong 0, \qquad \text{for } \theta = \pi/2 \text{ to } \pi$$

(5)
$$D^r_{s,n} = \Delta \cos \theta_n f^r_s D_d(a,\ell) e^{-\int_0^{T_n} dt/\lambda_d} e^{-\int_0^{T_r} dy/\lambda^r_s} \ell^2 P^r_s(\theta_n),$$

(6)
$$D^s_{s,n} = \Delta \cos \theta_n f^s_s D_d(a,\ell) e^{-\int_0^{T_n} dt/\lambda_d} e^{-\int_0^{T_s} dx/\lambda^s_s} \ell^2 P^s_s(\theta_n),$$

where

$D^r_{d,n}$ = dose rate at the point of interest in the crew compartment from the direct radiation arriving through the rear of the crew shield and originating in the nth conical shell of the reactor shield,

$D^r_{s,n}$, $D^s_{s,n}$ = dose rate at the point of interest in the crew compartment from scattered radiation arriving through the rear and side, respectively, of the crew shield and originating in the nth conical shell of the reactor shield,

$D_d(a,\ell) e^{-\int_0^{T_n} dt/\lambda_d}$ = direct dose rate at a distance ℓ from the reactor of radius a,

T_n = reactor shield thickness,

dt = increment of T_n,

T_r, T_s = thickness of shielding on the rear and side of the crew compartment, respectively,

dy, dx = increments of T_r and T_s, respectively,

λ_d = direct-beam relaxation length in reactor shield,

λ^r_d = direct-beam relaxation length in the rear of the crew compartment,

λ^r_s, λ^s_s = relaxation length of scattered radiation in the rear and side of the crew compartment, respectively,

$\cos \theta_n$ = $\cos \theta'_n - \cos \theta''_n$,

$P^r_s(\theta_n)$, $P^s_s(\theta_n)$ = probability of radiation from the nth shell scattering into the crew compartment rear and side, respectively.

Since for $\theta > 90$ deg the value of D^r_d is approximately zero, the dose rate measurements at the center of the crew compartment for $\theta > 90$ deg can be considered to consist only of scattered radiation. The ratio of dose rate scattered through the rear to that scattered through the sides of the crew compartment can then be evaluated as follows:

$$\frac{D^r_{s,n}}{D^s_{s,n}} = \frac{f^r_s P^r_s(\theta_n) e^{-\int_0^{T_r} dy/\lambda^r_s}}{f^s_s P^s_s(\theta_n) e^{-\int_0^{T_s} dx/\lambda^s_s}}.$$

The functions

$$P_s^r(\theta_n)\, e^{-\int_0^{T_r} dy/\lambda_s^r}$$

and

$$P_s^s(\theta_n)\, e^{-\int_0^{T_s} dx/\lambda_s^r}$$

were generated from the differential shielding experiments by using the dimensions of the GE crew compartment. Since $f_s^r \leqq 1$ and the theoretical f_s^s lies between 3.5 and 6.4 for cos θ and $\cos^5 \theta$ inside surface distributions, respectively, a limit for $D_{s,n}^r/D_{s,n}^s$ can be set. An estimate of this ratio for $0 \leqq \theta \leqq 180$ deg indicates that the dose rate scattered into the rear of the crew compartment is, at a maximum, about 5% of the side-scattered contribution. Therefore the dose rate measured in the center of the crew compartment for $\theta > 90$ deg is considered to consist entirely of side-scattered radiation.

From Eq. 6 the relation $D_{s,n}^s/f_s^s$ can be found for the GE crew compartment. Since the experimental value obtained at the center of a crew compartment is for a line beam, it can be multiplied by 2π to obtain the corresponding value of $D_{s,n}^s$ for the conical shell beam. The factor f_s^s can then be estimated by the ratio of $D_{s,n}^s/f_s^s$ for $\theta > 90$ deg, as shown in Table 15.2. The average value of f_s^s corresponds most closely to the theoretical angular distribution of $\cos^5 \theta$ (Table 15.1).

If the assumption is made that f_s^s is constant for all θ, an estimate of the scattered dose rate at the center of the crew compartment from a line beam can be made. The data are compared with the measured dose rate in the center of the crew compartment in Fig. 15.27.

If there had been less variation in the data, an estimate could have been made of f_d^r. In order to do this it would be necessary to assume that the shape of the y traverse in the crew compartment for $\theta > 90$ deg was that due to scattered radiation and that this shape did not change for $0 < \theta < 90$ deg. By using the information previously obtained on the scattered dose rate in the center of the crew compartment for $\theta = 0$ deg, shown in Fig. 15.27, the difference in the y traverse for total radiation and that for side-scattered radiation yields the direct dose, as well as the rear-scattered radiation, as a function of y (Fig. 15.28). An estimate of D_s^r/D_d^r indicated that D_s^r was negligible, even if it was assumed that

TABLE 15.2. VALUES OF f_s^s FOR THE GE CREW COMPARTMENT AS A FUNCTION OF θ

θ (deg)	D_s^s/f_s^s	$D_T^* \cong D_{s,n}^s$ (mrep/hr)	f_s^s
90	3.6×10^{-7}	2.01×10^{-6}	5.6
105	2.3×10^{-7}	1.44×10^{-6}	6.28
120	1.5×10^{-7}	1.00×10^{-6}	6.70
180	5.6×10^{-7}	345×10^{-6}	6.15
		Av	6.19

*Total measured dose rate.

$f^r_s = 10\, f^r_d$. Therefore, for $\theta = 0$ deg the ratio of the dose rate at the center of the crew compartment to that at the rear inside surface is the value of f^r_d; that is,

$$\frac{D^r_d \text{ for } y = 169 \text{ cm}}{D^r_d \text{ for } y = 89.9 \text{ cm}} = f^r_d \ .$$

From Fig. 15.28 it can be seen that the estimated value of f^r_d is about 0.25, which corresponds to a surface distribution of $\cos^2 \theta$.

The factor f^s_r for rear-scattered radiation can be no greater than 1. Since estimates indicate that D^r_s is negligible compared with D^s_s and D^r_s, very little error will be introduced by assuming $f^s_r = 0.5$.

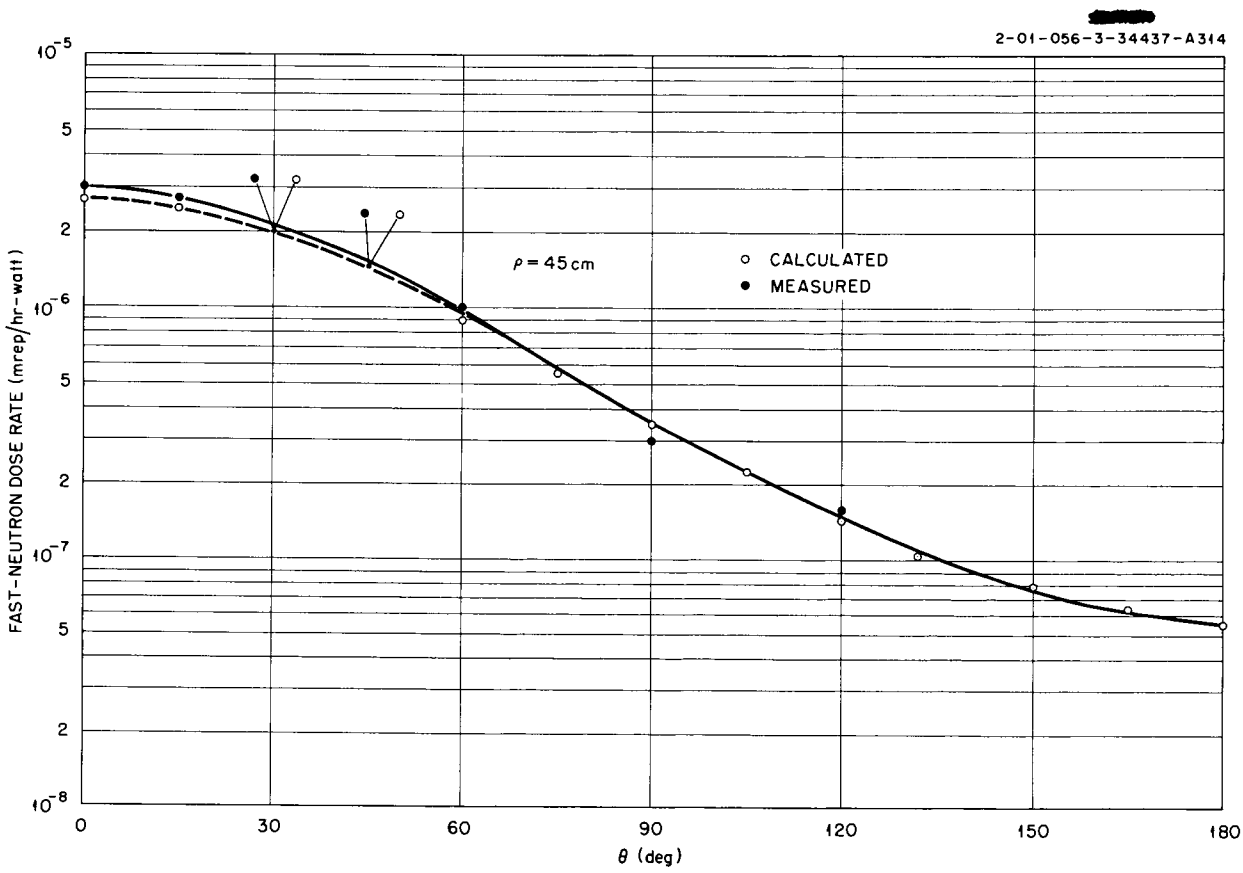

Fig. 15.27. Comparison of Total Measured Dose Rate at Center of GE R1 Crew Compartment with Calculated Scattered Dose Rate from a Line Beam.

[redacted]

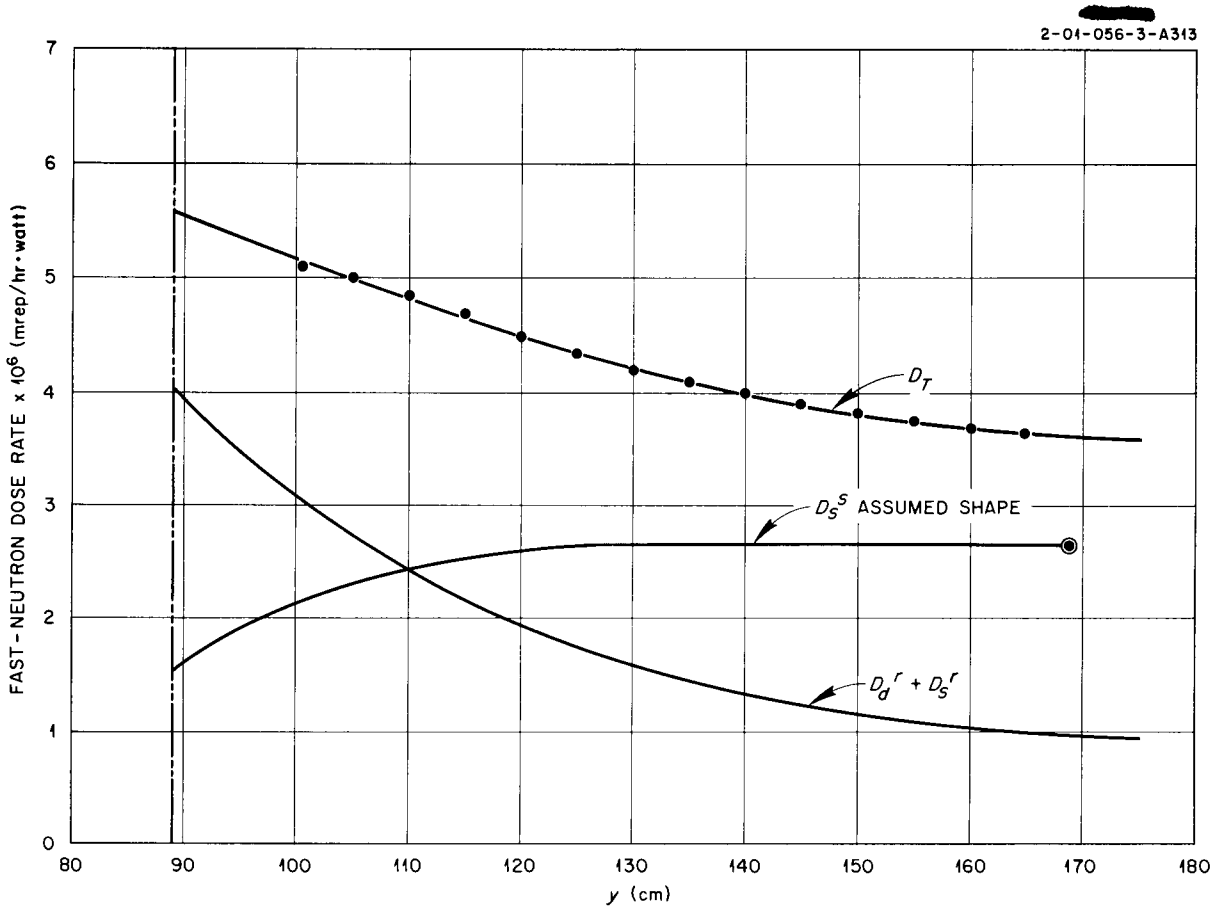

Fig. 15.28. Fast-Neutron Dose Rate in GE R1 Crew Compartment for $\theta = 0$ deg, $\rho = 45$ cm.

16. AIRCRAFT SHIELD DESIGN

C. E. Clifford
F. L. Keller
S. K. Penny D. K. Trubey
L. B. Holland
Applied Nuclear Physics Division
C. A. Goetz H. C. Woodsum
Pratt & Whitney Aircraft
R. M. Davis, Glenn L. Martin Co.

PROCEDURE FOR THE OPTIMIZATION OF A DIVIDED GAMMA-RAY SHIELD FOR CIRCULATING-FUEL REACTORS

H. C. Woodsum

Total divided-shield weights for various circulating-fuel reactors were calculated previously.[1,2] The optimization procedure described here is the procedure that was used to determine the thicknesses of the gamma-ray shielding. The method is useful primarily for choosing the proper distribution of gamma-ray shielding material between the reactor and the crew compartment, but it also gives a distribution at these locations which probably is not far from that for a minimum weight.

In the procedure it is assumed that the neutron shield for a specified neutron dose rate in the crew compartment has already been optimized[3] and that it will not be greatly affected by the optimization of the gamma-ray shield, and vice versa. The method of Lagrangian multipliers is then used to derive expressions for the optimum thickness of the lead at both the reactor and the crew compartment.

Expression for Total Crew-Compartment Gamma-Ray Dose Rate

As a first step, the total dose rate (D_T) specified for the crew compartment is expressed in terms of the direct dose rate (D_o) at the outside rear surface of the crew compartment (no shadow shield) and as a function of the shadow-shield and crew-compartment lead thicknesses:

$$D_T = D_o e^{-\mu_R t_R} \left(e^{-\mu_{pl} t_{pl}} e^{-\mu_r t_r} + P e^{-\mu_s t_s} \right) , \tag{1}$$

where

t_R = maximum thickness of the tapered lead shadow shield at the reactor,

t_r, t_s = thickness of lead at the rear and sides of the crew compartment, respectively,

μ_R, μ_r, μ_s = linear attenuation coefficients for gamma rays in the lead of the shadow shield and in the lead at rear and sides of the crew compartment, respectively,

$e^{-\mu_{pl} t_{pl}}$ = attenuation in the plastic on the rear of the crew compartment,

P = probability of dose scattering into the sides of the crew compartment for a given side plastic thickness and no lead (derivation given below).

Thus the first term inside the parentheses times $D_o e^{-\mu_R t_R}$ is the direct dose rate through the rear of the crew compartment, and the second term times $D_o e^{-\mu_R t_R}$ is the scattered dose rate through the sides

[1] J. B. Dee *et al.*, *ANP Quar. Prog. Rep. Sept. 10, 1955*, ORNL-1947, p 190.

[2] J. B. Dee *et al.*, *ANP Quar. Prog. Rep. Dec. 10, 1955*, ORNL-2012, Part IV, p 29.

[3] M. F. Valerino and F. L. Keller, *ANP Quar. Prog. Rep. Sept. 10, 1955*, ORNL-1947, p 205.

of the crew compartment. The scattered dose rate through the rear is neglected, since it is a negligible fraction of the total gamma-ray dose rate for lead thicknesses, on the rear, of 1 in. or greater.

Expression for Total Gamma-Ray Shield Weight

The total weight (W_T) of the lead gamma-ray shield at the reactor and the crew compartment also can be written in terms of the lead thicknesses:

$$W_T = \rho_{Pb}\left(A_r t_r + A_s t_s + k t_R e^{a t_R}\right) , \tag{2}$$

where

ρ_{Pb} = density of the lead (g/cm^3),

A_r, A_s = "effective" areas (cm^2) of the rear and sides of the crew compartment, respectively,

ke^{at_R} = "effective" area (cm^2) of the shadow shield (see below).

Determination of Shadow-Shield Volume

Since the shadow shield was shaped, that is, the thickness decreased with increasing angle, it was necessary to obtain its volume by integration:

$$V_R = 2\pi \int_0^{\theta_0} \int_{r_0}^{r_0 + t_R(\theta)} r^2(\theta)\, dr \sin\theta\, d\theta ,$$

where

θ = angle from the reactor–crew-compartment axis (θ_0 is at the edge of shadow shield, as shown in Fig. 16.1),

r_0 = inside radius of the shadow shield,

r = outside radius of the shadow shield

$= r_0 + t_R(\theta)$.

[redacted]
2-01-059-37

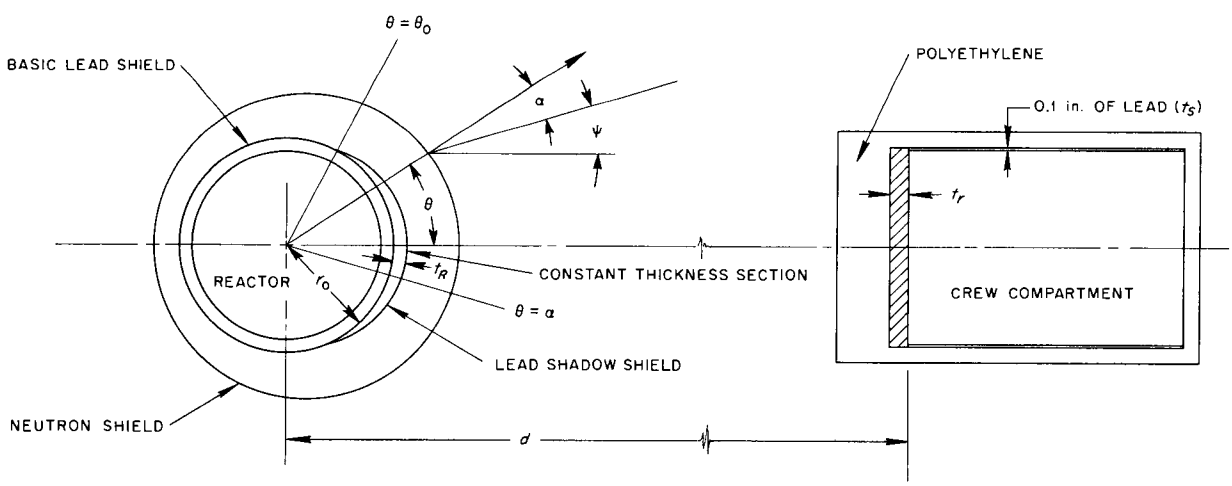

Fig. 16.1. Geometry for Optimization of a Divided Gamma-Ray Shield.

When the volume was plotted as a function of t_R, it was found that the expression could be fitted by a constant times the thickness t_R times an exponential, that is, by $kt_R e^{at_R}$, the term used in Eq. 2.

Method of Tapering the Shadow Shield

Because of the uncertainties in the dose as a result of the assumption of radial emission of gamma rays, a "disadvantage" angle α of 15 deg is arbitrarily assumed for the shadow shield (Fig. 16.1) to allow for the angular spread. In other words the gamma rays for $\theta > 15$ deg are presumed to come out more nearly in the forward direction by 15 deg, and for $\theta < 15$ deg they are assumed to come out exactly in the forward direction. As explained previously,[1,2] this assumption results in a constant thickness for the portion of the shadow shield between $\theta = 0$ and 15 deg, after which it tapers to zero thickness at some angle θ_0. It was also assumed in integrating the NDA $f(\psi)$ curves[4] to obtain the total dose scattering probability that the gamma rays emerging from the reactor shield at 15 deg from the reactor–crew-compartment axis would have the same probability of scattering as those emerging at 0 deg from a radial source. [The NDA $f(\psi)$ curves are plots of the dose-scattering probability in dose per unit source strength at angle ψ (θ in this paper) at a distance of 50 ft (1524 cm).] Since the NDA curves fall nearly exponentially at a rate of about one factor of e for every 12.5 deg, it was decided, as a matter of convenience, to taper the shadow shield from $\theta = 15$ deg to θ_0 by removing one relaxation length (2.1 cm) of lead every 12.5 deg. This gives a constant $f(\theta)$ between $\theta = 0$ to $\theta - 15$ deg (or $\theta = 0$ to $\theta - 0.262$ radian), which permits an analytical solution for the optimum gamma-ray shield thickness. The cutoff angle θ_0 is therefore determined by the maximum thickness of the shadow shield, since

$$\theta_0 = 15 + 12.5 \frac{t_R}{2.1} \text{ deg} ,$$

or

$$\theta_0 = 0.262 + 0.218 \frac{t_R}{2.1} \text{ radians} .$$

Determination of the Scattering Probability

Since the dose from the shield is allowed to increase by a factor of e for every 12.5 deg, the integrated dose from $\theta = 0$ to $\theta_0 - 0.262$ radian is

$$\int_0^{\theta_0 - 0.262} f(\theta)\, d\theta = f(\theta = 0)(\theta_0 - 0.262) ,$$

and, if the exponential fall-off is assumed for $f(\theta) > \theta_0$,

$$\int_{\theta_0}^{\pi} f(\theta)\, d\theta = f(\theta_0 = 0) \int_{\theta_0 - 0.262}^{\pi} e^{-[\theta - (\theta_0 - 0.262)]/0.218}\, d\theta .$$

When the terms have been combined, it is seen that

$$\int_0^{\pi} f(\theta)\, d\theta = f(\theta = 0) \left\{(\theta - 0.262) + (0.218) \left[1 - e^{-(\pi - \theta_0 + 0.262)/0.218}\right]\right\} .$$

---

[4] E. P. Blizard and H. Goldstein (eds.), *Report of the 1953 Summer Shielding Session*, ORNL-1575, p 167–235 (June 14, 1954).

Since θ_0 is usually small (~45 deg), the last term within the braces can be neglected, and, since

$$\theta_0 - 0.262 = \frac{t_R}{2.1} 0.218 ,$$

the integral, expressed as a function of t_R, is

$$\int_0^{\pi} f(\theta)\, d\theta = f(\theta = 0)\,(0.104 t_R + 0.218) .$$

In practice, since 0.218 is only about 20% of the total quantity in parentheses for $t_R > 10$ cm, the constant 0.104 can be replaced by a function $C(t_R)$, which will vary slowly with t_R and which will include the constant 0.218. For example, if $t_R = 15$ cm,

$$\int_0^{\pi} f(\theta)\, d\theta \approx f(\theta = 0)\, 0.119 t_R ,$$

and, if $t_R = 10$ cm,

$$\int_0^{\pi} f(\theta)\, d\theta \approx f(\theta = 0)\, 0.126 t_R .$$

A single iteration should be sufficient to fix t_R, approximately, and hence $C(t_R)$. The total dose scattering probability as a function of t_R can then be expressed as

$$P = K t_R ;$$

where

$K = 4\pi d^2 c(E)\,(1524/d)\,[f(\psi = 0)\, C(t_R)]$,

d = reactor–crew–compartment separation distance (cm)

= 1952 cm (64 ft) in this case,

$c(E)$ = flux-to-dose conversion factor

= 5.5×10^5 (Mev/sec·cm^2) (r/hr),

$f(\psi)$ = scattered dose probability at 50 ft at angle ψ (or for this paper at angle θ) [(r/hr)/(Mev/sec)].

Application of Lagrange Multipliers to Obtain Lead Thicknesses

Since the total gamma-ray dose rate and total gamma-ray shield weight have been expressed as rather simple functions of t_R, t_s, and t_r, it is now possible to apply Lagrange multipliers to derive equations for these thicknesses under the condition that there be a minimum weight. According to the system of Lagrange multipliers,

$$\frac{\partial W_T}{\partial t_R} + \frac{1}{L}\frac{\partial D_T}{\partial t_R} = \frac{\partial W_T}{\partial t_r} + \frac{1}{L}\frac{\partial D_T}{\partial t_r} = \frac{\partial W_T}{\partial t_s} + \frac{1}{L}\frac{\partial D_T}{\partial t_s} = 0 , \tag{3}$$

which must be satisfied for a value of the total dose rate (D_T) specified for the particular shield design. The solution to this set of equations, in terms of the thicknesses and constants involved, is as follows:

$$e^{at_R}(1 + at_R) + \frac{A_s}{kt_R\mu_s} = \frac{\mu_R}{k}\left(\frac{A_r}{\mu_r} + \frac{A_s}{\mu_s}\right) , \tag{4}$$

(5) $$L = -\frac{D_T \mu_R}{\rho_{Pb}} \left[\frac{1}{k e^{a t_R} (1 + a t_R) + A_s / \mu_s t_R} \right]$$

(6) $$t_s = \frac{\ln \left[\mu_s D_o K t_R / (-L)\, \rho_{Pb} A_s \right] - \mu_R t_R}{\mu_s} ,$$

(7) $$t_r = \frac{\ln \left[\mu_r D_o e^{-\mu_{pl} t_{pl}} / (-L)\, \rho_{Pb} A_r \right] - \mu_R t_R}{\mu_r} .$$

Although t_R could not be solved for explicitly because of the exponential and linear terms on the left side of the equation, Eq. 4 does contain only t_R. Therefore a unique solution may easily be obtained by plotting separately the left and right sides of Eq. 4 as functions of t_R. The point at which these two plots intersect is the optimum thickness t_R. Once t_R is determined, it can be substituted into Eq. 5 to obtain the Lagrange multiplier, L. Then, with L and t_R known, t_s and t_r are found by substitution into Eqs. 6 and 7.

Determination of Gamma-Ray Linear Attenuation Coefficients

The values of μ_R, μ_r, and μ_s are determined in the following manner. The direct gamma-ray dose rate 64 ft from the reactor is plotted as a function of lead thickness around the reactor by using the procedure outlined previously.[1] For the first 5 in. of lead the plot is approximately a straight line on semilogarithmic paper, but for greater thicknesses the increasing importance of secondary gamma rays causes the plot to deviate upward from the exponential.

For shadow-shield thicknesses t_R of less than 5 in., the exponential portion of the direct dose plot can be used as the attenuation coefficient μ_R. If the procedure indicates that a greater shadow-shield thickness is required, however, it will be necessary to choose from the plot the μ_R that corresponds to that particular thickness. Since the solution for t_R in Eq. 4 may differ from the chosen t_R, some iteration may be necessary for agreement of t_R and μ_R.

It is assumed that this deviation of the direct dose plot from the exponential does not affect μ_r and μ_s, since the neutron shielding between the shadow shield and the lead on the crew compartment is so large that the neutron captures in the crew compartment rear and sides do not contribute significantly to the total dose. Therefore, the coefficient of attenuation in the first few inches of lead on the reactor is chosen for μ_r. The value of μ_s is obtained by plotting $f(\psi = 0)$ for a given plastic side thickness and three different lead side thicknesses and choosing the coefficient of attenuation for a 0.1-in. lead thickness from the plot. (In practice, t_s usually comes out zero or negative, which indicates that the lead should be placed elsewhere. Owing to uncertainties in the dose from captures outside the reactor, however, a minimum thickness of 0.1 in. of lead is always placed on the sides.)

For the case where t_s is a constant, Eqs. 4 and 5 become

(8) $$e^{a t_R} (1 + a t_R) = \frac{A_r}{k \mu_r} \left[\mu_R + \frac{K D_o e^{-\mu_R t_R} e^{-\mu_s t_s} (\mu_R t_R - 1)}{D_T - D_o K t_R e^{-\mu_R t_R} e^{-\mu_s t_s}} \right]$$

and

$$L = -\frac{\mu_r}{\rho_{Pb} A_r}\left(D_T - D_o K t_R e^{-\mu_R t_R} e^{-\mu_s t_s}\right) \quad . \tag{9}$$

Equation 7 remains unchanged. Negative values for t_R, t_r, and t_s are, of course, not considered solutions of the above equations.

Sample Calculation

The optimization procedure presented above was used for a sample calculation for optimizing a divided gamma-ray shield for a circulating-fuel reactor having the following parameters:

Reflector thickness, in.	12.0
Island radius, in.	4.0
Core power density, kw/cm^3	4.125
Heat exchanger thickness, in.	6.5
Basic lead thickness (in rear), in.	3.0
Outside radius of basic lead, cm	83.0
Gamma-ray dose rate at 50 ft, r/hr	1000
Total design dose rate in crew compartment, rem/hr	1

The constants used in the calculation were:

$$\mu_R = 0.450 \text{ cm}^{-1} , \qquad \text{for } t_R = 7.5 \text{ cm} ,$$

$$= 0.372 \text{ cm}^{-1} , \qquad \text{for } t_R = 10 \text{ cm} ,$$

$$\mu_r = 0.477 \text{ cm}^{-1} ,$$

$$\mu_s = 1.44 \text{ cm}^{-1} ,$$

$$e^{-\mu_{pl} t_{pl}} = e^{-43/31} = 0.25 ,$$

$$K = 4\pi\,(1952)^2 \left(\frac{1524}{1952}\right) [f(\psi = 0)_{t=14 \text{ cm}}\ 0.135] ,$$

$$= 2.78 \times 10^{12} f(\psi = 0) ,$$

$$= 3.75 \times 10^{-3} ,$$

$$r_0 = 83 \text{ cm} ,$$

$$k = 1.04 r_0^2 ,$$

$$= 7.165 \times 10^3 \text{ cm}^2 ,$$

$$A_r = 35 \times (30.48)^2 ,$$

$$= 3.253 \times 10^4 \text{ cm}^2 ,$$

$$A_s = (225 + 35)\,(30.48)^2 ,$$

$$= 2.418 \times 10^5 \text{ cm}^2 ,$$

$$\rho_{Pb} = 11.3 \text{ g/cm}^3 ,$$

$$a = 0.0927 \text{ cm}^{-1} ,$$

$$D_o = 1000 \text{ r/hr at 50 ft},$$
$$= 610 \text{ r/hr at 64 ft},$$
$$D_T = 0.75 \text{ r/hr}.$$

Substitution of the constants in Eq. 4 gives

$$e^{0.0927t_R}(1 + 0.0927t_R) + \left[\frac{2.418 \times 10^5}{(7.165 \times 10^3)\,1.44}\right]\frac{1}{t_R} = \frac{0.450}{7.165 \times 10^3}\left(\frac{3.253 \times 10^4}{0.477} + \frac{2.418 \times 10^5}{1.44}\right),$$

the simplest form of which is

$$e^{0.0927t_R}(1 + 0.0927t_R) + \frac{23.43}{t_R} = 14.83 .$$

By substitution of various values of t_R in the left side of the equation, it is found that $t_R = 17.5$ cm most nearly satisfies the equation, as follows:

t_R (cm)	Value of Left Side
5	7.00
10	7.17
15	11.16
20	19.4

For $t_R = 17.5$ cm, however, μ_R is obviously too large. A better estimate would be $\mu_R = 0.350$ cm^{-1}. The constant then becomes

$$\frac{0.350}{0.450} \times 14.83 = 11.53$$

and $t_R = 16.0$ cm. Thus, by successive iteration t_R is found to be about 16.5 cm. Substitution of this value of t_R and other constants listed above into Eq. 5 gives

$$L = -\frac{(0.75)(0.35)}{11.3}\left\{\frac{1}{7.165 \times 10^3\, e^{(0.0927)(16.5)}\,[1 + (0.0927)(16.5)] + (2.418 \times 10^5)/(1.44 \times 16.5)}\right\}$$
$$= -2.48 \times 10^{-7} .$$

The value of t_s is then obtained from Eq. 6:

$$t_s = \frac{\ln\left[\dfrac{(1.44)(610)(3.75 \times 10^{-3})(16.5)}{(2.48 \times 10^{-7})(11.3)(2.418 \times 10^5)}\right] - (0.350)(16.5)}{1.44}$$
$$= \frac{4.39 - 5.77}{1.44} = -0.96 \text{ cm} .$$

This solution is unsatisfactory, since it gives a negative thickness on the sides of the crew compartment. Therefore, 0.1 in. of lead is placed on the sides of the crew compartment and t_R is re-evaluated by using Eq. 8. This is done to reduce the buildup of gamma rays in the plastic on the side shield.

If t_s = 0.1 in. (0.254 cm) is used, along with the constants obtained above, Eq. 8 becomes

$$e^{0.0927t_R}(1 + 0.0927t_R) = \frac{3.253 \times 10^4}{(7.165 \times 10^3)(0.477)}\left[\mu_R + \frac{(3.75 \times 10^{-3})(0.610 \times 10^3)\, e^{-(1.44)(0.254)}\, e^{-\mu_R t_R}(\mu_R t_R - 1)}{0.75 - (0.610 \times 10^3)(3.75 \times 10^{-3})\, e^{-(1.44)(0.254)}\, t_R\, e^{-\mu_R t_R}}\right].$$

The right side can then be simplified to give

$$e^{0.0927t_R}(1 + 0.0927t_R) = 9.53\left[\mu_R + \frac{1.585\, e^{-\mu_R t_R}(\mu_R t_R - 1)}{0.75 - 1.585 t_R\, e^{-\mu_R t_R}}\right].$$

Values for the left and right sides of this equation for various values of t_R are listed below:

t_R (cm)	Left Side	Right Side
6	2.71	14.1
8	3.66	8.13
10	4.86	5.49

Therefore the optimum thickness for t_R in this case is found to be 10.25 (4.03 in.). It may then be found from Eq. 9 that

$$L = -\frac{0.477}{(11.3)(3.253 \times 10^4)}\left[0.75 - (610)(3.75 \times 10^{-3})(10.25)\, e^{-(0.372)(10.25)}\, e^{-(1.44)(0.254)}\right]$$

$$= -5.08 \times 10^{-7}$$

and from Eq. 7 that

$$t_r = \frac{\ln\left[\dfrac{(0.477)(610)(0.25)}{(5.08 \times 10^{-7})(11.3)(3.253 \times 10^4)}\right] - (10.25)(0.372)}{0.477}$$

$$= 4.52 \text{ cm} = 1.78 \text{ in.}$$

Thus the results of the optimization give the following values:

$$t_s = 0.1 \text{ in.}$$
$$t_R = 4.03 \text{ in.}$$
$$t_r = 1.78 \text{ in.}$$

As a check, the total gamma-ray dose rate in the crew compartment is

$$D_T = 610\, e^{-(10.25)(0.372)}(0.25)\, e^{-(0.477)(4.52)} = (3.75 \times 10^{-3})(10.25)\, e^{-(1.44)(0.254)}$$

$$= 0.732 \text{ r/hr}.$$

SHIELD DESIGN STUDY FOR A CIRCULATING-FUEL REACTOR WITH A FUEL-TO-AIR RADIATOR

L. B. Holland S. K. Penny
D. K. Trubey

A limiting feature of a nuclear-powered aircraft system is the weight of the reactor and crew-compartment shield, and therefore some knowledge of the weight is desirable before a complete investigation of a new system is attempted. A circulating-fuel reactor with a direct fuel-to-air radiator was considered previously,[5] but it was rejected on the assumption that the shield weight would be excessive. There is a possibility, however, that an increase in efficiency and reliability might offset the increase in shield weight; therefore a shielding study was carried out to determine the feasibility of a more thorough investigation of this type of system.

Two fuel-to-air radiator configurations were considered in the study. The first configuration was the standard circulating-fuel wrap-around radiator, and the second was a tandem arrangement of reactor and radiator. Weights for each arrangement were determined for total radiation-damage limitations of 1,000 and 100,000 rep/hr at 50 ft.

Reactor, Radiator, and Crew Compartment

The reactor was assumed to be a 28.5-in.-dia circulating-fuel reflector-moderated reactor with an 8-in.-thick beryllium reflector. It was felt that this reflector thickness was sufficient, since there was no NaK activation problem and criticality would not be greatly affected. The reactor dimensions and weights are shown in Tables 16.1 and 16.2, respectively.

The radiator volume was estimated[6] to be 200 ft^3, which included an allowance for the ducting that was not designed into the shield. Design data for a sodium-to-air radiator, previously reported,[7] were used to determine the volume fractions of the various materials in the radiator, although the selection of materials differed somewhat. In the present study it was considered that Inconel tubes were needed to contain the fused-fluoride-salt fuel and that copper fins with stainless steel cladding would give the best performance. The following radiator specifications were assumed:

Fins	
Number per inch	15
Thickness, in.	0.010
Inconel tubes	
Outside diameter, in.	0.1875
Wall thickness, in.	0.015
Center-to-center spacing (square array), in.	0.667
Density,[6] lb/ft^3	98

[5] A. P. Fraas and A. W. Savolainen, *ORNL Aircraft Nuclear Power Plant Designs*, ORNL-1721, p 72 (Nov. 10, 1954).

[6] A. P. Fraas, private communication.

[7] W. S. Farmer *et al.*, *Preliminary Design and Performance Studies of Sodium-to-Air Radiators*, ORNL-1509, p 62 (Aug. 3, 1953).

TABLE 16.1. DIMENSIONS OF A CIRCULATING-FUEL REACTOR WITH A FUEL-TO-AIR RADIATOR

Reactor Region	Thickness (in.)	Inner Radius (in.)	
		Tandem Arrangement	Wrap-Around Arrangement
Beryllium island	4.0		
Outer sodium annulus of island	0.187	4.0	4.0
Core cladding (Inconel) of island	0.125	4.187	4.187
Core	9.938	4.312	4.312
Inner cladding (Inconel) of beryllium reflector	0.156	14.250	14.250
Inner sodium annulus of reflector	0.187	14.406	14.406
Reflector	8.000	14.593	14.593
Outer sodium passage of reflector	0.066	22.593	22.593
Outer cladding (Inconel) of reflector	0.010	22.659	22.659
Inner cladding (Inconel X) on B_4C-Cu sintered layer	0.01	22.669	22.669
B_4C-Cu sintered layer	0.20	22.679	22.679
Outer cladding (Inconel X) on sintered layer	0.01	22.879	22.879
Sodium passage	0.066	22.889	22.889
Air radiator (including Inconel shells on inside and outside)	23.195		22.955
Thermal shield	1.000	22.955	46.150
Sodium cooling layer	0.035	23.95	47.150
Pressure shell	1.00	23.990	47.185
Insulation	0.250	24.990	48.185
Outer cladding (Inconel X) on insulation	0.032	25.240	48.435

TABLE 16.2. WEIGHTS OF A CIRCULATING-FUEL REACTOR* WITH A FUEL-TO-AIR RADIATOR

Reactor Region	Weight (lb)	
	Tandem Arrangement	Wrap-Around Arrangement
Inconel	5,870	18,780
Sodium	70	70
Radiator	20,150	20,150
Beryllium	2,430	2,430
Insulation	220	220
Miscellaneous**	2,780	2,780
Total	31,520	44,430

*Spherical shells assumed for calculation.

**Decking, ducting, and expansion tanks, 500 lb; two sodium pumps and drives, 1100 lb; two fuel pumps and drives, 1080 lb; control rod and island support, 100 lb.

The volume fractions of the materials in the section of the radiator that contained the fins were:

Stainless steel	0.0750
Copper	0.0750
Inconel	0.0287
Fuel	0.0333
Air	0.7880
	1.000

At 3 Mev these volume fractions yield a value of 0.0567 cm^{-1} for the gamma-ray total absorption coefficient.

In order to estimate the gamma-ray flux originating in the heat exchanger, the fraction of the total fuel in the radiator had to be specified. If three-fourths of the 200-ft^3 volume is occupied by fins, the fuel volume is 5 ft^3 (150 $ft^3 \times 0.0333$). The headers were assumed to contain an equal amount. At an average power density of 2.5 kw/cm^3 in the core and a total power of 300 Mw, the core fuel volume is 4.24 ft^3. If 2 ft^3 is allowed for miscellaneous volumes, the total fuel volume is 16.2 ft^3, of which 62% is in the radiator. This figure is arbitrary, but the uncertainty does not introduce a large uncertainty in the shield weight. The crew compartment chosen was a 6.67-ft-dia cylinder 10.8 ft long.

Dose-Rate Criteria

For this shielding study the permissible total dose rate inside the crew compartment was 1 rem/hr with a gamma-ray–to–neutron ratio of 3 to 1. Since the current radiation-damage criterion being used at ORNL specifies that the total dose rate at 50 ft from the reactor cannot exceed 1000 rep/hr, shield weights were calculated for this limitation. In addition, weights were calculated for a total dose rate of 100,000 rep/hr at 50 ft. An arbitrary upper limit of the total neutron dose rate at 50 ft was set at 100 rem/hr because of uncertainties in neutron capture in air and neutron activation of structural members. A lower limit of $\frac{1}{8}$ in. of lead on the crew compartment was used to compensate for the buildup of soft gamma radiation in the crew-compartment plastic.

In the case of the tandem radiator, an arbitrary ratio of the total dose rate from the sides of the radiator and the reactor had to be set because of the uncertainties in the calculation of this ratio for minimum shield weight. The ratio chosen was that of the projected areas of the radiator and reactor.

Shield Design for a Circulating-Fuel Reactor with a Wrap-Around Radiator

The thickness of the wrap-around radiator was required by its volume limitation of 200 ft^3 to be 23 in. Since the reactor-radiator arrangement is spherical, the shield design was inherently similar to the shield design for the circulating-fuel reflector-moderated reactor presently being studied by ORNL and Pratt & Whitney, and the methods used for obtaining that design could be used.

Neutron Shield. – The neutron shield was designed first on the usual assumption that substitution of gamma-ray shielding for some of the neutron shielding would not affect the neutron dose rate, since the removal cross section of lead is nearly the same as that of water. This assumption introduces some

error when the neutron shielding is thin. In the design the contribution to the dose rate by delayed neutrons was assumed to be negligible, since the radiator and water thicknesses were large.

The design utilized the TSF neutron shield optimization procedure,[8] with an assumed $\cos^{10}$ angular distribution of neutrons at the shield surface. The procedure was modified, however, as shown in the following section (S. K. Penny, "Modification of the Procedure for Using TSF Data for the Optimization of a Divided Neutron Shield"). The neutron dose rate used in the procedure was the dose rate a distance d of 64 ft from the center of the reactor as a function of water thickness around the reactor. This dose rate was calculated from LTSF CFRMR mockup data,[9] as follows:

$$D_R\,(64\text{ ft}) = D_{LT}(z)\,H(a,z)\,\frac{r_c r_s}{d^2}\,\frac{\rho_R}{\rho_{LT}}\,C_{HX}C_R\ ,$$

where

D_R = neutron dose rate at a distance d from the reactor,

D_{LT} = neutron dose rate at a distance z from the LTSF source plate,

$H(a,z)$ = Hurwitz correction (a = radius of LTSF source plate),

r_c = reactor core radius,

r_s = reactor shield radius,

ρ_R = reactor surface source strength,

ρ_{LT} = LTSF surface source strength,

C_{HX} = correction for substitution of the reactor radiator for the LTSF heat exchanger mockup on the basis of removal cross sections,

C_R = correction for substitution of the reactor materials, other than for the radiator and reflector, for similar materials in the LTSF mockup on the basis of removal cross sections.

The neutron shield (Table 16.3 and Fig. 16.2) designed by the above procedure allowed the 0.25 rem/hr neutron dose rate specified for the crew compartment and thus was the same for both cases, that is, 10^3 and 10^5 rep/hr at 50 ft. The optimization indicated that no neutron shielding was required on the rear of the reactor. However, the water thickness around the reactor was not allowed to fall below 20 cm in order to prevent the total neutron dose rate at any point 50 ft from the reactor from exceeding the specified 100 rem/hr.

Gamma-Ray Shield. – The gamma-ray shield was determined by using experimental data from the LTSF CFRMR mockup tests and the optimization procedure described in the preceding section (H. C. Woodsum, "Procedure for the Optimization of a Divided Gamma-Ray Shield for Circulating-Fuel Reactors"). In order to maintain a total dose rate of 10^3 rep/hr at 50 ft, it was necessary to design both a basic lead shield and a shadow shield. For the 10^5 rep/hr case, however, only the shadow shield was required, since the reactor with no shielding yielded only 4.2×10^4 rep/hr at 50 ft.

In the determination of the dose rate to be used in the optimization procedure it was necessary to consider two sources of radiation – primary and fission-product-decay gamma rays. The primary gamma-

[8] M. F. Valerino and F. L. Keller, *ANP Quar. Prog. Rep. Sept. 10, 1955*, ORNL-1947, p 205.

[9] J. B. Dee *et al.*, *ANP Quar. Prog. Rep. Dec. 10, 1955*, ORNL-2012, Part IV, p 25.

TABLE 16.3. THICKNESS OF TOTAL NEUTRON SHIELD FOR A CIRCULATING-FUEL REACTOR WITH A WRAP-AROUND RADIATOR

Dose rate: 10^3 or 10^5 rep/hr at 50 ft

Shield Section	Shield Thickness (in.)
Reactor (water)	
$\Delta\theta$* = 0 to 15 deg	19.3
$\Delta\theta$ = 15 to 45 deg	15.6
$\Delta\theta$ = 45 to 75 deg	9.1
$\Delta\theta$ = 75 to 105 deg	5.8**
$\Delta\theta$ = 105 to 180 deg	0**
Crew Compartment (plastic)	
Side	8.3
Front	8.3
Rear	17.3

*Polar angle increment.

**Augmented to 7.9 in. as a safety factor.

ray dose rate was calculated by using the following expression:

$$D_P = \frac{r_c r_s}{d^2} \frac{P_R/4\pi r_c^2}{P_{LT}/\pi a^2} H(a,z)\, D_{P,LT}(z)\, C_{HX} C_R \ ,$$

where

D_P = primary gamma-ray dose rate at a distance d from the reactor,

P_R = power of the reactor,

P_{LT} = power of the LTSF source plate,

$H(a,z)$ = conversion from finite disk to infinite plane source

$$= \frac{E_1(\mu z)}{E_1(\mu z) - E_1\left(\mu\sqrt{z^2 + a^2}\right)} \ ,$$

$$E_1(\mu z) = \int_{\mu z}^{\infty} \frac{e^{-y}}{y}\, dy \ ,$$

μ = effective linear absorption coefficient for the reactor shielding materials based on a gamma-ray energy of 6 to 8 Mev,

$D_{P,LT}$ = primary gamma-ray dose rate at distance z from the LTSF source plate,

C_{HX}, C_R = corrections similar to those defined previously except that they are based on an effective linear absorption coefficient for a gamma-ray energy of 6 to 8 Mev.

[redacted]

2-01-059-62

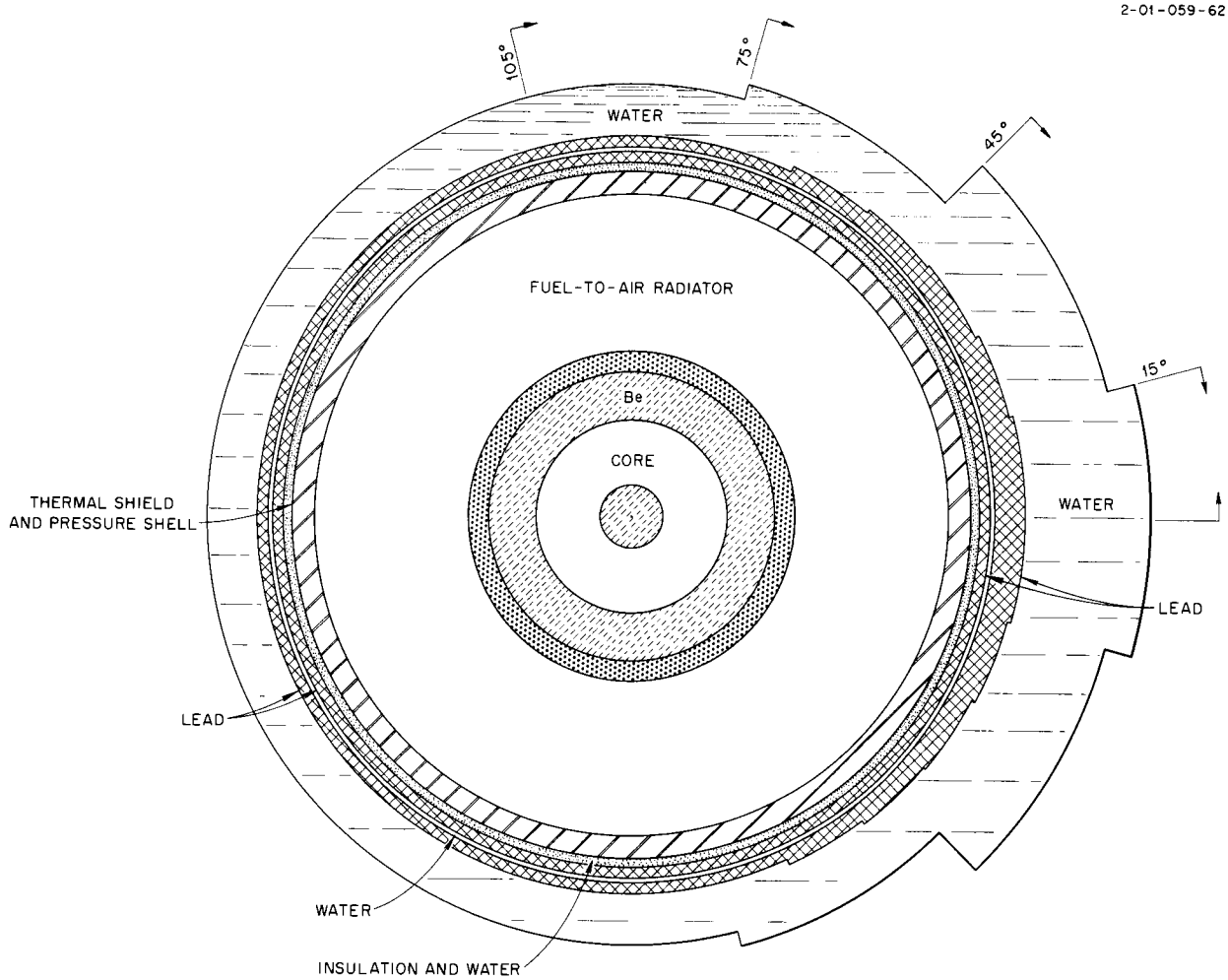

Fig. 16.2. Shield for a Circulating-Fuel Reactor with a Wrap-Around Fuel-to-Air Radiator.

The fission-product-decay gamma-ray dose rate was computed by using the following expression:

$$D_{HX} = N v_f \frac{P_R}{V_f} \frac{r_{HX_o} r_s}{d^2} \lambda(\bar{E}) \int_0^\infty \frac{B(\mu t)\, E_1(\mu t)\, N(E)\, dE}{2c(E)} ,$$

where

N = 3.1×10^{10} fissions/sec·watt,

D_{HX} = fission-product-decay gamma-ray dose rate at distance d from the reactor,

v_f = volume fraction of the radiator that contains fuel,

V_f = total volume of fuel in the system,

r_{HX_o} = outside radius of the radiator,

$\lambda(\bar{E})$ = effective mean free path of the radiator based on a gamma-ray energy of 2.7 Mev,

μt = number of mean free paths of lead and water shielding, as well as Inconel (shells), outside the radiator for gamma rays of energy E,

$B(\mu t)$ = dose buildup factor for μt mean free paths,

$N(E)$ = number of photons per fission of energy E per unit energy interval

$= 7\,e^{-1.2E}$,

$c(E)$ = flux-to-dose conversion factor.

The optimization procedure mentioned above assumed the lead shadow shield to be tapered by a 12.5-deg relaxation angle coupled with a disadvantage angle of 15 deg. This permits the dose rate emission per unit polar angle to increase exponentially to compensate for the exponential decrease in the probability of scattered radiation penetrating the crew-compartment sides. The tapering is based on a gamma-ray energy of 6.8 Mev.

The basic lead shield required to maintain 10^3 rep/hr at a distance of 50 ft is given in Table 16.4. This shield plus the shadow shield was divided so that lead and water shield layers could be alternated to cool the lead and to suppress capture gamma-ray production in the lead. For the 10^3 rep/hr case there was first an annulus of water 0.375 in. thick. The thickness of the rest of the lead varied with polar angle. For the 10^5 rep/hr case, where only the shadow shield was required, the lead was separated from the radiator by a water thickness of 0.375 in. The variations with polar angle are shown for the two cases in Table 16.5 and Fig. 16.2.

TABLE 16.4. THICKNESS OF BASIC GAMMA-RAY SHIELD FOR A CIRCULATING-FUEL REACTOR WITH A WRAP-AROUND RADIATOR

Dose rate: 10^3 rep/hr at 50 ft

$\Delta\theta$, Polar Angle Increment (deg)	Lead Thickness* (in.)
0–15	1.35
15–45	1.85
45–75	2.25
75–180	2.4

*Excluding shadow shield.

Shield Design for a Circulating-Fuel Reactor with a Tandem Radiator

The arrangement for the fuel-to-air radiator in tandem with the reactor is shown in Fig. 16.3. It was assumed that a reasonable radiator shape would be a 6-ft-dia cylinder 7 ft long. The reactor acts as a shield at one end. The shield around the remainder of the radiator was assumed to be a shell with no penetrating holes. The resulting total weight for this idealized system might be considered a lower limit. However, it must be remembered that the total shield weight was based on a radiator volume that allowed for ducting and that it also included patch weights. Thus two major problems were left unexplored – radiator design and duct design.

TABLE 16.5. THICKNESS OF TOTAL GAMMA-RAY SHIELD FOR A CIRCULATING-FUEL REACTOR WITH A WRAP-AROUND RADIATOR

Shield Section	Lead Thickness (in.)			
	For a Dose Rate of 10^3 rep/hr at 50 ft			For a Dose Rate of 10^5 rep/hr at 50 ft*
	First Layer	Second Layer**	Total	
Reactor				
$\Delta\theta$*** = 0 to 15 deg	1.35	4.32	5.67	4.47
$\Delta\theta$ = 15 to 27.5 deg	1.35	3.99	5.34	3.64
$\Delta\theta$ = 27.5 to 40 deg	1.35	3.17	4.52	2.82
$\Delta\theta$ = 40 to 52.5 deg	1.35	2.74	4.09	1.99
$\Delta\theta$ = 52.5 to 65 deg	1.35	1.89	3.24	1.16
$\Delta\theta$ = 65 to 77.5 deg	1.35	1.07	2.42	0.335
$\Delta\theta$ = 77.5 to 180 deg	1.35	1.05	2.40	0.0
Crew Compartment				
Side			0.125	0.125
Front			0	0
Rear			0.478	2.46

*Only one layer required.
**Part of basic shield plus all of shadow shield.
***Polar angle increment.

Reactor Shielding. – The shielding required on the reactor was determined by the comparison method, as it was for the wrap-around radiator design. The most recent LTSF data were employed, and they were adjusted for the attenuation by the radiator by using neutron-removal cross-section and gamma-ray absorption coefficients. It was assumed that one-fourth the total gamma-ray dose rate in the central vertical plane of the reactor-radiator system came from the reactor. This was based on the ratio of the projected areas of the reactor and radiators.

Radiator Shielding. – In calculating the gamma-ray shield for the radiator it was assumed that the fuel circulation time was so fast that the gamma-ray sources were uniform over the system. A surface source strength was then determined. The two methods used for calculating the attenuation through the shield are summarized below:

(1) Method 1:[10]

$$D_1 = \frac{P_0\lambda}{c}\,\frac{r_s^2}{d}\sqrt{\frac{r_{rad}}{r_s}}\,\frac{E_1(\mu t)}{2}\,B(\mu t)\ ;$$

(2) Method 2:[11]

$$D_2 = \frac{P_0\lambda}{2c\sqrt{\pi}}\,\frac{r_{rad}{}^b}{d^2}\,\frac{\mathrm{erf}\,(\sqrt{\alpha})\,e^{-\mu t}}{\sqrt{\alpha}}\,B(\mu t)\ ,$$

[10]E. P. Blizard and H. Goldstein (eds.), *Report of the 1953 Summer Shielding Session*, ORNL-1575, p 92 (June 14, 1954).

[11]*Ibid.*, p 83.

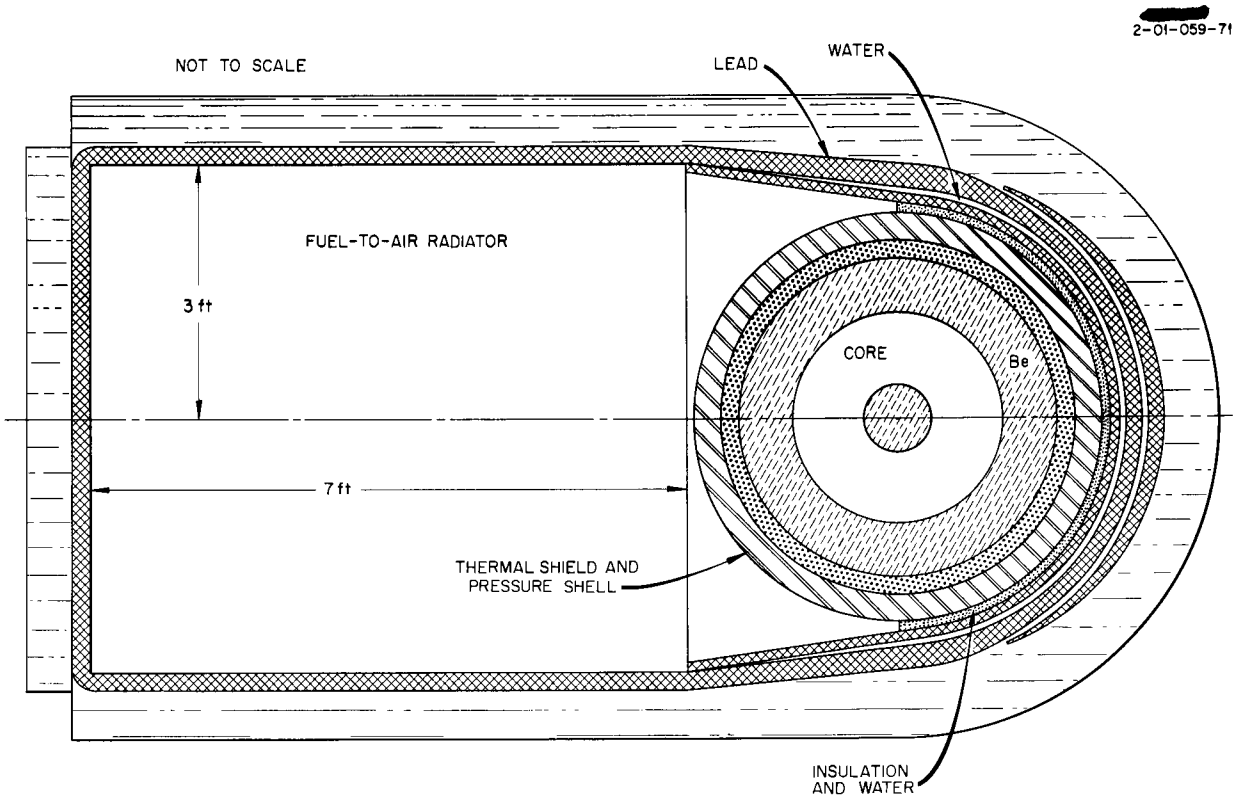

Fig. 16.3. Shield for a Circulating-Fuel Reactor with a Tandem Fuel-to-Air Radiator.

where

D_1, D_2 = gamma-ray dose rate at a distance d from the reactor,

P_0 = photon source density

$$= \frac{P_R}{V_{f(\mathrm{sys})}} \frac{V_{f(\mathrm{rad})}\,\Gamma N}{V_{\mathrm{rad}}} ,$$

P_R = power of the reactor,

$V_{f(\mathrm{sys})}$ = volume of fuel in the system,

$V_{f(\mathrm{rad})}$ = volume of fuel in the radiator,

V_{rad} = volume of radiator,

Γ = number of photons per fission,

N = 3.1×10^{10} fissions/sec·watt,

λ = gamma-ray mean free path in the radiator,

r_s = outer radius of the lead shield,

r_{rad} = outer radius of the radiator,

$t = r_s - r_{\mathrm{rad}}$,

$$E_1(\mu t) = \int_{\mu t}^{\infty} \frac{e^{-y}}{y}\, dy ,$$

c = flux-to-dose conversion factor,

$2b$ = heat-exchanger length,

$$\alpha = \frac{1}{2}\int_{r_{rad}}^{r_s} \frac{(r_{rad})^2}{r^2}\,\mu\,dr = \frac{(r_{rad})^2\mu}{2}\left(\frac{1}{r_{rad}} - \frac{1}{r_s}\right),$$

$$\text{erf}\,(\sqrt{\alpha}) = \frac{2}{\sqrt{\pi}}\int_0^{\sqrt{\alpha}} e^{-u^2}\,du \cong 1,$$

$B(\mu t)$ = dose buildup factor in lead.

The equations imply that the effective number of photons per fission, the source average mean free path, and the average absorption coefficient in the shield are known. These uncertainties may be removed by integrating over the spectrum of gamma-ray energies. Thus Eq. 1 may be written

$$D_1 = \frac{P_R}{V_f}\,\frac{V_{f(rad)}}{V_{rad}}\left(\frac{r_s}{d}\right)^2\sqrt{\frac{r_{rad}}{r_s}}\,\lambda A\,, \tag{3}$$

where

$$\lambda A = \frac{N}{2}\int_0^{\infty} \frac{N(E)\,E_1(\mu t,E)\,B(\mu t,E)\,dE}{c(E)\,\mu(E)}\,,$$

$N(E)$ = number of photons per fission of energy E per unit energy interval

$= 7\,e^{-1.2E}$,

$\mu(E)$ = gamma-ray absorption coefficient in the radiator.

Also

$$N\frac{B}{c}\,\frac{\lambda\Gamma}{2} = \frac{\lambda A}{\overline{E}_1}\,.$$

Then

$$D_2 = \frac{P_R}{V_f}\,\frac{V_{f(rad)}}{V_{rad}}\,\frac{r_{rad}{}^b}{\sqrt{\pi}\,d^2}\,\frac{\text{erf}\,\sqrt{\alpha}}{\sqrt{\alpha}}\,e^{-\mu t}\,\frac{\lambda A}{\overline{E}_1(\mu t)}\,. \tag{4}$$

Thus a check may be obtained on the estimation of the dose resulting from Method 1 (Eq. 3) by using Method 2 (Eq. 4). Method 2 yielded a slightly thicker gamma-ray shield for the case of 10^3 rep/hr at 50 ft. This thickness was used in the design in order to be conservative. Method 2 failed for the case of 10^3 rep/hr at 50 ft, and thus the thickness given by Method 1 was used.

In the calculation of the lead shield, delayed neutrons from the fuel were not considered, since it is very difficult to estimate the source strength of delayed neutrons at the surface of the radiator and also to calculate their attenuation through the shield. Therefore, the maximum dose rate from delayed neutrons was calculated by assuming zero circulation time and no attenuation from a point source. The dose at 50 ft under these conditions is about 30,000 rep/hr. The LTSF data indicate a very short relaxation length in water for delayed neutrons. If a reduction by a factor of 10^4 is desired, 10 in. of water will be required. With the water placed at the outside and replacing the same number of gamma-

ray mean free paths of lead, the additional weight is only 590 lb in the 10^3 rep/hr case. If, in the 10^5 rep/hr case, a reduction of 10^4 is desired, the additional weight is 4470 lb.

The plastic on the crew compartment was determined from the air-scattering considerations outlined previously.[12] The thicknesses on the side and front are given by:

$$t_{ps} = 1.77 \ln \left[2\pi \left(\frac{\overline{K}}{l} \right) d \, \frac{I_{dn}}{\phi_{sn}} \right] ,$$

where

d = reactor-crew compartment separation distance (cm),

I_{dn} = direct neutron dose rate outside the crew compartment,

ϕ_{sn} = desired crew compartment scattered dose rate,

$2\pi \left(\frac{\overline{K}}{l} \right) = 1.695 \times 10^{-4}$ for a symmetric shield.[13]

The thickness on the rear is given by:

$$t_{pr} = 2.84 \ln \frac{I_{dn}}{\phi_{dn}} ,$$

where ϕ_{dn} is the desired crew-compartment direct dose rate.

The resulting plastic thicknesses were used in the gamma-ray shield optimization procedure mentioned above to determine the lead thicknesses on the crew compartment and in the shadow shield. The shield thicknesses for the tandem arrangement are given in Table 16.6.

Total Weights

The total weights given in Table 16.7 for the two systems do not appear to be excessive. Before conclusions can be reached with any degree of certainty, however, a more thorough study must be made in which consideration is given to the fuel-to-air radiator design and to the increase in engine efficiency obtained by elimination of an intermediate heat exchanger. The reactor weight for the tandem case is less because the Inconel shells have a much smaller diameter.

MODIFICATION OF THE PROCEDURE FOR USING TSF DATA FOR THE OPTIMIZATION OF A DIVIDED NEUTRON SHIELD

S. K. Penny

The procedure for using TSF data[14] for the optimization of a divided neutron shield has been modified in two respects: a derivative term was included which was neglected previously, and the iteration procedure was changed so that one of the Lagrangian multipliers would converge more rapidly. Some useful curves have been plotted as an aid in following the procedure. The effect that these modifications have on the shield thicknesses and weights has been determined by a sample shield calculation for the reactor and crew-compartment system used previously. Neither the geometry nor the definitions of terms

[12] *Ibid.*, pp 221, 355.

[13] This term is defined in ref. 12.

[14] C. E. Clifford *et al.*, *ANP Quar. Prog. Rep. Sept. 10, 1955*, ORNL-1947, p 205.

TABLE 16.6. THICKNESS OF TOTAL NEUTRON AND GAMMA-RAY SHIELD FOR A CIRCULATING-FUEL REACTOR WITH A TANDEM RADIATOR

Shield Section	Shield Thickness (in.)	
	For a Dose Rate of 10^3 rep/hr at 50 ft	For a Dose Rate of 10^5 rep/hr at 50 ft
Reactor		
Lead at front	2.25	0
Lead at side[a]	3.2	0.2
Water at front and side	21.25 minus lead thickness[b]	
Shadow shield at center line	5.16	6.66
Radiator		
Lead at front and side	3.9[c]	0.5[d]
Water at front and side	*e*	*e*
Crew Compartment		
Lead at front and side	0.125	0.125
Lead at rear	0.125	2.08
Plastic at front and side	8.18	8.18
Plastic at rear	20.2	20.2

[a]Larger than the front thickness because the radiator contributes to the side gamma-ray dose rate.

[b]Thus total shield thickness = 21.25 in.

[c]Obtained by Method 2 (Method 1 gives 3.4 in.). This thickness is reduced to 3 in. if 10 in. of water is added as a delayed-neutron shield.

[d]Obtained by Method 1 (Method 2 fails at small lead thicknesses). This thickness is eliminated if 10 in. of water is added as a delayed-neutron shield.

[e]Ten inches of water can be added as a delayed-neutron shield and the lead thickness reduced (see *c* and *d*).

are repeated here, since it would require considerable repetition of the earlier report. Reference to that report[14] therefore will be necessary to an understanding of this report.

Neglected Derivative Term

The derivative term neglected previously occurs because the relaxation lengths in the side and rear of the crew compartment depend on the thickness of water on a conical shell as follows:

$$\lambda_s^s(T_n,\theta_n,t) = \frac{\lambda_s^s(45,\theta_n,t)\,\lambda_d(T_n + t)}{1.14\lambda_d(45 + t)} , \tag{1}$$

$$\lambda_s^r(T_n) = \frac{7.0\lambda_d(T_n + 15)}{1.14\lambda_d(45 + 15)} , \tag{2}$$

$$\lambda_d^r(T_n,t) = \frac{\lambda_d(T_n + t)}{1.14} . \tag{3}$$

TABLE 16.7. REACTOR AND SHIELD WEIGHTS FOR CIRCULATING-FUEL REACTORS WITH WRAP-AROUND AND TANDEM RADIATORS

Component	Weight (lb)			
	For a Dose Rate of 10^3 rep/hr at 50 ft		For a Dose Rate of 10^5 rep/hr at 50 ft	
	Wrap-Around Arrangement	Tandem[a] Arrangement	Wrap-Around Arrangement	Tandem[a] Arrangement
Reactor[b]	44,400	31,500	44,400	31,500
Reactor lead shield[c]	37,400	18,200	12,600	9,900
Reactor water shield	9,000	8,600	9,200	9,800
Radiator lead shield		38,400[d]		4,800
Structure[e,f]	2,500	2,500	2,400	2,500
Patch[f]	5,000	5,000	5,000	5,000
Crew compartment lead shield	2,700	1,700	6,700	3,000
Crew compartment plastic shield	14,400	14,700	14,400	14,700
Total	115,400	120,600	94,700	81,200
Delayed neutron shield[g]		600		4,500
Total		121,200		85,700

[a]Weights for shield specified in Table 16.6.
[b]Includes estimate for decking, pumps and drives, control rod, island support, radiator (20,000 lb), etc.
[c]Includes shadow shield.
[d]Method 1 gives 33,200 lb.
[e]Includes neutron shield container.
[f]Estimated from information given in ORNL-1575, *Report of the 1953 Summer Shielding Session*, E. P. Blizard and H. Goldstein (eds.) (June 14, 1954).
[g]Additional weight incurred if lead is replaced by water as described above under "Radiator Shielding."

The neglected terms appear when the partial derivative of the total dose in the crew compartment is taken with respect to T_n as follows:

$$(4)\quad \frac{\partial D_{\text{total}}}{\partial T_n} = -\left\{ D_n^{s,\text{side}} \left[\frac{1}{\lambda_d(T_n)} + \int_0^{T_s} \frac{\partial}{\partial T_n}\left(\frac{1}{\lambda_s^s(T_n, \theta_n, t)} \right) dt \right] \right.$$

$$\left. + D_n^{s,\text{rear}} \left[\frac{1}{\lambda_d(T_n)} + \int_0^{T_r} \frac{\partial}{\partial T_n}\left(\frac{1}{\lambda_s^r(T_n)} \right) dt \right] + D_n^{d,\text{rear}} \left[\frac{1}{\lambda_d(T_n)} + \int_0^{T_r} \frac{\partial}{\partial T_n}\left(\frac{1}{\lambda_d^r(T_n, t)} \right) dt \right] \right\} .$$

The terms involving integrals are the previously neglected terms and can be estimated as follows:

$$(5)\quad \frac{\partial}{\partial T_n}\left(\frac{1}{\lambda_s^s} \right) = -\frac{1}{(\lambda_s^s)^2} \frac{\partial \lambda_s^s}{\partial T_n} = -\frac{1.14\lambda_d(45 + t)}{\lambda_s^s(45, \theta_n, t)\, \lambda_d^2(T_n + t)} \frac{\partial \lambda_d(T_n + t)}{\partial T_n} ,$$

[redacted]

$$\frac{\partial}{\partial T_n}\left(\frac{1}{\lambda_s^r}\right) = -\frac{1}{(\lambda_s^r)^2}\frac{\partial \lambda_s^r}{\partial T_n} = -\frac{1.14\lambda_d(T_n + 15)}{7.0\lambda_d^2(T_n + 15)}\frac{d\lambda_d(T_n + 15)}{dT_n}, \tag{6}$$

$$\frac{\partial}{\partial T_n}\left(\frac{1}{\lambda_d^r}\right) = -\frac{1}{(\lambda_d^r)^2}\frac{\partial \lambda_d^r}{\partial T_n} = -\frac{1.14}{\lambda_d^2(T_n + t)}\frac{\partial \lambda_d(T_n + t)}{\partial T_n}. \tag{7}$$

It may be noted that

$$\frac{\partial \lambda_d(T_n + t)}{\partial T_n} = \frac{d\lambda_d(T_n + t)}{d(T_n + t)}. \tag{8}$$

Thus the partial derivative above may be evaluated from the slope of the plot of $\lambda_d(x)$ vs x. Equations 8 and 5 were used to numerically evaluate the quantity

$$-\int_0^{T_s}\frac{\partial}{\partial T_n}\left(\frac{1}{\lambda_s^s}\right)dt,$$

which is plotted as a function of T_s with θ_n and T_n as parameters in Figs. 16.4 through 16.6. From Eqs. 8 and 6,

$$-\int_0^{T_r}\frac{\partial}{\partial T_n}\left(\frac{1}{\lambda_s^r}\right)dt = \frac{1.14\lambda_d(60)\,T_r}{7.0\lambda_d^2(T_n + 15)}\left.\frac{d\lambda_d(x)}{dx}\right]_{x=T_n+15}.$$

The term $\dfrac{1}{\lambda_d^2(x)}\dfrac{d\lambda_d(x)}{dx}$ is plotted as a function of x in Fig. 16.7. By using Eqs. 8 and 7,

$$-\int_0^{T_r}\frac{\partial}{\partial T_n}\left(\frac{1}{\lambda_d^r}\right)dt = 1.14\left[\frac{1}{\lambda_d(T_n)} - \frac{1}{\lambda_d(T_n + T_r)}\right].$$

Then,

$$L_n = \frac{D_n^{s,\text{side}}\left[\dfrac{1}{\lambda_d} + \displaystyle\int_0^{T_s}\frac{\partial}{\partial T_n}\left(\frac{1}{\lambda_s^s}\right)dt\right] + D_n^{s,\text{rear}}\left[\dfrac{1}{\lambda_d} + \displaystyle\int_0^{T_r}\frac{\partial}{\partial T_n}\left(\frac{1}{\lambda_s^r}\right)dt\right] + D_n^{d,\text{rear}}\left[\dfrac{1}{\lambda_d} + \displaystyle\int_0^{T_r}\frac{\partial}{\partial T_n}\left(\frac{1}{\lambda_d^r}\right)dt\right]}{A(\theta_n)(T_n + a)^2}, \tag{9}$$

and the equation used in step c[14] of the procedure becomes

$$\frac{\lambda_d(T_n + a)^2}{D_d(a,e)\,e^{-\int_0^{T_n}(1/\lambda_d)dt}} = \frac{B_n e^{-\int_0^{T_s}(1/\lambda_s^s)dt}\left[1 + \lambda_d\displaystyle\int_0^{T_s}\frac{\partial}{\partial T_n}\left(\frac{1}{\lambda_s^s}\right)dt\right] + C_n e^{-\int_0^{T_r}(1/\lambda_s^r)dt}\left[1 + \lambda_d\displaystyle\int_0^{T_r}\frac{\partial}{\partial T_n}\left(\frac{1}{\lambda_s^r}\right)dt\right] + J_n e^{-\int_0^{T_r}(1/\lambda_d^r)dt}\left[1 + \lambda_d\displaystyle\int_0^{T_r}\frac{\partial}{\partial T_n}\left(\frac{1}{\lambda_d^r}\right)dt\right]}{L_n A(\theta_n)}, \tag{10}$$

[redacted]

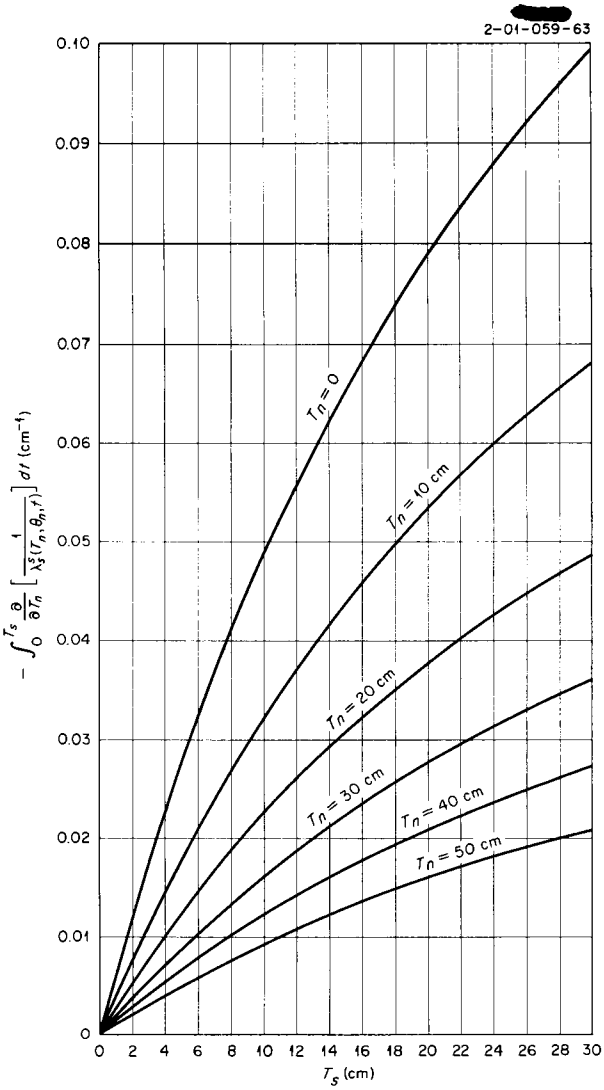

Fig. 16.4. $-\int_0^{T_s} \frac{\partial}{\partial T_n}\left[\frac{1}{\lambda_s^s(T_n,\theta_n,t)}\right] dt$ **as a function of** T_s **for** $\theta = 0$ **to 30 deg.**

[redacted]

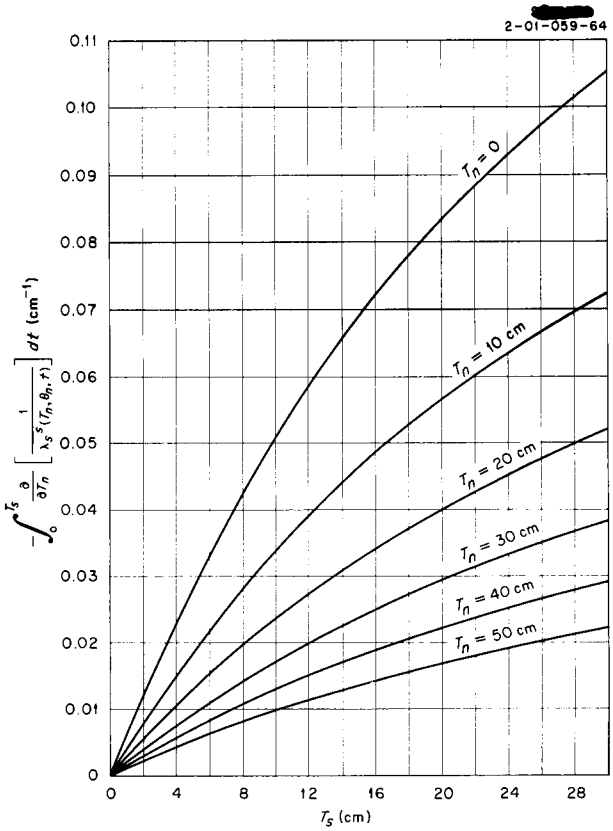

Fig. 16.5. $-\int_0^{T_s} \frac{\partial}{\partial T_n}\left[\frac{1}{\lambda_s^s(T_n,\theta_n,t)}\right] dt$ **as a function of** T_s **for** $\theta = 60$ **to 90 deg.**

[redacted]

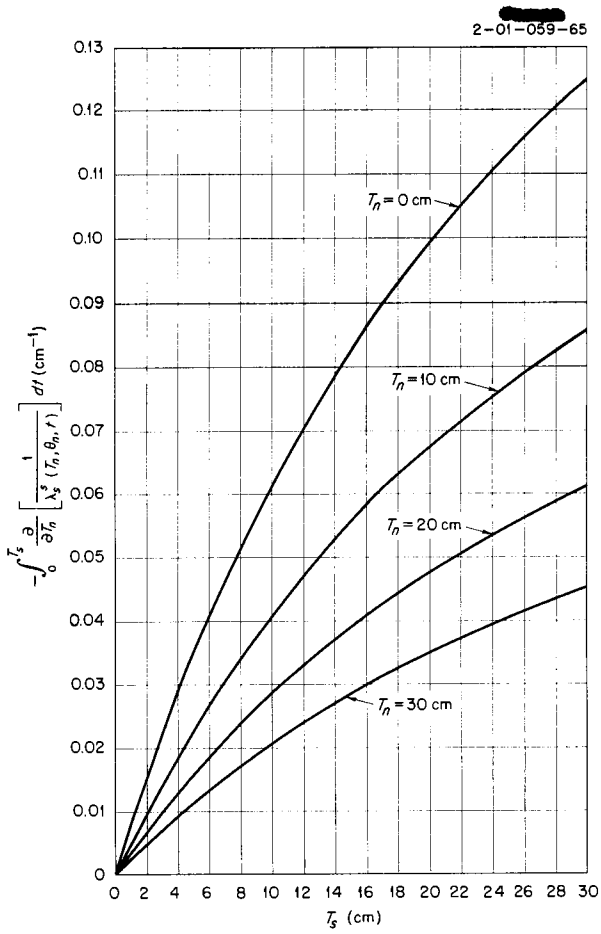

Fig. 16.6. $-\int_0^{T_s} \frac{\partial}{\partial T_n}\left[\frac{1}{\lambda_s^s(T_n,\theta_n,t)}\right] dt$ **as a function of** T_s **for** θ **= 135 to 180 deg.**

where $T_r = Q(T_s)$. In Eq. 10, the terms in brackets, $\left[1 + \lambda_d \int \frac{\partial}{\partial T_n}\left(\frac{1}{\lambda}\right) dt\right]$, may be as low as 0.32, whereas in the previous procedure they were exactly unity.

Changed Iteration Procedure

The Lagrangian multiplier for the rear of the crew compartment converges faster if the following changes are made. Let

$$\frac{1}{\lambda_d^r} \equiv \frac{\sum_{n=1}^{N} D_n^{d,\text{rear}}/\lambda_d^r}{\sum_{n=1}^{N} D_n^{d,\text{rear}}} ;$$

[redacted] [redacted]

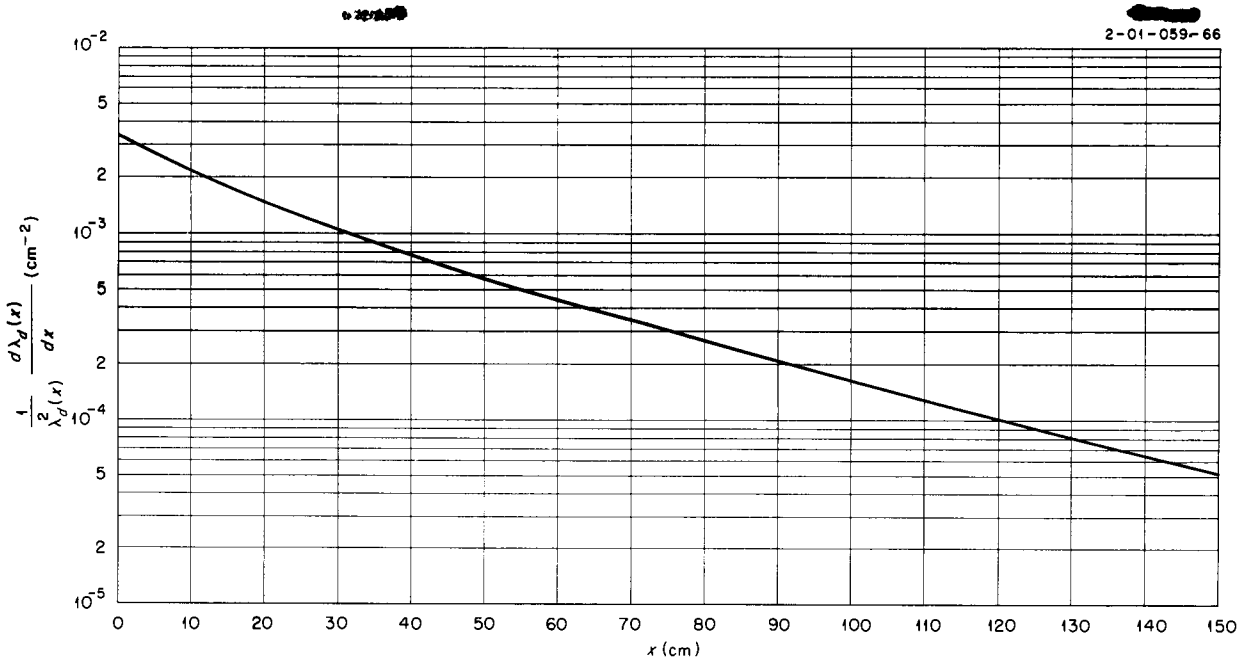

Fig. 16.7. $\dfrac{1}{\lambda_d^2(x)} \dfrac{d\lambda_d(x)}{dx}$ **as a function of** x.

then

$$L = \frac{D_{\text{total}} + \left[(\overline{\lambda_d^r}/\overline{\lambda_s^r}) - 1\right] \sum_{n=1}^{N} D_n^{s,\text{rear}}}{\overline{\lambda_s^s}(\partial W_{\text{total}}/\partial T_s) + \overline{\lambda_d^r}(\partial W_{\text{total}}/\partial T_r)}$$

so that near the optimum

$$D_{\text{total}} \gg \left(\frac{\overline{\lambda_d^r}}{\overline{\lambda_s^r}} - 1\right) \sum_{n=1}^{N} D_n^{s,\text{rear}}$$

is truly realistic and L varies very slowly from one iteration to the next. Let

$$e^{-T_r/\overline{\overline{\lambda_d^r}}} \equiv \frac{\sum_{n=1}^{N} J_n e^{-\int_0^{T_n}(1/\lambda_d)dt} e^{-\int_0^{T_r}(1/\lambda_d^r)dt}}{\sum_{n=1}^{N} J_n e^{-\int_0^{T_n}(1/\lambda_d)dt}},$$

and let

$$\alpha \equiv \frac{(\partial W_{\text{total}}/\partial T_s)\,\overline{\lambda_s^s}}{(\partial W_{\text{total}}/\partial T_r)\,\overline{\lambda_d^r}} \;;$$

then

$$\frac{1}{\alpha}\, e^{-T_s/\overline{\overline{\lambda_s^s}}} = \frac{\sum_{n=1}^{N} C_n\, e^{-\int_0^{T_n}(1/\lambda_d)\,dt}}{\sum_{n=1}^{N} B_n\, e^{-\int_0^{T_n}(1/\lambda_d)\,dt}}\;\frac{\overline{\lambda_d^r}}{\overline{\overline{\lambda_s^r}}}\; e^{-T_r/\overline{\overline{\lambda_s^r}}} + \frac{\sum_{n=1}^{N} J_n\, e^{-\int_0^{T_n}(1/\lambda_d)\,dt}}{\sum_{n=1}^{N} B_n\, e^{-\int_0^{T_n}(1/\lambda_d)\,dt}}\; e^{-T_r/\overline{\overline{\lambda_d^r}}} \;.$$

The basic steps a, b, c, and d are the same as in the previous procedure[14] except that the equations shown above have been changed. To aid in following the procedure, $\int_0^{T_s}(1/\lambda_s^s)\,dt$ is shown plotted as a function of T_s with θ_n and T_n as parameters in Figs. 16.8 through 16.10. The quantity $e^{-\int_0^{x}(1/\lambda_d)\,dt}$, from which $e^{-\int_0^{T_r}(1/\lambda_d)\,dt}$ can be determined, is shown in Fig. 16.11.

Results of a Sample Calculation

The results after three iterations, with the use of the new procedure and beginning with the shield thickness presented previously,[14] are shown in Table 16.8. The thicknesses on the last two conical shells tended to become negative and thus were dropped from the optimization procedure and set equal to zero. The dose rate criterion in the crew compartment was 0.25 rem/hr, which is the same as that for the previous system.

TABLE 16.8. OPTIMIZATION OF NEUTRON SHIELDING FOR A 300-Mw CIRCULATING-FUEL REFLECTOR-MODERATED REACTOR

Shield Region	Old Procedure			New Procedure		
	Shielding Thickness (cm)	Lagrangian Multiplier ($\times 10^8$)	Weight of Shield (tons)	Shielding Thickness (cm)	Lagrangian Multiplier ($\times 10^8$)	Weight of Shield (tons)
Reactor shield						
$\Delta\theta$* = 0 to 15 deg	43.4	16.8	0.15	36.8	17.7	0.12
$\Delta\theta$ = 15 to 45 deg	39.3	17.0	0.96	32.0	18.7	0.74
$\Delta\theta$ = 45 to 75 deg	28.6	18.3	1.11	20.3	18.7	0.72
$\Delta\theta$ = 75 to 105 deg	21.3	18.9	0.89	12.2	17.3	0.47
$\Delta\theta$ = 105 to 165 deg	10.4	17.8	0.53	0.0		0.00
$\Delta\theta$ = 165 to 180 deg	7.8	18.0	0.02	0.0		0.00
Rear of crew compartment	43.8	11.9	1.47	46.3	17.4	1.54
Side and front of crew compartment	16.8	18.0	4.52	20.6	18.2	5.54
Total weight			9.65			9.13

*Polar angle increment.

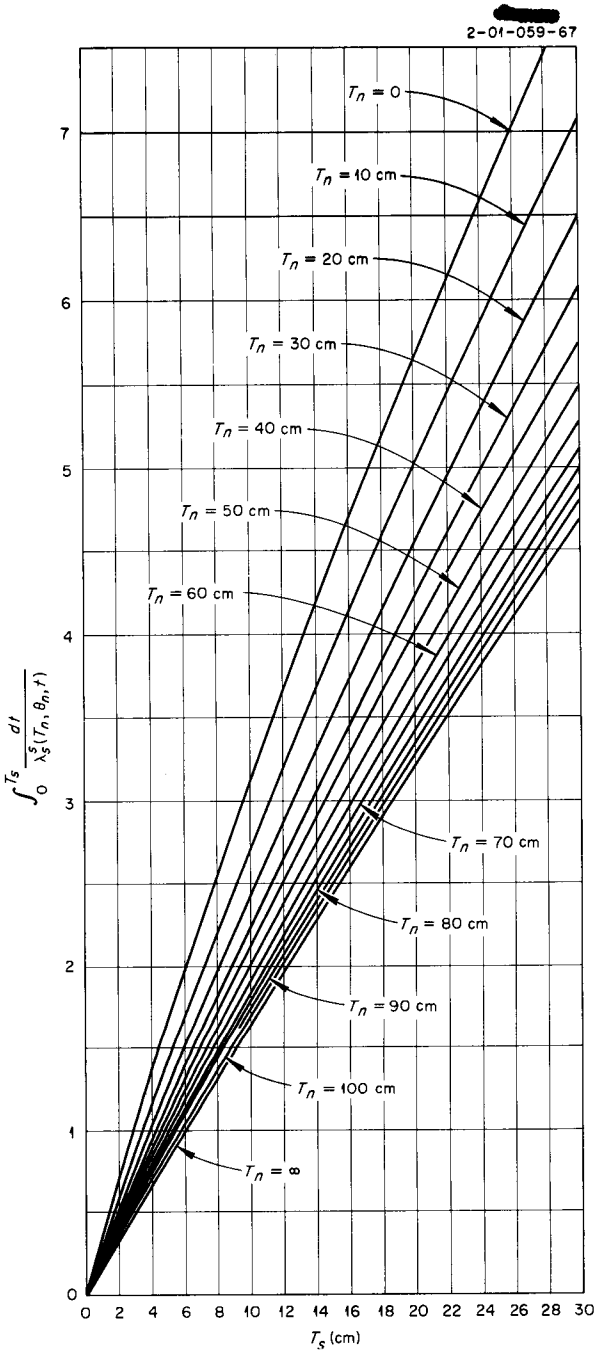

Fig. 16.8. $\int_0^{T_s} \frac{1}{\lambda_s^s(T_n, \theta_n, t)}\, dt$ **as a function of** T_s **for** $\theta = 0$ **to 30 deg.**

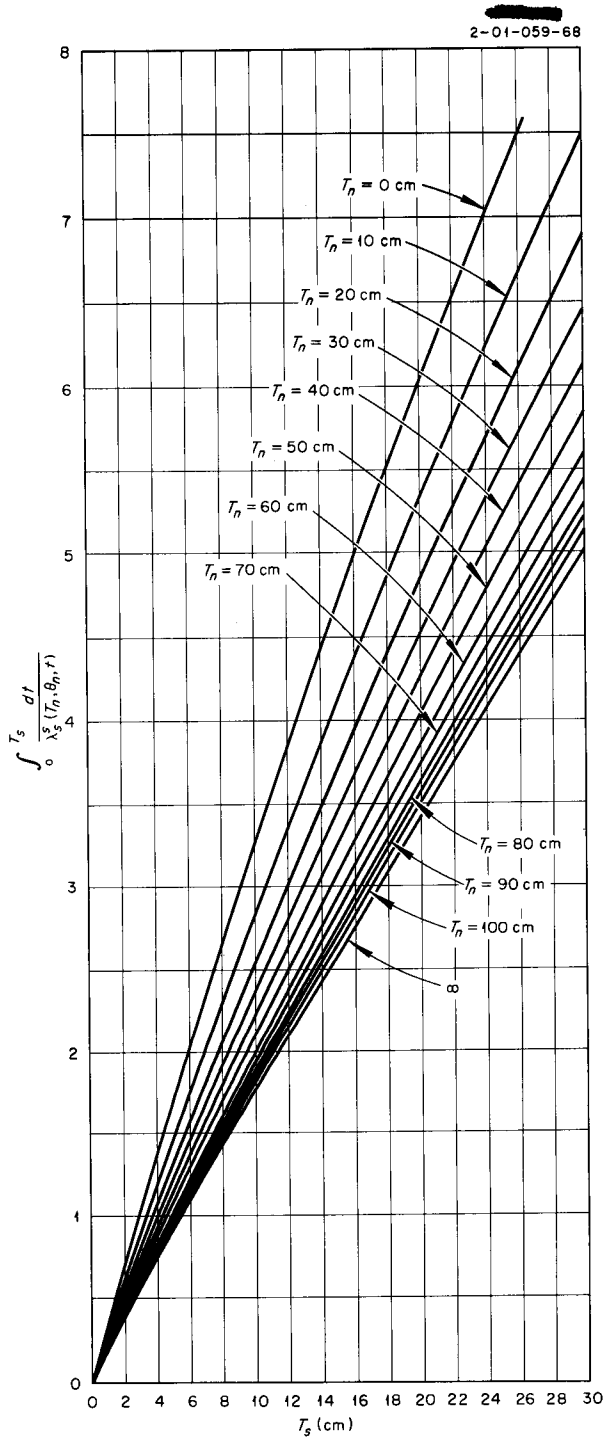

Fig. 16.9. $\int_0^{T_s} \frac{1}{\lambda_s^s(T_n, \theta_n, t)}\, dt$ **as a function of** T_s **for** $\theta = 60$ **to 90 deg.**

[redacted]

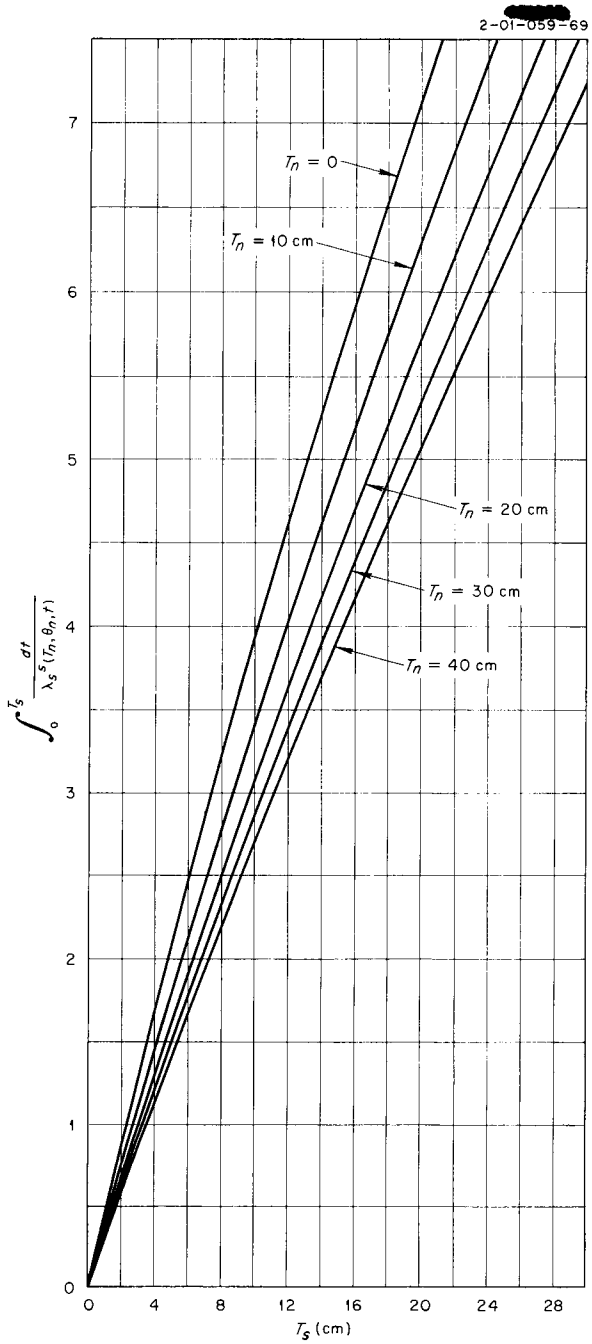

Fig. 16.10. $\int_0^{T_s} \frac{1}{\lambda_s^s(T_n, \theta_n, t)}\, dt$ **as a function of** T_s **for** θ **= 135 to 180 deg.**

[redacted] [redacted]

2-01-059-70

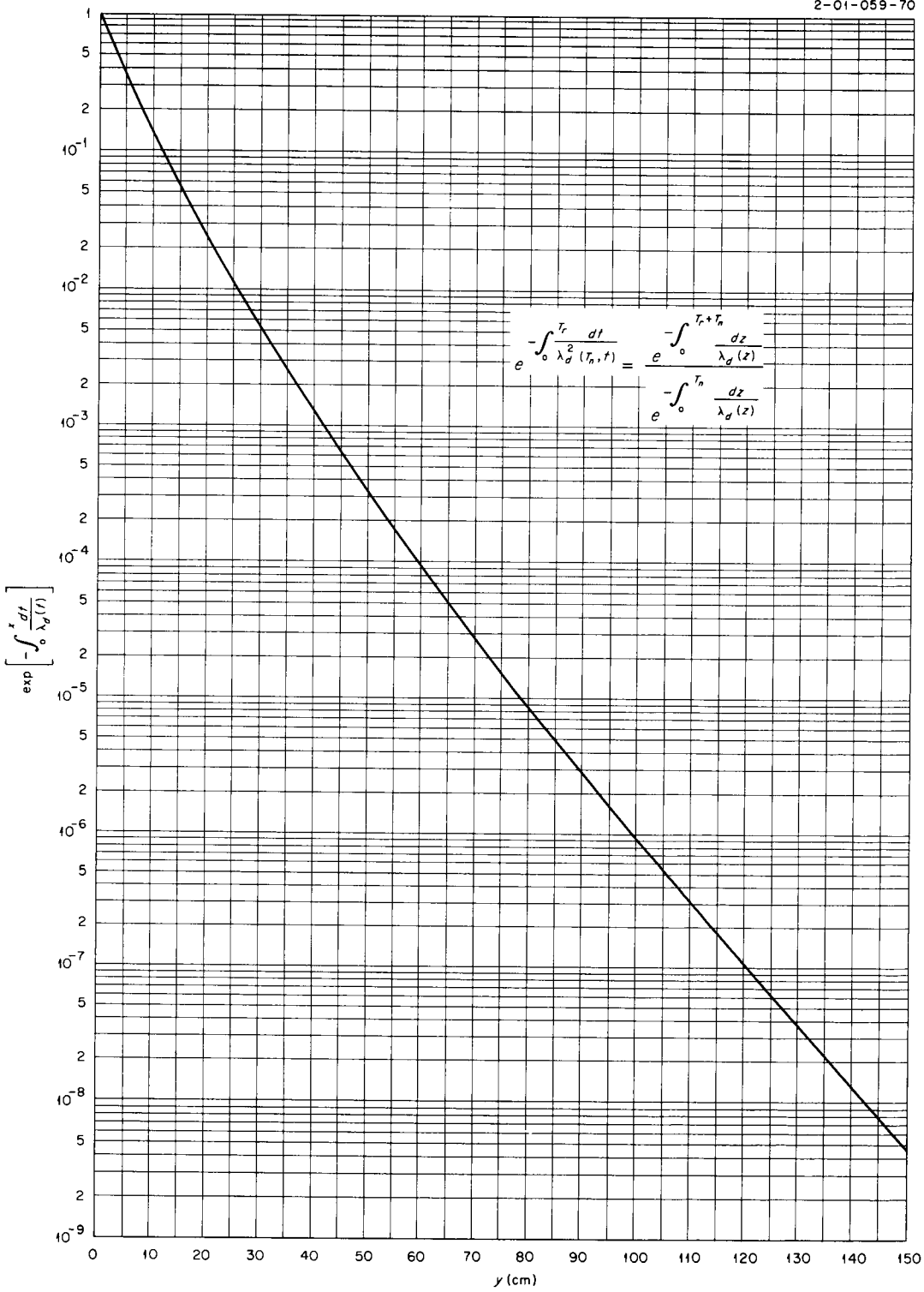

Fig. 16.11. $\exp\left[-\int_0^x \frac{dt}{\lambda_d(t)}\right]$ **as a function of** x.